Journal of Molecular Structure 1069 (2014) 23–49

Contents lists available at ScienceDirect

Journal of Molecular Structure

journal homepage: www.elsevier.com/locate/molstruc

Frontiers of two-dimensional correlation spectroscopy. Part 2. Perturbation methods, fields of applications, and types of analytical probes

Isao Noda *

Department of Materials Science and Engineering, University of Delaware, Newark, DE 19716, USA

HIGHLIGHTS

- Comprehensive survey on experimental practices in 2D correlation spectroscopy.
- Perturbation methods, fields of applications, and types of analytical probes.
- Physical phenomena, chemical reactions, and biological processes with effects of temperature, concentration, pressure, etc.
- Applications, like polymers, proteins, composites, solution mixtures, etc.
- Probes, like IR, Raman, NIR, fluorescence, NMR, X-ray, Mass spectrometry, etc.

GRAPHICAL ABSTRACT

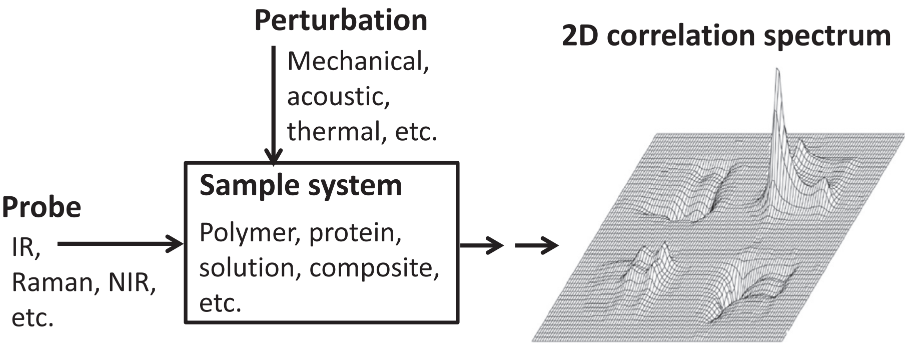

ARTICLE INFO

Article history:
Available online 21 January 2014

Keywords:
Two-dimensional correlation
Spectroscopy
Review
Survey
2DCOS

ABSTRACT

Noteworthy experimental practices, which are advancing forward the frontiers of the field of two-dimensional (2D) correlation spectroscopy, are reviewed with the focus on various perturbation methods currently practiced to induce spectral changes, pertinent examples of applications in various fields, and types of analytical probes employed. Types of perturbation methods found in the published literature are very diverse, encompassing both dynamic and static effects. Although a sizable portion of publications report the use of dynamic perturbatuions, much greater number of studies employ static effect, especially that of temperature. Fields of applications covered by the literature are also very broad, ranging from fundamental research to practical applications in a number of physical, chemical and biological systems, such as synthetic polymers, composites and biomolecules. Aside from IR spectroscopy, which is the most commonly used tool, many other analytical probes are used in 2D correlation analysis. The ever expanding trend in depth, breadth and versatility of 2D correlation spectroscopy techniques and their broad applications all point to the robust and healthy state of the field.

© 2014 Elsevier B.V. All rights reserved.

Abbreviations: ATR, attenuated total reflectance; BSA, bovine serum albumin; DFT, density functional theory; DRIFTS, diffuse reflectance Fourier transform IR spectroscopy; HDPE, high-density polyethylene; IR, infrared; IRRAS, infrared reflection absorption spectroscopy; LCST, lower critical solution temperature; LDPE, low-density polyethylene; LLDPE, linear low density polyethylene; NIR, near infrared; PAS, photoacoustic spectroscopy; PCA, principal component analysis; PCL, polycaprolactone; PEG, polyethylene glycol; PEO, polyethylene oxide; PET, poly(ethylene terephthalate); PHA, poly(3-hydoroxyalkanoate); PHB, poly(3-hydroxybutyrate); PHBHx, poly(3-hydroxybutyrate-*co*-3-hydroxyhexanoate); PLA, poly(lactic acid); PLLA, poly(L-lactic acid); PNIPAM, poly(*N*-isopropylacrylamide); PP, polypropylene; PPO, polypropylene oxide; PS, polystyrene; PVME, poly(vinyl methyl ether); ROA, Raman optical activities; STOCSY, statistical total correlation spectroscopy; SAXS, small angle X-ray scattering; SEIRAS, surface-enhanced IR absorption spectroscopy; SERS, surface enhanced Raman spectroscopy; THz, terahertz; UV, ultraviolet; WAXD, wide angle X-ray diffraction; XANES, X-ray adsorption near edge structure; XAS, X-ray absorption spectroscopy; XPS, X-ray photoelectron spectroscopy; 2D, two-dimensional.

* Tel.: +1 513 858 3362.
E-mail address: noda@udel.edu

http://dx.doi.org/10.1016/j.molstruc.2014.01.016
0022-2860/© 2014 Elsevier B.V. All rights reserved.

1. Introduction

This survey review was compiled as the second part of the seventh in the series of comprehensive reviews [1–6] to mark the occasion of the Seventh International Symposium on Two-Dimensional Correlation Spectroscopy (2DCOS-7) held in Seoul, Korea in August 2013, covering the period between August 6, 2009 and July 31, 2013. This article is a companion piece for another survey review prepared to cover the new concepts or ideas and emerging developments in the field [7]. Current review focuses on noteworthy experimental practices in the field of two-dimensional (2D) correlation spectroscopy, including the topics of various perturbation methods currently used in 2D correlation spectroscopy experiments, types of analytical probes employed, and pertinent examples of fundamental and practical applications.

2D correlation spectroscopy was originally developed as an obscure mathematical tool to sort out information found in a time-resolved IR linear dichroism spectrum observed for a polymer film undergoing a small-amplitude dynamic deformation [8,9]. The basic idea of treating systematic time-dependent variations of spectral intensities induced by an external perturbation to construct 2D correlation spectra was established at this point. The introduction of the concept of so-called generalized 2D correlation analysis [10–12] dramatically expanded the field 2D correlation spectroscopy. Today, the experimental practices of 2D correlation spectroscopy routinely incorporate the use of various forms of perturbation methods, such as thermal, electrical, and chemical perturbations, application of different types of modern analytical probes, such as IR, Raman, NMR, X-ray, and fluorescence, and both fundamental and applied studies of a vast number of chemical, physical and biological systems [13]. The current survey discusses the itemized topics of recent activities in the field.

2. Dynamic or transient perturbations

A sizable portion of the 2D correlation spectroscopy studies employ dynamic or transient perturbation methods, which induce time-dependent spectral intensity variations reflecting the system response to a perturbation applied to the sample system. Fig. 1 shows the distribution among 113 publications related to time-dependent phenomena studied by 2D correlation spectroscopy. Transient physical processes, such as dynamic response of a sample to mechanical or acoustic stimuli, sorption, diffusion, evaporation and other spontaneous processes, crystallization and other physical phenomena are extensively studied representing about 44% of the literature on dynamic systems. Chemical reactions and kinetics studies, such as polymerization and crosslinking, are also often reported. In the recent years, the number of reports has increased in the 2D correlation spectroscopy study of transient biological processes. Effects of the duration of exposure time to various treatments are also explored here.

2.1. Physical process

2.1.1. Repetitive or pulsed perturbations

In early days, because of the advantage of signal-to-noise ratio gain in cumulative repetitive measurements, 2D correlation spectroscopy experiments often utilized a fixed-frequency sinusoidal perturbation, such as small-amplitude dynamic mechanical deformation and acoustic stimuli, to induce similar sinusoidally varying spectral intensity responses suited for the subsequent 2D correlation analysis [8,9]. Interestingly, there has been rather limited number of such sinusoidal perturbation schemes used in 2D correlation spectroscopy today. Li and Zhang [14] carried out dynamic 2D IR photoacoustic spectroscopy (PAS) study of a layered polymer sample by using a step-scan FT IR spectrometer. Modulated PAS signals were generated by the repetitive fixed-frequency irradiation of IR beam to the sample to achieve the depth profiling of layered materials.

In contrast to the use of a simple sinusoidal perturbation, there have been some activities in the application of multiplexed or pulsed stimuli, which contains more than one frequency component of perturbation effect. Nishikawa et al. [15] reported the 2D correlation spectroscopy based on pulsed compression experiment, which was carried out with a step-scan ATR (attenuated total reflectance) FT IR instrument. In their approach, a series of soft pulses comprising a short duration of mechanical compression with a fixed frequency around microsecond time resolution was used. The resulting IR data were analyzed by the double Fourier transformation along the time axis of mechanical perturbation and the mirror position of the interferometer. This development is particularly significant in the field that it represents the possible emergence of pulse-based 2D correlation spectroscopy outside of NMR or nonlinear optical spectroscopy. Similarly, Rivallan et al. [16] reported the 2D pressure-jump adsorbed species IR technique. The Fourier analysis of time evolution of IR spectrum after sudden pressure change was carried out for the platinum-containing zeolite sample, and different CO oxidation activities were successfully detected for different locations.

2.1.2. Sorption, penetration, diffusion and evaporation

There have been a large number of reports related to the 2D correlation spectroscopy studies of time-dependent spontaneous physical processes which were induced by other than repetitive or pulsed perturbations. Spontaneous sorption, penetration and diffusion of small molecules interacting with host matrices were often studied. For example, Haider et al. [17] reported the 2D ATR-IR study of time-resolved adsorption–desorption spectra to detect the band shift effect, and selective poisoning of colloidal Au catalysis with thiols was explored. Chowdhury [18] used 2D surface enhanced Raman spectroscopy (SERS) to investigate the time-dependent adsorption of 2-aminobenzithiazole onto nanocolloidal silver surface. Le Bihan et al. [19] reported the 2D correlation study of liquid chromatography/mass spectrometry (LC/MS) data obtained for peptide fragments from cytoplasmic proteins. They found fragments with even similar mass and hydrophobicity could be differentiated with 2D correlation by taking advantage of slight difference in elution profiles, suggesting the potential of

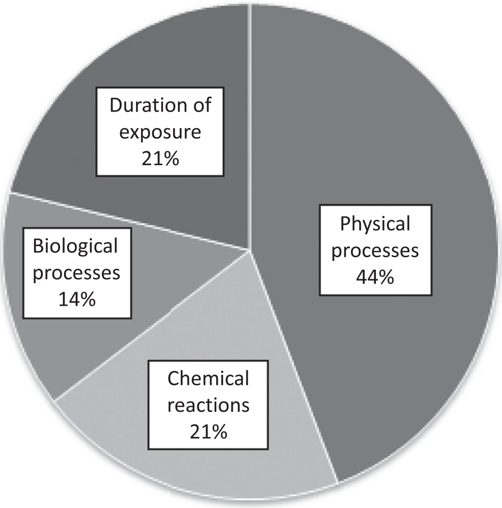

Fig. 1. Time-dependent phenomena studied by 2D correlation spectroscopy.

deciphering various peptide fragments without any prior knowledge of their origin.

Liu et al. [20] used 2D ATR IR to examine the water desorption process from water-soaked cotton fibers. Hwang and Kim [21] used 2D IR to study the plasma enhanced chemical vapor deposition as a function of precursor flow rate, which controls the chemical reaction. Correlation among structural modes and bonding groups were explored in this study. Tang et al. [22] reported 2D localized surface plasmon resonance spectra generated from time-resolved excitation spectroscopy results. Interaction between bovine serum albumin (BSA) and silver or gold nanoparticles was explored. Kawabe et al. [23] discussed the 2D IR correlation study of time-resolved changes of polymer film with environmental effect imposed by using a flow cell. Khesbak et al. [24] reported the 2D IR study of isothermal transition and conformational states of DNA based on transient IR spectra collected after pulsed hydration. Sinelli et al. [25] reported 2D NIR study of osmo-air dehydration process for blueberries by using various sugar solutions, and Kachrimanis and Griesser [26] studied time-dependent dehydration process of a pharmaceutical ingredient carbamazepine dihydridate by 2D IR.

Musto et al. [27] used 2D IR for the investigation of the sorption process of water vapor in polyimide films. Different water molecules, such as self-associated and single monomeric water interacting with C═O groups, were detected. Water sorption and desorption processes with a pharmaceutical amphiphilic copolymer poly(3-(2-methoxyethyl)-*N*-vinyl-2-pyrrolidone) investigated with 2D IR was reported by Lai and Wu [28], and different states of hydrogen-bonded water molecules were detected. Takumi et al. [29] used 2D correlation for external reflection–absorption IR spectra representing the time-dependent adsorption dynamics of hexadecylpyridinium and sodium dodecyl sulfate to air and water interface. Yang et al. [30] reported the 2D ATR IR study of dynamic adsorption of catechol on goethite, which was influenced by pH but not by ionic strength. In another study, Yan et al. [31] examined the effect of dissolved organic matter on the desorption process of enrofloxacin onto montmorillonite under different pH. Katayama et al. [32] used NIR-ATR IR hetero-spectral correlation to characterize the rehydration process of *Domyoji-ko*, which is 100% amylopectin starch obtained from glutinous rice flour and is capable of gelatinization either by heating or rehydration without heating.

Spontaneous evaporation of volatile components provides a source of time-dependent spectra suitable for 2D correlation analysis. Giangiacomo et al. [33] used 2D NIR to study the osmotic dehydration process of apple with hypertonic sugar solution to elucidate the chemical and spatial interactions of water and sugar. Sinelli et al. [34] used 2D diffuse reflectance NIR to study the osmo-air dehydration of blueberries during the drying process. Noda [35,36] discussed the application of 2D IR correlation in the analysis of time-dependent evaporation of mixed solvents which can be decomposed to individual component contributions. Pi et al. [37] used 2D ATR IR for the time-dependent evaporation of ethanol from the mixture with oleic acid or linoleic acid. Sequential order of steps involving the dissociation of carboxylic acid complex, followed by the formation of carboxylic acid dimers, leading to the self-assembly of dimers to form quasi-smectic liquid crystalline structure was determined. Chen et al. [38] used 2D IR to examine the room temperature volatilization of sweet and dry wine samples.

Time-dependent diffusion and penetration processes have been extensively studied by 2D correlation spectroscopy. For example, Wang et al. [39] reported the 2D ATR IR study of the diffusion of water in poly(ether urethane) block copolymer to determine the sequential order of diffusion processes. Li et al. [40] used 2D IR and 2D NIR to probe the water diffusion in epoxy resins. Local chain reorientation and bond dissociation of water molecules were explored, and four types of different water molecules were identified. Wang and Wu [41] reported the 2D IR study of water diffusion in poly(ε-caprolactone). Diffusion of water in low-density polyethylelen (LDPE) film at different temperature was also studied by Wang et al. [42]. Similar behavior consisting of three different types (i.e., free, cluster, and bulk) of water was observed at different temperature.

Hattori and Otsuka [43] used 2D NIR to analyze time-dependent water penetration into and interaction with disaccharide excipient of pharmaceutical tablets. Jin et al. [44,45] reported the 2D ATR-IR study of water diffusion in poly(metaphenylene trimesamide) layer of thin film composite membrane and in polylactic acid–polyethylene glycol block copolymer, and three different states of water molecules were detected. Fu and Lim [46] reported the 2D ATR IR study of the diffusion of multiple flavor components, including 2-octanone, hexyl acetate, octanal, limonene and linalool, in linear low density polyethylene (LLDPE). Sequential order of diffusion processes was determined. Lai et al. [47] used 2D ATR IR for diffusion of plasticizer tri-2-ethylhyxyltrimellitate in poly(vinyl chloride) film at different temperature, and specific interaction between C—Cl and C═O groups was noted.

2.1.3. Crystallization process

Crystallization processes of various compounds are also studied in detail by 2D correlation spectroscopy. For example, time-dependent crystallization process of polybutene-1 which was accelerated with super critical CO_2 was studied with 2D IR by Shi et al. [48] to probe the crystallization mechanism. Zheng et al. [49] used 2D correlation for the time-dependent IR spectra collected during the isothermal crystallization of syndiotactic polystyrene. Similarly, Liu et al. [50] applied 2D correlation to time-dependent IR spectra for the isothermal crystallization process of ice in poly(vinyl methl ether) solution. Smirnova et al. [51] reported the 2D synchrotron SAXS (small angle X-ray scattering) study and SAXS–WAXS (wide angle X-ray diffraction) hetero-correlation study of non-isothermal crystallization of hydrogenated polybutadiene with varying time and temperature. Three different regimes of structure development were identified.

Ando et al. [52] applied 2D correlation for the analysis of time-dependent IR spectra during the isothermal melt crystallization of poly(ʟ-lactic acid) (PLLA) nanocomposite with organically modified layered silicate. Sequence and mechanism of crystallization for nanocomposite was different from the neat PLLA. Chen et al. [53] used 2D IR to provide the detailed band assignments for poly(ethylene terephthalate) (PET) based on temperature dependence during the cooling from melt and time-dependence during the isothermal crystallization. Such spectra are very complex due to the effects of crystallinity and orientation. Guo et al. [54] reported the 2D WAXD and 2D SAXS, as well as WAXD–SAXS hetero-correlation study, of time-dependent isothermal crystallization of poly(hydroxybutyrate) (PHB). Multiple step processes of crystallization were suggested.

Hoshina et al. [55–57] reported the use of 2D terahertz (THz) spectroscopy in the analysis of temporal spectral evolution of PHB during the isothermal crystallization process. Two-step process involving the initial C—H···O═C hydrogen bond formation followed by the development of well-defined crystal structure was noted. Zhou and Xin [58] used 2D correlation for the time-resolved IR spectra observed during the isothermal crystallization of isotactic polypropylene (PP) containing various benzilidene acetal nucleating agents. With the nucleator, changes in methyl occurs before that for methane and C—C skeleton of PP, which is opposite of the neat PP. Xu et al. [59] studied the isothermal crystallization kinetics of isotactic PP containing grapheme oxide nanosheet, acting as a nucleation aid, with 2D IR. It was found that conformational ordering occurs as a vanguard prior to the crystallization at the growth boundary. Wang et al. [60] reported the 2D IR study of the gradual cooling crystallization process of α-*trans*-1,4-polyisoprene. Presence of an intermediate state was detected prior to 2_1 helix formation.

2.1.4. Other transient physical phenomena

Many other transient physical processes are analyzed by 2D correlation spectroscopy. Piccinini et al. [61] used 2D NIR FT Raman spectroscopy to analyze the starch retrogression process observed during the aging of Semolina bread crumb. De la Arada et al. [62] used 2D IR to probe the aggregation process of amyloid fibril formation for bovine and human serum albumin. Tang et al. [63] applied 2D correlation analysis to time-resolved light scattering during the phase separation of epoxy-amine-polyethersulphone blend. Sequential order of domain size coarsening processes in both diffusion regime and hydrodynamic regime were determined.

Park and Kim [64] reported an interesting application of 2D SERS. Strong synchronous correlation, indicative of spectral wondering observed in time-dependent charge-transfer-enhanced single molecule SERS of 4-aminobenzenethiol, was reported. Kim et al. [65] used 2D diffuse reflectance IR spectroscopy (DRIFTS) to study the thermal annealing mechanism and micro-structural changes of tin-doped indium oxide nanoparticles. Luo et al. [66] reported the use of 2D NIR for the on-line detection of time-dependent variations of sugar content of jujube. Park et al. [67] used 2D ATR IR to study the gelation process of poly(*N*-isopropylacrylamide) (PNIPAM) hydrogel above and below the lower critical solution temperature (LCST). Zhang et al. carried out a systematic study of 2D NIR of glucose solution aimed at the detection of chance correlation, such as instrument time drift, sample temperature variations, and interferent compositions.

2.2. Chemical reactions

2.2.1. Polymerization and crosslinking

2D correlation spectroscopy has been extensively utilized in the analysis of time-dependent spectral data obtained during various chemical reactions, including polymerization and curing or crosslinking reactions. For example, Ryu et al. [69] reported 2D IR and IR-NMR hetero-spectral correlation study of a free radical polymerization process of poly(vinylpyrrolidone) with $AgNO_3$ chain transfer agent. Su et al. [70] used 2D IR for the real-time monitoring of the polymerization reaction of partially crosslinked polyacrylamide. Huang and Kuo [71] used 2D IR to study the curing kinetics and mechanisms of polybenzoxazine and polyhedral oligomeric silsesquxanes nanocomposite. Spegazzini et al. [72,73] reported the 2D IR study of the cross linking reaction of epoxy resin diglycidyl ether of bisphenol A with rare earth triflate initiators, and presence of two reaction mechanisms was confirmed.

Curing process of epoxy resin was also studied by Yu et al. [74], who reported the 2D IR study of parallel reactions of cationic polymerization and esterification progressing together during the curing process of epoxy resin with a polyoxometalate catalyst along the reaction time. Yamasaki and Morita [75] used 2D IR, 2D NIR, and IR-NIR hetero-spectral correlation to elucidate the reaction mechanisms and kinetics of isothermal curing process of bisphenol A epoxy resin with polyamine reagent by distinguishing dynamics of the primary and secondary amine. Chae et al. [76] used 2D IR to study thermal cure kinetics and structural changes of phenylethyl end-capped imide compound.

2.2.2. Other chemical reactions

Many other chemical reactions were also studied. Lednev and Shashilov [77] reported the 2D deep UV resonance Raman study of the H/D exchange reaction of *in vivo* protein structural evolution of amyloid fibril, especially at the early stage of fibrillation. Tang et al. [78] reported the UV–visible extinction spectroscopy study of halide ion etching reaction of silver nanoprism to nanodisks. The transformation of nano particle shape was probed by the intensity time-evolution of surface plasmon resonance peaks, which are characteristic to shape and size of noble metal nanoparticles. Complete synchronization of the disappearance of nanoprisms and appearance of nanodisks indicated the pseudo-first-order reaction. Del Rio et al. [79] used 2D NIR to demonstrate the competing amidation of oxirane ring opening and amide formation reactions in epoxidized methyl oleate and aniline system to simulate curing of epoxy resin.

Fernandez et al. [80] reported the 2D IR study of zeolite catalysis of isomerization of *o*-xylene. Sun and Wu [81] generated 2D ATR-IR spectra from real-time monitoring of Cu(I)-catalyzed azide–alkyne “click” cycloaddition reaction to provide mechanistic understanding of the consumption of alkyne and azide followed by the formation of 1,2,3-triazide product. Mezzetti et al. [82] carried out 2D IR study based on the time-resolved difference spectra obtained during the photo-induced ubiquinol formation in the reaction centers isolated from *Rhodobacter sphaeroides*. Quaroni et al. [83] reported the 2D synchrotron FT IR study of living retinal rod cells by using time-resolved spectra collected after photo-stimulation. Rodrigues et al. [84] reported the 2D NMR correlation study of beer under forced aging reaction, and inter-compound dependences of degradation products were detected. Sun et al. [85] used 2D fluorescence correlation to examine the oxidation reaction of tyrosine. Yan et al. [86] applied 2D correlation to time-resolved surface-enhanced IR absorption spectroscopy (SEIRAS) during the electrochemical reaction of water at CO predosed Pt electrode interface under strong hydrogen evolution.

Zrelli et al. [87] reported an intriguing temperature modulation technique, which can be potentially applicable to dynamic 2D correlation analysis. Selective titration of biological mixture samples undergoing two-state exchange reaction was described, indicating the out-of-phase concentration oscillation. Andraka et al. [88] reported the 2D IR study of metabolic changes of normal and cancerous keratinocyte cells with time after irradiation with different dosage. Cheon et al. [89] used 2D IR combined with chemometrics to study chemical reaction dynamics of sterically hindered alkanolamine and CO_2. Choi et al. [90] used 2D IR for time-dependent conversion of carbanion to bicarbonaion in the aqueous reaction of CO_2 and NH_3. Doan et al. [91] reported the application of 2D correlation in ultrafast spectroscopy. Time-resolved spectra of photo-induced decarbonylation reaction of nanocrystalline diphenylcyclopropenone were analyzed.

Musto et al. [92] reported the use of 2D ATR IR spectroscopy in the study of photo-oxidative degradation reaction dynamics of epoxy resin stabilized with polyhedral oligomeric silsesquioxane nano filler, as an organic–inorganic hybrid composite. Qu et al. [93] applied 2D IR to a hydrolytic condensation reaction process of polyhedral oligomeric silsequioxanes, and synthesis of linear, cyclic and then cage-like siloxanes were observed. Spegazzini et al. [94] reported the use of 2D NIR to study the chemical reaction process of phenol with phenylisocyanate to produce diphenylurethane isomers. Xiang et al. [95] used 2D IR to study a thermo oxidative degradation process of styrene–butadiene rubber. Popescu and Simionescu [96] reported the 2D IR study of environmental weathering process for acrylic copolymer film and acrylic coated lime wood (*Tillia cordata* Mill).

2.3. Biological processes and related topics

Applications of 2D correlation spectroscopy in the time-dependent processes associated with biology, life science and medical field have expanded considerably. A number of publications appeared on the use of NMR spectroscopy coupled with statistical treatment on time-dependent metabolic systems. Guyett et al. [97] used statistical total correlation 2D NMR or STOCSY to detect signals originating from the same compound during the enzymatic conversion of UDP-α-D-glucuroic acid. Kirwan et al. [98] reported the 2D correlation NMR applied to metabonomics time study of human blood plasma obtained from subjects recovering from exhaustive exercise with ingestion of controlled diet. Robinette et al. [99] used 2D correlation NMR combined with cluster analysis to analyze the time-dependent variation of rat urine during the L-arginine induced pancreatitis development. Sonker et al. [100] also used STOCSY for transient metabolic flux of phage infection. Xu et al. [101] reported the statistical hetero-sample correlation between urine and serum ^{1}H NMR spectra from metabolomic data sets.

The use of 2D correlation in biological processes is not limited to NMR studies. Yao et al. [102] reported a form of 2D correlation spectroscopy based on UV–visible reflectance spectro-radiometry. Winter wheat leaf nitrogen accumulation per soil area (LNA) was correlated over time against ratio spectral index (RSI), which is a ratio between reflectance measured at two different wavelengths. Statistical coefficient of determination obtained by the regression analysis was plotted as a 2D map to detect the most reliable RSI indicator for LNA. Liu et al. [103,104] used 2D ATR IR for cotton fibers with different maturity stages, determined by the days after flowering. Saskura et al. [105] applied 2D IR for time-dependent secondary structure changes of Ca^{2+}-binding protein calmodulin with its antagonist. Sikirzhytski et al. [106] used 2D deep UV resonance Raman to determine the sequence of the fibrillation process of genetically engineered model polypeptide. Saguer et al. [107] applied 2D IR to the study of porcine blood plasma proteins, and kinetics of thermally induced aggregation process at different pH was determined.

Yu et al. [108] used 2D IR, 2D NMR and IR-NMR hetero-spectral correlation to study the extracellular polymeric substances in biofilms developed during composting as a function of time. Wang et al. [109] used 2D IR to study biopolymer degradation during the composting process of rapeseed meal and what bran. Degradation sequence influenced by the distribution pattern was identified as cellulose first, then heteropolysaccharides, followed by proteins. Kirwan et al. [110] reported 2D correlation ^{31}P NMR study of growth process of a plant pathogen *Phytophthora palmivora* with and without phophonate. Nishi et al. [111] reported 2D NIR-IR hetero-correlation for monitoring the ethanol content during fermentation process with a newly developed dual region spectrometer. Ricci et al. [112] reported the ^{13}C NMR STOCSY applied to the time course study of yeast *Saccharomyces cerevisiae* fermentation with different ethanol concentration.

2.4. Duration of exposure to stimuli

While dynamic perturbations may induce time-dependent spectral responses of samples, static perturbations should result in more or less steady or stationary spectral responses not varying but remain constant with time when spectra are collected. This distinction becomes somewhat ambiguous if the perturbation variable turned out to be a period of time during which the sample is being exposed to some sort of stimulus. One must expect that the constituents of the sample system must be dynamically evolving during the exposure time. However, once the exposure is terminated, and the spectral measurement is carried out after the exposure, the system might have already ceased to change as a function of time. In any case, 2D correlation spectra can still be readily constructed and analyzed by using the exposure time, not the time during the spectral measurement, as the perturbation variable.

There are a number of 2D correlation spectroscopy studies that utilize the sample treatment time as a perturbation variable. For example, Caerdà-Costa et al. [113] reported the 2D IR study of temperature-induced conformational reorganization and aggregation of activation domain of human procarboxypeptide as a function of incubation time at 90 °C. Mecozzi et al. [114] used 2D IR and UV–visible-IR hetero-correlation to study the aggregate formation process of marine mucilage as a function of incubation period. Popescu et al. [115–118] reported the 2D IR study of lime wood exposed for different time period to various factors, including soft-rot fungus to induce decay. Detailed steps of enzymatic oxidation and hydrolysis of cellulose and hemicellulose were elucidated. Gasper et al. [119] reported the 2D IR study of human prostate cancer cells in the presence of two different cardenolides with different incubation time after the exposure. Palszkiewicz et al. [120] applied 2D IR to nucleation and growth of apatite on a nanocomposite comprising chitosan and montmorillonite, which was exposed to simulated body fluid for different incubation period up to 18 days.

Irradiation of samples with an electromagnetic wave, such as UV light, is a very common dosage-dependent perturbation method used in 2D correlation spectroscopy. For example, Kim et al. [121] and Lee et al. [122] studied UV-irradiation-induced molecular reorientation of photosensitive polyimide with cinnamate side group and *trans–cis* isomerization of photo-sensitive polymer poly(4-methacryloyloxazobenzene) under different UV doses with 2D IR. Hur et al. [123] reported the 2D fluorescence study of leaf litter humic substance and Suwannee River fulric acid under different UV irradiation time. Lee et al. [124] reported the 2D IR study of photodegradation of PET film with varying UV-irradiation time to identify the degradation products. Zhong et al. [125] used 2D IR to examine photochromic behavior of polyoxometalate in cured epoxy resin after UV irradiation to determine the sequence of electron movements.

Wang et al. [126,127] reported the 2D IR study of the photo-induced orientation of epoxy-based polymers with azo chromophores under different irradiation time of polarized laser. Mäkie et al. [128] reported the 2D DRIFTS study of solar-light-mediated degradation reaction of organophosphane compounds on hematite or goethite nanoparticles with different irradiation time. Cozzolino et al. [129] used 2D NIR reflectance for red grape homogenate exposed to different microwave heating time. Gomaa et al. [130] used 2D IR to probe the effect of microwave exposure treatment and temperature on the H/D exchange of β-lactoglobulin in D_2O. Sui et al. [131] used 2D derivative thermogravimetry to study the decomposition reaction of polyester–urethane adhesive with different doses of γ-ray irradiation.

Duration of exposure to physical phenomenon as a perturbation is not limited to electromagnetic irradiation. Shinzawa et al. [132] reported the 2D correlation study of time-dependent NIR spectra during the spontaneous evaporation of moisture from cellulose excipient for pharmaceutical tablets to probe the effect of the duration of preparatory grinding operation, which lowers the crystallinity, and consequently the distribution of the absorbed, bound and free water content. Kamerzell et al. [133] applied 2D correlation to size exclusion chromatography to probe the stability and relative sequence of the hinge region fragmentation of immunoglobulin gamma under different storage time and elution time.

Duration of chemical exposure time is also used in 2D correlation spectroscopy applications. Andary et al. [134] used 2D correlation chromatography to study valorization of olive stones by dilute acid hydrolysis followed by varying the duration of over-liming process to increase sugar content. Pietroletti et al. [135] reported the 2D IR study of pollutant removal by marine alga *Caulerpa racemosa* exposed to various hydrocarbons. Mäkie et al. [136] reported the 2D DRIFTS study of the adsorption of trimethyl phosphate onto nanoparticles of hematite, maghemite, or goethite with varying dosing time of organophosphate.

3. Static perturbations

Perturbation of samples with some form of a static effect represents the dominant form of 2D correlation spectroscopy experiments today. The number of published papers is about three times greater than the case for dynamic perturbations. Fig. 2 shows the distributions among 298 publications found using static perturbations for 2D correlation spectroscopy. Temperature effects are the most popular form of static perturbation methods, representing about 54% of published literature in this category. Spectral variations arising from changes in concentrations are also actively studied in 2D correlation, showing about 28% of publications. Electromagnetic effects and other forms of static perturbations are also used in a number of publications.

3.1. Temperature

By far the most popular perturbation method used in 2D correlations spectroscopy is the effect of temperature variation. There are numerous reports on the analyses of spectral data obtained under increasing or decreasing temperature to induce reversible or irreversible changes of the samples. Examples of temperature effects studied by 2D correlation spectroscopy include conformational changes of proteins, aggregation of colloidal systems, various hydrogen bonding interactions, structural changes of metal–organic complexes, melting and crystallization processes, phase transition phenomena, and the like.

3.1.1. Conformational changes of proteins

2D correlation spectroscopy study of thermally induced conformational changes of the secondary structures of various proteins is a very active area of research. For example, Das et al. [137] reported the 2D SERS study of the temperature-induced conformational changes of proteins, e.g., bovine serum albumin, lysozyme, ribonuclease A, and myoglobin, with nano-structured SERS substrates. De la Arada et al. [138] used 2D IR to study the temperature-induced conformational transition of peptide. Fabian et al. [139] carried out the 2D IR analysis to determine the sequential order of the thermal unfolding of Cro repressor of the λ phage and its variants. Popescu et al. [140] used 2D IR to probe the mechanism of temperature-induced secondary protein structure changes of soluble elastin.

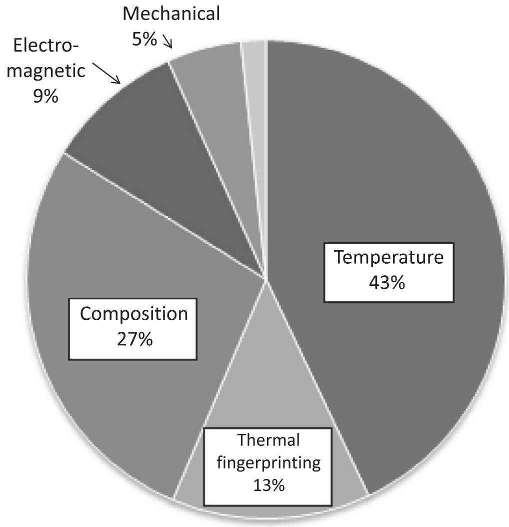

Fig. 2. Static perturbation effects used in 2D correlation spectroscopy.

Wang et al. [141] used 2D IR for the temperature-induced unfolding of conformational structures of glucose oxidase protein. Zhang et al. [142] reported the use of concatenated 2D IR correlation analysis to detect the heating and cooling hysteresis observed for the thermally induced unfolding of bovine pancreatic ribonuclease A. Gao et al. [143] used 2D IR for thermally induced conformational changes of apoptosis inhibitor protein. Li and Li [144] reported the 2D fluorescence study of temperature-induced denaturation process of collagen dissolved in glycerol or 2-propanol and found that the former promote dissociation while latter aggregation. Sovová et al. [145] used 2D IR, 2D Raman, and IR-Raman hetero-spectral correlation to study the thermal dynamics of natural killer cell receptor proteins.

Ausilli et al. [146] reported the 2D IR study of three-step thermal unfolding of zinc-dependent alcohol dehydrogenase obtained from hyper thermophilic archeon microorganism. Chen et al. [147] used 2D IR for the thermal denaturation study of uncrosslinked and crosslinked collagen. Guo et al. [148] also used 2D IR for the study of temperature-induced denaturation of aqueous collagen solution. Pastrana-Rios and Lloro-Manzano [149] were granted a United States patent on the method for determining the aggregation, stability and viability of proteins, peptides and peptoids based on 2D IR study of thermally induced unfolding. Tian et al. [150] used 2D IR for the thermally induced conformational transition of soy protein and noted that some changes are reversible. Scirè et al. [151] used 2D IR for the temperature effect on rat odorant-binding protein, and intermediate state was detected before aggregation and denaturation. Sosa et al. [152] reported the 2D IR study of thermally induced structural changes of complex between calcium binding protein centrin and model peptide melittin.

3.1.2. Association, self-assembly and gelation

Association, self-assembly and gelation are also very popular topics in temperature-based 2D correlation spectroscopy. For example, Sun et al. [153] used 2D NIR to probe the temperature-induced transformation of aggregate species of pyrrole from polymer to dimer to monomer form. Transformation of dimers from T-shaped geometry to anti-parallel geometry was indicated. Tang et al. [154] studied the temperature effect on the self-association of 2-pyrrolidone in the pure liquid with 2D NIR. Park et al. [155] used 2D DRIFTS to study the temperature effect on self-assembled thin films of sensitizing dye for solar cells on nanocrystalline TiO_2 surfaces. Shi et al. [156] used 2D IR to determine the sequential responses of components to thermal perturbation of polystyrene and ionic liquid composite membrane, and local aggregate domain distribution within polymeric network was elucidated. Shinzawa et al. [157] investigated the self-assembly of oleic acid with 2D ATR IR under the multiple-perturbation consisting of pressure and temperature.

Jia et al. [158] used 2D IR to examine the step-by-step molecular level mechanism of the temperature-induced micellization process of an aqueous solution of a block copolymer, involving conformational transition, dehydration, hydrogen bond breaking, and hydrophobic association. Sun and Wu [159] studied the gelation microdynamics of *N*-octyl-D-gluconamide upon cooling by 2D NIR. Sequential order analysis revealed the continuous dehydration process from the octyl tail to the chiral carbohydrate head group. Wang and Wu [160] studied the temperature induced gelation microdynamics of poly(*N*-isopropylacrylamide) (PNIPAM) in ionic liquid by 2D IR. Saguer et al. [161] reported the 2D IR study of the heat-induced gelation of whole porcine blood plasma and serum proteins.

3.1.3. Hydrogen bonding

Hydrogen bonding plays an important role in the molecular interactions of various chemical and biological systems. The temperature sensitivity of hydrogen bonding is one of the very active areas of research in 2D correlation spectroscopy. For example, Li et al. [162] studied the temperature-induced changes in the hydrogen bonding of sodium salt of carboxymethyl cellulose by 2D IR. Czarnecki et al. [163] reported the 2D NIR study, assisted with density functional theory calculation, of hydrogen bonding interaction in cyclohexanol and water mixtures under different temperature. Haufa and Czarnecki [164] reported the 2D NIR study of aminoalcohols in the pure liquid state, as well as in CCl_4 and water with varying temperature. Both inter- and intra-molecular hydrogen bonds were detected in their study.

Liu et al. [165] studied the temperature effect on methanol and ethanol to probe the evolution of different hydrogen bonding association structures by 2D NIR. Liu et al. [166] reported the 2D IR study of the temperature-dependent interaction between 4-aminopyridine and methacrylic acid. Sun and Wu [167] used 2D NIR to study the thermally induced evolution of mixtures of an ionic liquid, 1-butyl-3-methylimidazolium tetrafluoroborate, with water to probe the detailed mechanisms of various hydrogen-bonding interactions. Szyc et al. [168] reported the 2D IR study of the temperature-dependent complexation chemistry of 2-pyridone, which isomerizes to 2-hydroxypyridine, in CD_2Cl_2. Cyclic dimer, solute–solvent complex, and chain-like dimer were detected. Balevicius et al. [169] carried out the 2D IR study of matrix-isolated propanol clusters under thermal perturbation to probe hydrogen-bonded aggregates. Radice et al. [170] used 2D IR for the temperature study of hydrogen bonding in fluorinated amide.

The position of the peak maximum of IR absorption associated with hydrogen bonding is known to shift with temperature. 2D correlation spectroscopy is a good tool to determine the origin of this apparent peak position shift. Ryu et al. [171] examined with 2D IR such peak position shift phenomena. Moving window principal component analysis (PCA) along the wavenumber axis turned out to be a useful tool because true band frequency shift cannot be modeled by a linear combination of only a few factors. It was concluded that the apparent shift of a hydrogen-bonding absorption peak usually originates from the overlapped contributions of different species which changes their population distributions with temperature.

Further 2D IR work combined with various forms of waterfall plots was carried out by Ryu et al. [172] to probe the peak position shift phenomenon. Simulated spectra, temperature dependent IR spectra of ethylene glycol, and concentration dependent spectra of acetone in $CHCl_3$ and CCl_4 mixture were studied. 2D correlation spectra can clearly distinguish the true shift of band frequency vs. effect of relative intensity changes of overlapped bands, while waterfall plots often fails to give unambiguous distinction. Czarnecki [173] also examined the temperature-induced peak position shift of hydrogen-bonded systems, like cyclohexanol, by 2D NIR. It was concluded that in most cases, changes in intensities of adjacent bands instead of frequency shift of a single band is a more plausible cause to explain the peak shift. Czarnecki [174] also reported the 2D NIR study of the temperature dependence of the hydrogen bonding of diamine–water mixture. Li et al. [175] studied the temperature dependence of hydrogen bonding of thermoplastic segmented polyurethane.

Noncovalent interactions, such as π–π interaction and hydrogen bonding, play an important role in structural development and stability of a number of metal and organic ligand complex systems. While the former may be probed by magnetic perturbation, the latter is most effectively studied by thermal perturbation. For example, Chai et al. [176] used thermal and magnetic perturbations of hydrothermally synthesized compound made from bismuth and a flexible ligand *N,N′*-diacetic acid imidazolium chloride. Chen et al. [177] reported the 2D IR and 2D UV study of hydrothermally synthesized rare earth 3-bi-pyridine polymer under thermal and magnetic perturbation. Lei et al. [178] used 2D IR to study samples of hydrothermally synthesized divalent transition metal carboxyarylphosphonates with different structures under thermal and magnetic perturbation. Dramatically different 2D IR spectra obtained by their study indicate different sensitivities of groups to different stimuli.

2D IR study of crystals of carboxylate metal coordination compounds hydrothermally synthesized with 3-methylbenzoic acid was reported by Chen et al. [179]. Li et al. [180,181] also reported 2D IR study of porous organic–inorganic hybrid compound of polyoxovanadium borate under magnetic and thermal perturbations. By using 2D IR, Chen et al. [182] examined temperature-induced changes of clusters of polyoxometalates, which were hydrothermally synthesized with different carboxylic ligands and photocatalytic activities, having different stability. Hu et al. [183] reported the 2D IR study of organically templated aluminoborate with quasi-aromaticity, showing the thermal sensitivity of hydrogen bonding and magnetic sensitivity of π bonds. Mei et al. [184] studied hydrothermally synthesized lanthanide 2-hydroxynicotinic acid coordination polymer by 2D IR under thermal and magnetic perturbations. Sun et al. [185] reported the 2D IR study of polyoxovanadium borate organic–inorganic hybrid, based on the structural changes under magnetic and thermal perturbations.

The application of 2D IR spectroscopy in the study of organic–inorganic complex with combined thermal and magnetic perturbations has been fully established as a technique of choice indicated by a steady stream of publications. Chen et al. [186] used 2D IR for characterizing hydrothermally synthesized Keggin-type heteropolytungustates with thermal and magnetic perturbations. Chen et al. [187] also reported the 2D IR study of temperature and magnetic intensity effects on hydrothermally synthesized nitrogen-heterocyclic β-octamolybdate supported metal–organic compounds. Ge et al. [188] reported the 2D IR study of newly synthesized cadmium thiolato-carboxylate coordination complexes. Temperature-induced structural changes, reflecting the effect on hydrogen bonding and π–π stacking interaction between aromatic rings, were noted. Wu et al. [189] used 2D IR to study the temperature effect on weak interactions, like C—H···O hydrogen ponding, π–π stacking, and C—H···π interaction, within manganese complex with 4,4′-bipyridine and methyl benzoate ligands. Zhao et al. [190] used 2D IR to probe the temperature- and magnetism-induced structural changes of hydrothermally synthesized rare earth compounds with 3-methylbenzoic acid.

3.1.4. Melting, crystallization and glass transition

Melting and crystallization of various chemical compounds, including polymeric materials, is one of the very active areas of temperature-variation-based 2D correlation spectroscopy studies. Unger et al. [191–193] reported the 2D IR study of annealed and non-annealed poly(3-hydroxybutyrate) (PHB) and blend of PHB and polycaprolactone (PCL) with varying temperature. Recrystallization and melting phenomena were observed, and two crystalline forms, i.e., well-ordered and less ordered, were detected. Furthermore, two apparently different amorphous contributions were found, suggesting the possible existence of amorphous component with some structure. They also reported the 2D IR study of the detailed crystallization behavior of polymers under variable temperature. Unger et al. [194] further extended their temperature-dependent 2D IR study beyond the analysis of polymers. They reported the temperature effect on oleic acid to elucidate the recrystallization of γ-phase and melting.

Many other researchers used 2D correlation spectroscopy to examine the melting and crystallization processes. Zhou et al.

[195] reported the 2D IR study of the melting of poly(ethylene oxide) (PEO), and intermediate state, probably associated with the disordered helical conformation formed first at the front of lamellae, was detected. Popescu and Vasile [196] used 2D IR to study the temperature induced melting and partial miscibility of poly(tetrahydrofuran) and cholesteryl palmitate. Watanabe et al. [197] reported the 2D correlation analysis of light microscopy retardance mapping histograms, representing the spatial distribution of higher order supramolecular structures, of various polyethylene samples during heating. Hoshina et al. [197] used 2D THz absorption spectroscopy for the study of PHB and poly(3-hydroxybutyrate-*co*-3-hydroxyhexanoate) (PHBHx) with varying temperature to obtain assignments for peaks characteristics to the crystalline and amorphous components. Li et al. [199] reported the 2D correlation study of the temperature-dependent IR spectra for non-isothermal crystallization and melting of polyoxymethylene, which has the hybrid complex structure of folded and extended chain crystals and also have low molecular weight cyclic polymers.

Chen et al. [53] applied 2D correlation to temperature dependent IR spectra obtained during the cooling of melt to give detailed band assignments for spectra of poly(ethylene terephthalate) (PET) complicated by the effects of crystallinity and orientation. Chen et al. [200] used 2D IR to examine the crystallization steps of polyoxymethylene and PEO blend during the cooling. Guo et al. [201] used 2D IR to probe the microstructure and phase transition of regioregular poly(3-dodecylthiophene) by temperature dependence. Kim et al. [202] reported the 2D IRRAS study of the spin-coated thin film of a blend of PHBHx with varying temperature. Null-space projection was used to filter out dominant crystalline contribution of PHBHx. Shinzawa et al. [203] used 2D Raman with wide area illumination scheme to examine the heating of high-density polyethylene (HDPE) and octene-1 LLDPE. Hetero-sample correlation was used to compare and identify different behavior of polyethylenes. It was found that the premelting was not prominent in HDPE. Choi et al. [204] studied spin-coated thin films PHBHx with different 3HHx content under increasing temperature. Kim et al. [205] reported the 2D IRRAS study of thermal behavior of spin-coated thin films of blends of PHBHx and polyethylene glycol (PEG) with varying composition.

In addition to the melting and crystallization studies of polymers, glass transition phenomena are also examined with 2D correlation methods. For example, Zimmermann and Vrsaljko [206] used the 2D ATR IR technique based on the moving-window and sample-sample correlation in the thermal analysis of polystyrene to identify glass transition. Wang et al. [207] applied the 2D correlation analysis to dynamic mechanical spectroscopy data, and resolution of temperature-dependent loss tangent peak under different deformation frequency for the glass-to-rubber transition of polyisobutylene was reported. Three modes of molecular motions, described by Rouse model, sub-Rouse model, and local segmental motions, were identified.

3.1.5. Other phase transitions

Various phase transition phenomena aside from simple melting and crystallization processes also provide very rich area of study for 2D correlation spectroscopy. Zimmermann and Baranović [208] reported an interesting use of 2D low-resolution FT IR spectroscopy based on the temperature-induced baseline variation for the detection of phase transition of polymorphic or mesomorphic compounds. Kurz et al. [209] used the sum-frequency 2D IR to study a thermo-responsive poly(*N*-isopropylacrylamide) (PNIPAM) thin film near the LCST. Lai and Wu [210] reported the 2D IR study of the LCST-type phase transition of aqueous solutions of PNIPAM and *N*-isopropylpropionamide with varying temperature. Similar mechanism consisting of three-step microscopic dehydration process was observed for both systems. Sun et al. [211] used 2D IR to study the thermally induced volume phase transition of PNIPAM hydrogel with D_2O for both heating and cooling process. Sun and Wu [212] used 2D IR to study the temperature effect around LCST of concentrated solution of PNIPAM in water or water methanol mixture. Inhibition of hydration process before hydrogen bonding association was found.

Szwed et al. [213] used the moving-window 2D analysis for temperature-dependent ATR IR spectra to probe the effect of incorporating fluphenazine into a model bilayer membrane of dipalmitoylphosphatidylcholin. Wu et al. [214] reported the 2D IR study of the temperature induced phase transition between lamellar and micellar phase of amphiphilic lysophospholipid 1-stearoyllysophosphatidylcholin to probe the cooperativity of phase transition phenomenon. Nonsynchronous behaviors of lipid head groups, disordering rearrangement of acyl tails, and hydrating process in the inter-chain region were observed. Zhang et al. [215] reported the concatenated 2D IR correlation analysis applied to the temperature-induced hydration and dehydration of poly(*N*-isopropylmethacrylamide) aqueous solution during the heating and cooling indicates a degree of path-dependent irreversibility of coil-globule transitions.

In the systematic error analysis of 2D spectra, Zhang et al. [216] used temperature effect on the mixture of ionic liquid and water as one of the illustrative examples. Zhou et al. [217] used 2D IR to study the temperature-dependent transitions of triblock copolymer, including order-order transition, order–disorder transition, and lattice disordering transition, driven by different parts of blocks. Chen et al. [218] used 2D IR to study the temperature-induced spectral changes of mesogen-jacketed liquid crystalline polymers with amide core and flexible tails of varying lengths. Luo et al. [219] reported the 2D IR study of the temperature dependence of polyamide around the Brill transition, and changes in hydrogen bonding interactions were detected. Sun et al. [220] used 2D IR to study the thermally induced volume phase transition of hydrogel made of poly(*N*-isopropylacrylamide-*co*-acrylic acid) and D_2O during heating and cooling. Sun et al. [221] also used 2D IR to probe the detailed micro dynamics mechanism of temperature-induced phase transition and hydrogen bonding of aqueous solution of poly(vinyl methyl ether) (PVME).

Sun and Wu [222] reported the 2D IR study of the temperature dependent dynamic dehydration of poly(*N*-vinylcaprolqactam) near the LCST. Sloop et al. [223] used 2D Raman to analyze the temperature-induced phase transition and keto–enol and enol–enol tautomerization of fluorinated aryl β-diketones. Wang et al. [224] used 2D IR to elucidate the molecular mechanism of thermally induced phase transition of hyperbranched poly(ethyleneimine) with isobutyramide groups in D_2O. Morita and Kitagawa [225] used the temperature effect of poly(2-methacryloyloxyetyl phophorylcholine) to illustrate the baseline drift effect on perturbation correlation moving-window 2D analysis. Popescu and Simionescu [226] reported the 2D IR study of the phase transition of allyl-terminated carbosilane dendrimer, involving the reorganization of core structure and conformational rearrangement of terminal units, with varying temperature.

Sun et al. [227] used 2D IR to examine the behavior of PNIPAM-based hydrophilic block copolymer with different arms in D_2O during heating. Wang et al. [228] used 2D IR for the study of the thermal phase behavior and microdynamics of PNIPAM-*b*-poly(1-butyl-3-vinylimidazolium bromide) aqueous solution, forming core–shell micellar structure. Wang and Wu [229] reported the 2D IR study of the effect of ionic liquid on PNIPAM under temperature variation. Wu et al. [230] used the 2D concatenated 2D IR correlation analysis for the quantitative measure of reversibility for individual molecular moieties during the temperature-induced folding and unfolding of ribonuclease A and temperature and pressure-induced globule to coil transition. Zhang et al. [231] also used the concatenated 2D IR correlation to probe reversibility of the coil–globule transition of aqueous solutions of PNIPAM and poly(*N*-isopropylmethacrylamide) with heating and cooling cycle undergoing thermally induced hydration and conformational changes.

Jin and Wu [232] used 2D IR and 2D NIR for the study of temperature-induced coil-to-globule and sol–gel phase transitions of hydroxypropylcellulose aqueous solution. Sun et al. [233] used 2D IR to study the LCST-type phase transition behavior of thermo-responsive dendritic polymer with hydrogen bonding in D_2O during the heating and cooling process. Sun and Wu [234] reported the 2D IR study of the thermally reversible hydration of thermo-responsive copolymer in D_2O. Sun et al. [235] used 2D IR to probe the thermo-sensitivity and self-assembly of PNIPAM block copolymer. Lai et al. [236] also used 2D IR to study the dehydration process around the LCST of poly(3-ethyl-*N*-vinyl-2-pyrrolidone) in water during the heating and cooling cycle. Different species of carbonyl groups hydrogen bonded with D_2O were detected.

3.1.6. Structural changes

The effects of temperature in many other systems were also reported. For example, Marcelli et al. [237] used 2D X-ray adsorption near edge structure (XANES) and 2D IR to probe the subtle spectral changes of metal endohedral fullerenes induced by temperature. Li and Wu [238] used 2D IR to examine the temperature-induced helical to planar zigzag conformational change of syndiotactic polystyrene. Morita and Kitagawa [239] used 2D IR to study the temperature-induced three-step structural changes (i.e., dehydration, protonation of side chain terminal sulfonate, and thermal degradation) of Nafion ionomer. Murawska et al. [240] reported the 2D ATR IR study of the structural change during the heating of two-component liposome. Tang et al. [241] reported the 2D Raman study of the conformational change of thermotropic liquid crystalline polymer poly[di(alkyl) vinylterephthalate] upon heating. Formation of mesophase by specific interaction among phenyl rings was observed.

Zhou et al. [242] used the moving window 2D correlation analysis for the variable temperature Raman study of melt intercalated PEO and clay hybrid nanocomposite. Distorted helical conformation in clay galleries due to crown-ether like association between cation and PEO oxygen was suggested. Chys et al. [243] reported the 2D IR study of thermal responses of alkali-pretreated gelatin fractions to probe the sequences of conformational changes. Morita et al. [244] discussed the use of 2D IR to study the temperature dependence of polyvinyl alcohol. Rettler et al. [245] used 2D IR to study the temperature effect on interaction with water and melting of poly(2-*N*-alkyl-2-oxazoline)s with different side chain lengths. Sun et al. [246] used 2D IR to study the temperature effect on thermotropic liquid crystalline polymer poly[di(butyl)vinylterephthalate], and splitting of carbonyl band corresponding to different conformations was noted.

Wang et al. [247] analyzed the temperature-dependent IR spectra of thermotropic liquid crystalline polymer poly[di(butyl)vinyl terephthalate]. Idrissi et al. [248] used 2D Raman to probe the temperature dependence of Fermi dyads of CO_2 with different local density. Vyalov et al. [249] applied 2D correlation analysis to molecular dynamics simulation, where reorientation and rotation relaxation of supercritical ammonia were calculated as a function of temperature or density. Shinzawa et al. [250] reported the temperature based 2D NMR study of nano-composite made of poly(lactic acid) (PLA) and montmorillonite nano clay. Kim et al. [251] used 2D Raman for lube base oil and adulterated olive oil with varying temperature. Chen et al. [252] filed a patent application based on the use of 2D correlation fluorescence spectra of edible vegetable oils under varying temperature as an identification method.

3.1.7. Temperature-induced chemical reactions

A number of chemical reactions were studied by 2D correlation spectroscopy where the reaction was induced by or carried out under the influence of temperature. Yamasaki and Morita [253] reported the 2D ATR-IR and 2D NIR study of the temperature-dependence of a two-step curing reaction of epoxy resin. The effect of temperature on the H/D exchange reaction of β-lactoglobulin in D_2O was studied with 2D IR by Gomaa et al. [130]. Vdovenko et al. [254] used 2D IR for probing the temperature effect on push–pull enantiomer equilibrium of enaminoketones with different solvents. Du et al. [255] reported the moving window 2D correlation analysis of the temperature dependent IR spectra of partially hydrolyzed poly(vinyl alcohol). Gredičak et al. [256] also used moving window 2D IR for examining the temperature-dependent Bergman cyclization reaction of enediyne. Cozzolino et al. [257] reported the use of 2D MS electric nose for the headspace analysis of wine with varying temperature for the selection of optimal sampling temperature for classification and fingerprinting.

Thermally induced degradation reactions of various compounds and subsequent spectral analysis of the degradation products are important areas of studies in 2D correlation spectroscopy. Peng et al. [258] reported the 2D IR study of the thermal degradation behavior of nanocomposite material comprising CoAl-layered double hydroxide and PCL. Jung et al. [259] used 2D DRIFTS for the surface-induced thermal degradation mechanism of self-assembled thin film of ruthenium complex dye containing polypyridyl ligand anchored on TiO_2 surface used for dye-sensitized solar cells. Harvey et al. [260] reported the 2D IR study of plant derived bio chars under heat treatment with rising temperature under oxygen-limited condition. Badia et al. [261,262] used 2D IR to study the evolved gas kinetics of reprocessed PLA by non-isothermal thermogravimetric analysis. via et al. [263] used ATR IR-NIR hetero-correlation for analyzing biomass changes of sweet gum, Loblolly pine and switch grass with torrefaction (roasting) process. Zimmermann and Baranović [264] reported the use of moving window 2D correlation analysis applied to the baseline variation of temperature-dependent IR for polymorphs of analgesic and antipyretic compound paracetamol for the detection of transition temperature.

2D IR correlation spectra reflecting the compositional changes of samples resulting from thermal reactions induced under a well-controlled temperature scan are extensively used for discriminating and classifying complex natural product mixtures, like traditional Chinese herbal medicine and food. The so-called IR macro-fingerprinting analysis pioneered by Sun [265] combines the examination of FT IR spectra, the second derivative spectra, and thermally induced 2D IR spectra to holistically compare the similarities and differences among complex mixtures. A number of publications appeared on the use of IR macro-fingerprinting technique, which will be discussed later in the field of applications section.

3.2. Composition and concentration

The variation of system constituent concentrations is another important class of static perturbation method extensively used in the field of 2D correlation spectroscopy. The correlation analysis of spectral data reflecting the effect of varying concentrations of contributing components also share some common interest and approaches used in the multivariate chemometrics calibration studies. While chemometrics studies traditionally bring out utility and applications in quantitative classification and prediction based on calibration model derived from statistical analysis of datasets, concentration-based 2D correlation analysis tends to focus on the mechanistic understanding of the system responses under the influence of concentration change by spectral interpretation.

3.2.1. Effect of pH

A number of reports relate to the analysis of the effect of pH on spectra. For example, Lindegren et al. [266] used 2D IR to probe the pH dependence on the adsorption of citrate and tricarballylate onto goethite suspended in water. Ashton and Blanch [267] reported the moving window 2D Raman analysis of the pH-dependent conformational transition of bovine α-lactalbumin. Li et al. [268] also used the moving window 2D analysis of enhanced Rayleigh scattering spectra for pH dependent complexation of poly(acrylic acid) and PEO. Olsson et al. [269] reported the 2D ATR IR study of the adsorption, desorption, and surface-promoted hydrolysis of glucose-1-phospahte based on pH-dependent surface complexes formation on goethite. Ashton et al. [270] used 2D Raman and 2D Raman optical activities (ROA) for the study of the pH effect on protein phosphorylation.

Bálint et al. [271] reported the 2D SERS study to determine a proper marker band for pH dependence of Raman spectrum of 4-mercaptobenzoic acid used as local pH monitoring within cancer cells. Chruszcz-Lipska et al. [272] reported the 2D Raman study of pH-dependence of oxirane ring opening reaction of antibiotic fosfomycyn. Ma et al. [273] used 2D UV-resonance Raman for the study of pH dependent side chain electrostatic interactions of poly-L-lysine. Ji et al. [274] used 2D SERS to elucidate the mechanism of pH-dependent signal enhancement effect for p-aminobenzenethiol on Ag nanoparticles. Litwińczuk et al. [275] reported the 2D polarized ATR IR study of the pH dependence of orientation of solid-supported bilayer of phospholipid 1,2-dipalmitoyl-*sn*-glycero-3-phophocholine (DPPC) by βν correlation analysis. Pienpinijtham et al. [276] used 2D SERS to study nurotensin, a peptide known to stimulate tumor growth, placed in a silver colloid solution under different pH.

3.2.2. Solution mixtures

Many different types of solution mixtures were studied by 2D correlation spectroscopy. Zhang et al. [68] used 2D NIR correlation to detect the chance correlation of interferant composition and analyte glucose concentration. Czarnecki et al. [163] studied the hydrogen bonding interaction in cyclohexanol and water solution mixtures under different concentration with 2D NIR. The concentration dependent complexation chemistry of 2-pyridone, which can also isomerize to 2-hydroxypyridine, in CD_2Cl_2 was reported by Szyc et al. [168]. Radice et al. [170] used 2D IR to probe the concentration effect on hydrogen bonding in fluorinated amide. 2D IR study detected the presence of cyclic dimer, solute–solvent complex, and chain-like dimer. Geng and Xiang [277] reported the 2D NIR study of sinomenine hydrochloride in methanol with varying concentration to demonstrate the utility of net analyte signal (NAS)-based 2D correlation approach.

Tong et al. [278] used 2D ATR IR to study the concentration dependence of 1-propanol and water mixture, and progressive destruction of hydrogen bonding network was noted. Biliškov et al. [279] reported the 2D IR study of the protonated Schiff base of n-butylretinal titrated with trifluoroacetic acid with varying molar ratio. Koeppe et al. [280] reported the 2D UV–visible and NMR hetero-spectral correlation of hydrogen-bonded complexes of 2-chloro-4-nitrophenol with acetate ion with varying concentration to locate the bridging proton in hydrogen bonding. Optical measurement was made directly inside the magnet of NMR spectrometer. Unger et al. [281] used 2D ATR IR for the study of solution mixtures of *N*,*N*-dimethyl formamide in methanol and *N*,*N*-dimethyl acetamide in methanol with varying concentration.

Ryu et al. [172] used 2D correlation to analyze the concentration dependent IR spectra of acetone in $CHCl_3$ and CCl_4 mixtures. Chen et al. [282] reported the 2D UV–visible and 2D IR work for the double asynchronous orthogonal sample design scheme based on concentration series to eliminate interfering peaks and identify specific molecular interactions in the iodine in benzene and CCl_4 mixtures. Díaz-Visurraga et al. [283] used 2D IR to study the interaction of antibacterial copper nanoparticles with sodium alginate at different content levels as a stabilizer. Gu et al. [284] used 2D NIR to study an organophosphorous insecticide phoxin in water at different concentration. Li et al. [285] studied acetone–butanone interactions in CCl_4 with varying concentration by using the asynchronous orthogonal sample design 2D IR. Szostak [286,287] reported the 2D Raman study of concentration dependence of tribromoacetamide solution in CCl_4/C_6D_{12} and self-aggregation of trichloroacetaldehyde in carbontetrachloride and deutrated cyclohexane. Wu et al. [288] used 2D fluorescence to study the concentration dependence of aggregation of type I collagen in acidic solution. Zhou et al. [289] used 2D NIR to select informative spectral interval for varying concentration of analyte in *Ginko biloba* extracts.

3.2.3. Ionic liquids, ionic species, dissolved gasses, etc.

Applications of ionic liquids have attracted interest in recent years. Several publications appeared for the 2D correlation analysis of ionic liquid systems with varying concentrations of mixtures. For example, Zhang et al. [216] used ionic liquid and water mixtures with varying concentrations to illustrate the error analysis associated with 2D correlation spectroscopy. Wu et al. [290] used 2D NIR to study the effect of ethanol addition with different concentration to an aqueous solution of ionic liquid. It was found ethanol seems to weaken the dissociation of ionic liquid in water and thus promote the formation of larger clusters.

Park et al. [291] used 2D IR to examine the concentration-dependent hydrogen bonding interactions of zwitterion-type ionic liquids in water. Wang et al. [292] used 2D ATR IR to study the concentration dependence of ionic liquid, 1-butylpyridinium tetrafluoroborate. Zhang et al. [293] also used 2D ATR IR to study the ionic liquid and water interaction with varying concentration affecting the hydrogen bonding. Aleska et al. [294] reported the 2D Raman study of ionic liquid aqueous solutions of 1-decyl-3-methyl-imidazolium bromide with increasing water content to detect different states of water. He et al. [295] used 2D ATR-IR to study the methanol and ionic liquid molecular interaction with varying concentration of 1-ethyl-3-methylimidazolium lactate.

Concentrations of ionic species in many systems were studied. Park et al. [296] used 2D Raman to study the electrochemical reaction at the electrode–electrolyte interface of $LiCoO_2/Li$ cell under high voltage. Raman spectra obtained under varying delithiation content could be analyzed. Aldon et al. [297] reported the 2D *in situ* and *operando* Mössbauer spectroscopy study of the electrochemical reaction of Li extraction from positive electrode by using Li concentration as perturbation, and isomer shift and quadrapole splitting were detected. Park et al. [298] used 2D X-ray photoelectron spectroscopy and 2D X-ray absorption spectroscopy to probe the electrochemical surface reaction of $LiCoO_2/Li$ cell under high voltage. Yen et al. [299] reported the 2D IR study of poly(amide urethane) solid state electrolyte with $LiClO_4$ addition as the environmental perturbation. Lithium cations interact with both ethylene oxide segments and urethane groups without affecting the self-complementary interaction in the polymer electrolyte.

Jiang et al. [300] used 2D UV to examine the molar ratio dependence leading to different forms of Al(III) complex with curcumin from turmeric for prevention of Alzheimer's disease. Park et al. [301] reported the 2D IR study of the concentration-dependent transition behavior and dynamics of ionic transport in crystalline ionic gel electrolytes. Hur and Lee [302,303] used 2D fluorescence quenching to probe the heterogeneous distribution of copper-binding characteristics of ultrafiltered size fractions of soil humic acid with varying copper concentration and of leaf litter humic substance and Suwannee River fulric acid under different UV irradiation time. Abdulla et al. [304] used 2D IR, 2D ^{13}C NMR correlation, and IR-NMR hetero-correlation to analyze the dissolved organic matter along an estuarine transect with varying salinity to identify nature of components. Abdulla et al. [305] also used 2D MS and MS-NMR hetero-correlation based on the FT ion cyclotron resonance MS to study the ultrafiltered dissolved organic matter from the lower Chesapeake Bay with salinity of water as a perturbation.

Wang et al. [306] examined the concentration dependent IR spectra by 2D correlation to determination of the optimal wavenumber range for the detection of gases, such as SO_2, NO, and NO_2. Morita et al. [307], as well as Shinzawa and Ritthiruangdej [308], discussed the application of 2D NIR to examine the concentration-dependent spectral changes induced by the evaporation of ethanol from a solution mixture with oleic acid. Chandra et al. [309] reported the 2D SERS study of the concentration dependence of 3-thiophene carboxylic acid adsorption onto silver nano colloids. 2D ATR IR was used by Simanova et al. [310] to study the reaction of different levels of oxalate or $Fe(C_2O_4)_3^{3-}$ adsorbed at water–geothite interface.

3.2.4. Designed concentration series

Particular patterns of carefully designed concentration variations are sometimes used to enhance the information content of the 2D IR spectra. For example, Li et al. [285] described the asynchronous orthogonal sample design coupled with modified reference spectrum derived from average of virtual mixture without intermolecular interactions to improve the signal-to-noise ratio and detection of weak signals observed in the acetone–butanone interactions in CCl_4 with varying concentration. Zhang et al. [311] reported the IR and UV–visible hetero-spectral correlation of benzene/I_2/CCl_4 under the double orthogonal sample design condition. Concentrations of two components were set such that one series was orthogonal not only to the other concentration series but also the quadrature to the series. Li et al. [312,313] reported the 2D IR study of butanone and dimethyl formamide in CCl_4 and based on the asynchronous orthogonal sample design. Specific concentration series were used to eliminate peaks due to effect linearly proportional to concentration and to detect deviations from Beer–Lambert law due to specific molecular interactions.

3.2.5. Blends and composites

Several polymer blends and composites were studied by 2D correlation spectroscopy. Nanocomposite made of PLA and different levels of montmorillonite nano clay was studied by Shinzawa et al. [250] by using 2D NMR. Huang et al. [314] used 2D IR to probe the specific molecular interaction of polymer nanocomposites made by blending different levels of polyhedral oligomeric silsesquioxane derivatives and PEO. Apparent peak frequency shift of OH stretching band is due to the competition between contributions reflecting the OH—OH and OH—ether interactions, and dipole–dipole and hydrogen bonding interactions of C═O groups were also detected.

Jelčić and Vranješ [315] reported the 2D NIR study of the blend of polystyrene and polyethylene with various concentration of a block copolymer compatibilizer, which affects specific interaction and conformational feature of polymer components. 2D IR was used by Kuo and Liu [316] for studying hydrogen bonding interactions of blends of PHB and poly(vinyl phenol) or copolymer melt with different compositions. Nurkhamidha et al. [317] used 2D IR to study the composition dependence of the melt blend of poly(ethylene succinate) and tannin, and strong hydrogen bonding interaction leading to the miscibility was observed. Wu et al. [318] reported the 2D dynamic mechanical spectroscopy study of polystyrene with different molecular weights to analyze the sub-Rouse mode. Both temperature–temperature and frequency–frequency 2D correlation maps were constructed.

3.2.6. Other concentration studies

2D correlation spectroscopy was applied to the analysis of many other systems involving the compositional variations. For example, De Almeida et al. [319] applied 2D ATR IR to study zein-based biofilms with different concentration of xanthan gum additive, which affects C═O and N—H groups of zein structure. Pereira and Pasquini [320] used 2D IR for the concentration perturbation study of gasoline by using a flow cell. Radice et al. [321] reported the 2D Raman study combined with density functional theory (DFT) calculations to study the polymer chain microstructure of perfluoropolyethers containing different concentration of peroxide groups. Brewster et al. [322] reported the moving window 2D Raman study of glycosilation status of protein by varying the concentration of native ribonuclease A and ribonuclease B glycoprotein. Fernandes et al. [323] used 2D IR to study diurea crosslinked bridged silsequioxanes derived from organosilane precursor with variable molecular composition of central spacer length.

Ferrari et al. [324] reported the NIR–NMR hetero-spectral correlation study of red wine samples which are color-enhanced with anthocyanins from grapevine or black rice. Park et al. [325] used 2D IR to study the thermal transition and physical gelation of binary gel consisting of zwitterionic compounds and lithium bis(trifluorosulfonyl)imide. Podstawska-Proniewicz et al. [326] reported the 2D SERS study of G-protein-linked nuropeptide neurotensin with various modifications, which were immobilized onto an electrochemically roughened silver electrode, with varying compositions of L- and D-conformations of amino acids. Popescu and Vasile [327] reported the 2D IR study of the blend of polyethylene adipate and liquid crystalline cholesteryl palmitate additive with varying compositions to probe specific interactions and conformational changes. Rudd et al. [328] reported the 2D NMR study of heparin with compositional changes caused by contaminants or natural structural variability.

Song and Boily [329] used 2D ATR IR for the study of the concentration dependence of the surface hydroxyl groups of akaganéite (β-FeOOH) particles. Tan et al. [330] reported the 2D IR study of conformational changes and specific interactions of blends of collagen and hyaluronic acid with varying compositions. Yu et al. [331] used 2D IR for the characterization of edible oil blends with varying compositions to give different saponification number. Tian et al. [332] used 2D IR to study the composition dependence of blends of collagen and chondroitin sulfate, and conformational changes and specific interactions were detected. Wu et al. [333] used 2D IR to probe the interaction of polyacrylonitrile with various solvents at different concentrations, and dipole–dipole interactions between C≡N groups and C═O or S═O were noted. Xu et al. [334] reported the 2D visible/NIR study of mixtures of goose down and duck down with different compositions.

Yu et al. [335] used 2D IR to assess the binding of organic ligands with Al(III) in soil dissolved organic matter with different Al(III) concentration. Zhang et al. [336] obtained 2D ATR-IR spectra based on blood glucose concentration. Brewster et al. [337] used Raman and fluorescence moving-window 2D analysis for chemically induced protein unfolding of ribonuclease A and B with different guanidine hydrochloride denaturant levels. Fudge et al. [338] used 2D IR for the identification of smoke-affected wine by using the concentration of a smoke taint marker guaiacol as perturbation. Shao et al. [339] used 2D ATR IR to probe the conformational changes of glucose oxidase upon adsorption onto graphine oxide with different protein concentration. Shinzawa et al. [340] reported the 2D NIR study of the state of cellulose affecting the packing and crystallinity under the compositional changes by water absorption.

3.3. Electro-magnetic effects

3.3.1. Electrode potential

A number of articles appeared on the use of electrical field as a source of perturbation for 2D correlation spectroscopy. Boily [341] reported the 2D IR study of oxyanions adsorbed on solid surfaces under varying electric field. Theoretical prediction of 2D spectra was provided based on DFT calculation of frequency shift and band broadening for different correlation peak cluster patterns reflecting the distinct electric field induced coordination. Podstawka and Niaura [342] reported the 2D SERS study of neurotransimitter bombesin which was chemisorpted on electrochemically roughened electrode surfaces with varying electrode potential at the physiological pH. Fen et al. [343] filed a patent application based on 2D NIR spectra to predict viscosity index of engine oil under electrical perturbation with voltage and frequency changes. Park et al. [344] reported the 2D X-ray photoelectron spectroscopy (XPS) study of the electrochemistry of at the solid electrolyte interface of a cathode electrode for lithium ion battery under different changing voltage.

Podstawka et al. [345] studied 2D SERS of phenylalanine-substituted bombesin fragment peptides adsorbed on various electrode surfaces under different electrode potential to robe the adsorption mechanism and specific interaction. Laredo et al. [346] reported the 2D photon polarizarion modulation IRRAS (infrared reflection absorption spectroscopy) study of gold-supported biomimetic membrane phospholipid bilayer containing ion channel peptide with electrode potential. Naumann et al. [347] used 2D SEIRAS for the study of electrochemistry of protein tethered bilayer lipid membrane as function of potential. Nowak et al. [348] used 2D SEIRAS to study the membrane redox protein cytochrome c oxidase with varying electrical potential. Ambrosio and Gewirth [349] used 2D SERS to probe the electrochemical reactions of alkaline aqueous solution at Ag electrode by cyclic voltammetry, and sequential order of liberated and binding bands of water was determined.

Colina et al. [350] used 2D low-resolution Raman to study the electrochemical oxidation of transparent single-walled carbon nanotubes during anodic voltametric scan. Whitman et al. [351] introduced a 2D cyclic voltammetry application to the electrochemistry with current measured as a function of potential with a number of potential cycle scans. Butcher et al. [352] used 2D shell-isolated nanoparticles-enhanced Raman to study the electrical potential dependent assembly of 2,2′-bipyridine on Au(1 0 0) and Au(1 1 1). Park et al. [353] used 2D X-ray absorption spectroscopy (XAS), 2D Raman, and XAS–Raman hetero-spectral correlation to study the electrochemical reaction of the overcharged cathode surface of lithium battery with varying voltage. Leitch et al. [354] used 2D polarization modulation IRRAS to study the voltage dependent change of phospholipid–cholesterol bilayer with cholera toxin B on Au(III) electrode surface. Su et al. [355] also used 2D polarization modulation IRRAS to study the electrochemistry of lipid bilayer assembled at Au(III) electrode surface for higher resolution.

3.3.2. Magnetic field

Magnetic field is extensively used as a convenient means to perturb π bonds encountered in various hydrothermally synthesized metal organic hybrid materials. Such studies often use thermal perturbation in parallel to probe the hydrogen bonding interactions of the system as well [176–187,190]. For example, magnetic perturbation of hydrothermally synthesized compound from bismuth and a flexible ligand *N*,*N*′-diacetic acid imidazolium chloride was studied with 2D IR by Chai et al. [176]. 2D IR and 2D UV study of rare earth 3-bi-pyridine polymer under magnetic perturbation was reported by Chen et al. [177]. 2D IR study of divalent transition metal carboxyarylphosphonate samples with different structures were investigated under magnetic perturbation by Lei et al. [178]. Crystals of carboxylate metal coordination compounds with 3-methylbenzoic acid were analyzed by Chen et al. [179] with 2D IR based on magnetic perturbation. 2D IR study of polyoxovanadium borate under magnetic perturbations was reported by Li et al. [180,181].

Magnetically induced changes of hydrothermally synthesized polyoxometalates with different carboxylic ligands and photocatalytic activities analyzed with 2D IR were reported by Chen et al. [182]. Magnetic sensitivity of π bond of organically template aluminoborte with quasi-aromaticity was studied with 2D IR by Hu et al. [183]. 2D IR study of lanthanide 2-hydroxynicotinic acid coordination polymer under magnetic perturbation was reported by Mei et al. [184]. Structural change of polyoxovanadium borate organic–inorganic hybrid probed by 2D IR study under magnetic perturbation was reported by Sun et al. [185]. Magnetic perturbation 2D IR study of hydrothermally synthesized Keggin-type heteropolytungustates was reported by Chai et al. [186]. 2D IR analysis of magnetic intensity effects on nitrogen-heterocyclic β-octamolybdate supported metal–organic compounds was studied by Chen et al. [187]. 2D IR study based on the magnetism-induced structural changes of rare earth compounds with 3-methylbenzoic acid was reported by Zhao et al. [190].

3.4. Mechanical perturbations

3.4.1. Deformation of samples

Mechanical perturbations, such as tensile deformation applied to a film, are used is the 2D correlation spectroscopy analysis of polymeric materials. In fact, the field of 2D IR correlation spectroscopy originally started with the analysis of IR responses of plastic films subjected to a small-amplitude repetitive deformation [1,8,9]. A number of articles related to the 2D correlation spectroscopy based on mechanical deformation effects appeared during this review period. Kawabe et al. [23] discussed the 2D correlation spectroscopy applied to the IR study of stretched adhesive tape. Unger and Siesler [356] used 2D IR for the dichroism study of PHB and PCL blend under uniaxial elongation to determine the directions and sequence of orientation processes of crystalline and amorphous components of PCL and PHB.

Burba et al. [357] reported the 2D IR study of the chain orientation of stretched polyelectrolyte film comprising salt of PEO with $LiCF_3SO_3$. Liu et al. [358] used 2D Raman spectroscopy to study the single walled carbon nanotube films under strain. Wang et al. [359] used 2D dielectric relaxation for probing the molecular dynamics of polyisobutylene around the glass transition temperature, and unambiguous identification of local segmental motion, sub-Rouse modes, and Rouse modes was possible. Rao et al. [360] reported the 2D SERS study applied to single-molecule force spectroscopy by using a dual optical trapping of DNA near Ag nanoparticles to induce extension at the molecular level.

3.4.2. Pressure and uniaxial compression

The application of pressure to a sample system is a popular mechanical perturbation method to obtain 2D correlation spectra. Wu et al. [230] used concatenated 2D IR correlation analysis to assess the reversibility for individual molecular moieties during the pressure-induced globule to coil transition of ribonuclease A. Zhang et al. [361] used 2D IR to study the pressure-induced conformational change of poly-L-lysine with different initial conformations. Zhang and Wu [362] carried out the 2D IR analysis of a number of proteins, including lysozyme, human serum albumin, ubiquitin, and ribonuclease A, with structural and hydration changes under pressure change. Piccirilli et al. [363] used 2D IR to probe the pressure effect on the aggregation of bovine pancreatic insulin amyloid.

Shinzawa et al. [364] used 2D X-ray diffraction and hetero-correlation between X-ray diffraction and dissolution profile of either active ingredient or water absorption profile. Pharmaceutical tablets containing cellulosic excipient and pentoxifylline under different compressive deformation, affecting both crystallinity and compaction, were studied. Shinzawa et al. [157] also used 2D ATR IR for examining the self-assembly of oleic acid under multiple-perturbation consisting of both pressure and temperature generating three-way dataset. Shinzawa et al. [340,365] used 2D NIR to study the pressure-induced variation affecting the packing and crystallinity of cellulose tablets. Zhang et al. [366] reported the 2D fluorescence correlation spectroscopy study of the pressure-induced fluorescence enhancement of bovine serum albumin-protected gold nano clusters.

3.5. Spatial distributions

Spectral variations of samples obtained at different spatial locations are also analyzed by 2D correlation spectroscopy. Abdulla et al. [304] conducted such spatial distribution based studies with 2D IR, 2D ^{13}C NMR, and IR-NMR hetero-correlation analyses. Dissolved organic matters sampled along locations of an estuarine transect was used as the perturbation variable to identify the nature of such components. Richardson and Wang [367] used the moving-window 2D correlation analysis for the Raman image of a single-wall carbon nanotube along the position of the specimen to enhance spectral resolution. Kwok and Taylor [368] reported the application of 2D correlation in the analysis of microscopic Raman images of pharmaceutical counterfeit packaging based on image coordinate scanning. Li et al. [369] used 2D IR to examine the diagenesis of organic matter in Lake Superior sediment sampled at different depth of core as the perturbation variable.

4. Fields of applications

2D correlation spectroscopy has been applied to a number of diverse categories of samples encountered in different fields of applications and research activities. Types of materials and systems studied by this technique include polymers, nano materials and composites, pharmaceuticals, medical and physiological applications, proteins and peptides. Other biomolecules, like lipids, saccharides, and DNA, are also studied. A number of practical samples found in food science, bio-sourced or natural materials, and environmental science, are also often studied by 2D correlation spectroscopy. Research activities are reported in classical physical chemistry field, such as the in-depth studies of pure liquids and solution mixtures, colloids and surfaces, and organic–inorganic hybrid materials. 2D correlation spectroscopy is also used in the analysis of chemical reactions, electrochemistry, industrial chemicals and materials, and many more applications. Fig. 3 shows the distribution of the different fields of applications among 421 published articles.

4.1. Polymers

Study of polymers and oligomers in various forms and states remains a very active area of research for 2D correlation spectroscopy, representing about 26% of the application-oriented articles reviewed here. 2D correlation spectroscopy analysis of polymeric samples utilized many different types of perturbation methods, such as temperature, composition, and chemical reactions. Aside from plastic films and fibers, many other forms of polymer samples were studied, including melts, solutions and dispersion, cross linked resins and elastomers, as well as blends and composites.

4.1.1. Bio-based and biodegradable polymers

In the recent years, the interest in bio-based or biodegradable polymers has dramatically increased. The growing number of publications on the use of 2D correlation spectroscopy for the analysis of such biodegradable materials also reflects this trend. Poly(3-hydoroxyalkanoate) or PHA belong to the class of polyesters produced by microorganisms capable of converting natural carbon sources, like lipids and saccharides, to polymers accumulated in their body as energy storage materials [370]. PHA bioplastics harvested from such microorganisms are viewed as a new promising class of materials sourced from nonpetroleum-based raw materials. Poly(3-hydoroxybutyrate) or PHB homopolymer is the simplest and most ubiquitous form of PHA, while copolymers, like poly(3-hydoroxybutyrate-*co*-3hydroxyhexanoate) (PHBHx), possess different material properties [371].

Unger et al. [191,192] used 2D IR to study the temperature dependence of annealed and non-annealed PHB, as well as the blend of PHB and polycaprolactone (PCL). The detection of recrystallization and melting processes has a significant practical implication for the industrial processing of this class of materials. Unger and Siesler [356] reported the 2D IR dichroism study of PHB and PCL blend under uniaxial elongation. Unger et al. [193] also studied the crystallization behavior of PHB, PCL, and blends of PHB and PCL under variable temperature with 2D IR. Hoshina [55] discussed the use of 2D THz spectroscopy to investigate PHB. Hoshina et al. [56,57] reported the 2D THz study of the time-dependent spectral evolution of PHB during the isothermal crystallization. Hoshina et al. [198] also used 2D THz absorption spectroscopy for the study of PHB and PHBHx with varying temperature to obtain assignments for crystalline and amorphous peaks.

Guo et al. [54] reported the 2D WAXD and 2D SAXS study of the time-dependent behavior of PHB during the isothermal crystallization. Nishikawa et al. [15] used dynamic compression for 2D ATR study of PET and PHBHx films. Choi et al. [204] reported the 2D IR and 2D XPS study of the spin-coated thin films PHBHx with different comonomer content under increasing temperature. Kim et al. [202,205] reported the 2D IRRAS study of the thermal behavior of spin-coated thin films of PHBHx and PEG blends. Kuo et al. [316] used 2D IR for the analysis of hydrogen bonding interactions of blends of PHB and poly(vinyl phenol). Poly(lactic acid) or PLA is another class of bioplastics synthesized from bio-based raw material. Ando et al. [52] used 2D correlation spectroscopy to study the

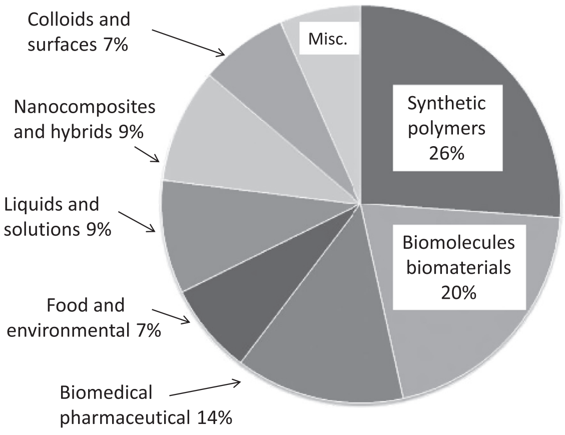

Fig. 3. Sample systems studied by 2D correlation spectroscopy.

time-dependent IR spectral evolution during the isothermal melt crystallization of PLA nanocomposite with organically modified layered silicate. Badia et al. [261,262] used 2D IR to study the evolved gas kinetics of reprocessed PLA by non-isothermal thermogravimetric analysis.

4.1.2. Thermo-responsive polymers

Intriguing aqueous solution behavior of thermo-responsive polymers, such as poly(*N*-isopropylacrylamide) or PNIPAM, has attracted interest of many researchers, and the number of published articles related to the 2D correlation spectroscopy study of this class of materials is increasing. Park et al. [67] used 2D ATR IR to study the gelation process of PNIPAM hydrogel above and below LCST. Wang and Wu [160] used 2D IR to study the temperature induced gelation microdynamics of PNIPAM in an ionic liquid. Kurz, et al. [209] reported the 2D IR sum-frequency spectroscopy study of a thermo-responsive PNIPAM thin film near the LCST. Lai and Wu [210] used 2D IR to study the LCST-type phase transition of aqueous solutions PNIPAM and *N*-isopropylpropionamide. Sun et al. [211] reported the 2D IR study of the thermally induced volume phase transition of PNIPAM hydrogel with D_2O for both heating and cooling process. Sun and Wu [212] studied the temperature effect around the LCST of concentrated solutions of PNIPAM in water or water methanol mixture by using 2D IR.

Sun et al. [227] used 2D IR to study the PNIPAM-based multihydrophilic block copolymer in D_2O during heating. Wang et al. [228] used 2D IR to analyze the thermal phase behavior and microdynamics of PNIPAM-*b*-poly(1-butyl-3-vinylimidazolium bromide) aqueous solution, forming core–shell micelle structure. Wang and Wu [229] used 2D IR to examine the effect of ionic liquid on the temperature dependence of PNIPAM. Zhang et al. [215,231] used concatenated 2D IR to study the temperature-induced hydration and dehydration of PNIPAM and poly(*N*-isopropylmethacrylamide) aqueous solution during the heating and cooling to assess the degree of path-dependent irreversibility of coil-globule transitions. Sun et al. [233] also studied the LCST-type phase transition behavior of thermo-responsive dendritic polymer with hydrogen bonding in D_2O during the heating and cooling process by 2D IR. Sun and Wu [234] used 2D IR to study the thermally reversible hydration of thermoresponsive copolymer in D_2O. Sun et al. [235] used 2D IR to study the thermo-sensitivity and self-assembly of a PNIPAM block copolymer.

4.1.3. Water-soluble polymers

Other water-soluble polymers were also subject matter of active 2D correlation spectroscopy studies. For example, Lai and Wu [28] studied the water sorption and desorption process of a pharmaceutical amphiphilic copolymer poly(3-(2-methoxyethyl)-*N*-vinyl-2-pyrrolidone) by 2D IR. Liu et al. [50] reported the 2 D IR study of the time-dependent IR of isothermal crystallization of ice in PVME solution. Sun et al. [220] used 2D IR to study the thermally induced volume phase transition of hydrogel during heating and cooling. Sun et al. [221] used 2D IR to probe the detailed micro dynamics mechanism of temperature-induced phase transition and hydrogen bonding of aqueous solution of poly(vinyl methyl ether). Li et al. [268] reported the 2D correlation analysis of enhanced Rayleigh scattering spectra for pH dependent complexation of poly(acrylic acid) and poly(ethylene oxide). Sun and Wu [222] reported the 2D IR study of the temperature dependent dynamic dehydration of poly(*N*-vinylcaprolactam) near the LCST. Wang et al. [224] studied the molecular mechanism of thermally induced phase transition of hyperbranched poly(ethyleneimine) with isobutyramide groups in D_2O by 2D IR. Lai et al. [236] used 2D IR to study the dehydration process of the LCST of poly(3-ethyl-N-vinyl-2-pyrrolidone) in water during the heating and cooling cycle.

4.1.4. Liquid crystalline polymers

Liquid crystalline polymers were also studied by many researchers. Sun et al. [246,372] reported the 2D IR study of the temperature induced self-assembly process of thermotropic liquid crystalline polymer without conventional mesogens. Tang et al. [241] reported the 2D Raman study of the conformational change of thermotropic liquid crystalline polymer poly[di(alkyl) vinylterephthalate] upon heating. Wang et al. [247] applied 2D correlation to temperature-dependent IR spectra of thermotropic liquid crystalline polymer poly[di(butylvinyl terephthalate).

Cheng et al. [218] reported the 2D IR study of the temperature-induced spectral change of mesogen-jacketed liquid crystalline polymers with amide core and flexible tails of varying lengths. Several ion-containing polymeric systems have also been studied. Morita and Kitagawa [239] studied Nafion ionomer by 2D IR and detected the temperature-induced three-step structural changes (i.e., dehydration, protonation of side chain terminal sulfonate, and thermal degradation). Shi et al. [156] reported the sequential responses of components to thermal perturbation of polystyrene and ionic liquid composite membrane by 2D IR. Yen et al. [299] reported the 2D IR study of poly(amide urethane) solid state electrolyte with $LiClO_4$ addition as perturbation. Burba et al. [357] reported the rheo-optical 2D IR study of the chain orientation of stretched polyelectrolyte film comprising salt of PEO with $LiCF_3SO_3$.

4.1.5. Thermosetting polymers

Thermosetting polymers, like epoxy resins, were also studied, especially during the curing process. Spegazzini et al. [72,73] studied the cross linking reaction of epoxy resin based on diglycidyl ether of bisphenol A with rare earth triflate initiators with 2D IR. Yu et al. [74] reported the 2D IR study of the parallel reactions of cationic polymerization and esterification during the curing of epoxy resin with a polyoxometalate catalyst. Yamasaki and Morita [253] studied the temperature-dependence of a two-step curing reaction of epoxy resin by 2D IR and 2D NIR. Tang et al. [63] applied 2D correlation analysis to the time-resolved light scattering data from the phase separation process of epoxy-amine-polyethersulphone blend. Zhong et al. [125] studied the photochromic behavior of polyoxometalate in cured epoxy resin after UV irradiation by 2D IR to determine the sequence of electron movements. Wang et al. [126] investigated the photo-induced orientation of epoxy-based polymers with azo chromophores under different duration of irradiation time with 2D IR. Morita et al. [244] discussed the curing reaction kinetics of epoxy resin studied by using 2D IR.

4.1.6. Block copolymers and blends

2D correlation spectroscopy was used for the analysis of block copolymers and polymer blends. Li and Zhang [14] used 2D IR photo-acoustic spectroscopy to the depth profile study of block polymer and polyester layered material. Jia et al. [158] reported the study of temperature-induced micellization process of an aqueous solution of a block copolymer involving conformational transition, dehydration, hydrogen bond breaking, and hydrophobic association by 2D IR. Zhou et al. [217] studied temperature-dependent transitions of polystyrene-*b*-poly(ethylene-co-1-butene)-*b*-polystyrene triblock copolymer with 2D IR. Chen et al. [200] studied the crystallization steps of polyoxymethylene and PEO blend during the cooling by 2D IR. Jelčić et al. [315] studied blends of polystyrene and polyethylene by 2D NIR with various concentration of triblock copolymer compatibilizer, which affects specific interaction and conformational feature of polymer components. Kuo et al. [374] used 2D correlation for time-dependent IR spectra of blends of poly(vinyl phenol) and polybenzoxazine undergoing copolymerization reaction to produce super hydrophobic surfaces.

4.1.7. Conventional polymers

Conventional synthetic polymers are routinely analyzed by 2D correlation spectroscopy. A number of publications related to the characterization of synthetic polymers appeared during this review period. For example, Chen et al. [53] gave the detailed band assignments by 2D IR for PET based on temperature dependent spectral changes during the cooling from the melt and time-dependence during the isothermal crystallization. Lee et al. [124] studied the photodegradation of PET film with UV-irradiation time by 2D IR. Virgin and reprocessed PET samples were studied with 2D IR by Badia et al. [373] for the kinetic model identification of the energetic valorization reaction by evolved gas analysis from temperature scan of thermogravimetric analysis. Luo et al. [219] studied the Brill transition of nylon 66 using temperature-dependent 2D IR.

Zhou and Xin [58] studied the time-resolved spectral change during the isothermal crystallization of isotactic PP containing various benzilidene acetal nucleating agents by 2D IR. Xu et al. [59] reported the isothermal crystallization kinetics of isotactic PP containing graphene oxide nanosheet. Watanabe et al. [197] studied various polyethylene samples during heating and applied 2D correlation analysis to the light microscopy retardance mapping histograms reflecting the spatial distribution of higher order supra molecular structure. Shinzawa et al. [203] studied the heating of HDPE and octene-1 LLDPE by 2D Raman. Smirnova et al. [51] studied the non-isothermal crystallization of hydrogenated polybutadiene by 2D SAXS. Zimmermann and Vrsaljko [206] applied 2D IR sample–sample correlation to thermal analysis for the identification of glass transition of polystyrene. Wu et al. [318] studied polystyrene with different MW by 2D dynamic mechanical spectroscopy to analyze the sub-Rouse mode response. Syndiotactic polystyrene was studied with 2D IR by Li and Wu [238] for the temperature-induced helical to planar zigzag conformational change. Zheng et al. [49] studied the time-dependent isothermal crystallization of syndiotactic polystyrene by 2D IR.

Shi et al. [48] reported the 2D IR study of the time-dependent crystallization of polybutene-1 accelerated with super critical CO_2 to probe crystallization mechanism. Wang et al. [60] studied the gradual cooling crystallization process of α-*trans*-1,4-polyisoprene by 2D IR. Wang et al. [207,359] analyzed dynamic mechanical and dielectric spectra of polyisobutylene by 2D correlation to resolve temperature-dependent loss tangent peak under different deformation frequency for the glass-to-rubber transition region. Melting process of PEO was studied with 2D IR by Zhou et al. [195]. Li et al. [199] studied the non-isothermal crystallization and melting of polyoxymethylene. Melt blends of poly(ethylene succinate) and tannin were studied by Nurkhamidha et al. [317] and Popescu and Vasile [327]. Partially hydrolyzed polyvinyl alcohol was studied by Du et al. [255]. Morita et al. [244] discussed the 2D IR analysis of poly(vinyl alcohol). Kawabe et al. [23] discussed the 2D IR correlation analysis of poly(vinyl acetate) adhesive tape under deformation. Guo et al. [201] studied the temperature dependence of microstructure and phase transition of regioregular poly(3-dodecylthiophene) by 2D IR. Rettler et al. [245] studied poly(2-*N*-alkyl-2-oxazoline)s with different side chain lengths by temperature based 2D IR.

Wu et al. [333] studied the interaction of polyacrylonitrile with various solvents at different concentrations by 2D IR. Li et al. [162] used 2D IR to study the temperature-induced changes in the hydrogen bonding of sodium salt of carboxymethyl cellulose. Jing and Wu [232] studied the temperature-induced coil-to-globule and sol–gel phase transitions of hydroxypropylcellulose aqueous solution by 2D IR and NIR. Popescu and Simionescu [226] reported the 2D IR study of the phase transition of allyl-terminated carbosilane dendrimer. Sui et al. [131] applied 2D correlation to derivative thermogravimetry to study the decomposition reaction of polyester–urethane adhesive with different doses of γ-ray irradiation. Li et al. [175] studied a thermoplastic segmented polyurethane by 2D IR. Ryu et al. [69] reported the 2D IR and NMR study of the free radical polymerization process of poly(vinylpyrrolidone) with $AgNO_3$ chain transfer agent. Su et al. [70] studied the polymerization reaction of partially cross linked polyacrylamide by 2D IR. Xiang et al. [95] reported the 2D IR study of the thermooxidative degradation process of styrene–butadiene rubber. Popescu and Simionescu [96] studied the environmental weathering of an acrylic copolymer film. Photosensitive polyimide with cinnamate side group undergoing UV-irradiation-induced molecular reorientation was studied with 2D IR by Kim et al. [121]. Photo-induced molecular reorientation and *trans–cis* isomerization of photosensitive polymer poly(4-methacryloyloxazobenzene) under different UV doses was reported by Lee et al. [122].

4.1.8. Small molecules within polymer matrices

Presence of small molecules, like water, within a polymer matrix is often studied effectively by 2D correlation spectroscopy. Wang et al. [39] used 2D ATR IR to investigate the diffusion of water in poly(ether urethane) block copolymer. Jun et al. [44,45] studied the water diffusion in poly(metaphenylene trimesamide) layer of a thin film composite membrane and in block copolymer. 2D IR and 2D NIR studies of water diffusion in epoxy resin were reported by Li et al. [40]. Water desorption process from water-soaked cotton fibers was studied by Liu et al. [20]. Wang and Wu [41] reported the 2D IR study of water diffusion in PCL. Wang et al. [42] also studied the diffusion of water in LDPE film under different temperature. 2D IR study of the sorption of water vapor in polyimide films was reported by Musto et al. [27]. Diffusion of small molecules other than water was also studied. Fu and Lin [46] reported the 2D ATR IR study of the diffusion of multiple flavor components, including 2-octanone, hexyl acetate, octanal, limonene and linalool, in LLDPE. Lai et al. [47] studied the diffusion of plasticizer tri-2-ethylhyxyltrimellitate in poly(vinyl chloride) film at different temperature by 2D IR.

4.2. Nanoparticles and nanocomposites

The interest in nanoparticles remains strong. Kim et al. [65] used 2D DRIFTS to study the thermal annealing mechanism and micro-structural changes of tin-doped indium oxide nanoparticles. Tang et al. [78] reported the UV–visible extinction spectroscopy study of the halide ion etching (i.e., shape conversion) reaction of producing silver nanoprism to nanodisks particles. Doan et al. [91] applied 2D correlation to time-resolved spectra of photo-induced decarbonylation reaction of nanocrystalline diphenylcyclopropenone. Díaz-Visurraga et al. [283] studied the interaction of antibacterial copper nanoparticles with sodium alginate at different content as a stabilizer by 2D IR. Shao et al. [339] reported the 2D ATR IR study of the conformational change of glucose oxidase upon adsorption onto graphine oxide. Liu et al. [358] used 2D Raman to study single walled carbon nanotube films under strain.

Zhang et al. [366] used 2D correlation fluorescence to study the pressure-induced fluorescence enhancement of bovine serum albumin-protected gold nano clusters. Richardson and Wang [367] applied 2D correlation to the Raman image of single-wall carbon nanotube along positions to enhance spectral resolution. Nano particles are incorporated into various polymeric matrices to produce nanocomposite materials with superior properties. Ando et al. [52] reported the 2D IR study of the isothermal melt crystallization of PLA nanocomposite with organically modified layered silicate. Huang and Kuo [71] used 2D IR to study the curing kinetics and mechanisms of nanocomposite made of polybenzoxazine and polyhedral oligomeric silsesquxanes. Musto et al. [92] used 2D IR to study the photo-oxidative degradation reaction dynamics of epoxy resin stabilized with polyhedral oligomeric silsesquioxane nano filler, as an organic–inorganic hybrid composite.

Palszkiewicz et al. [120] used 2D ATR IR to study the nucleation and growth of apatite on a nanocomposite comprising chitosan and montmorillonite. Zhou et al., [242] used 2D Raman to study the melt intercalated PEO and clay hybrid nanocomposite. Shinzawa et al. [250] reported the 2D correlation NMR study of nanocomposite made of PLA and montmorillonite nano clay. Peng et al. [258] used 2D IR to study the thermal degradation behavior of nanocomposite material comprising CoAl-layered double hydroxide and PCL. Huang et al. [314] studied the specific molecular interaction of polymer nanocomposites made by blending polyhedral oligomeric silsesquioxane derivatives and PEO by using 2D IR.

4.3. Proteins and peptides

A sizable number of articles were published on the 2D correlation spectroscopy study of proteins, polypeptides and related molecules. The enhanced spectral resolution achieved by the application of 2D correlation, as well as the capability to determine the coordinated and sequential changes of spectral band intensities, makes this technique especially attractive to the analysis of complex molecules. Tang et al. [22] used 2D localized surface plasmon resonance spectroscopy based on time-resolved excitation spectroscopy to study the interaction between bovine serum albumin (BSA) and silver or gold nanoparticles. Gomaa et al. [130] used 2D IR to study the effect of microwave exposure treatment and temperature on the H/D exchange of β-lactoglobulin in D_2O. Das et al. [137] investigated the temperature-induced conformational changes of studied a number of proteins, e.g., BSA, lysozyme, ribonuclease A, and myoglobin, by using 2D SERS with nano-structured substrates. Wang et al. [141] used 2D IR to study the temperature-induced unfolding of conformational structures of glucose oxidase protein.

Ausilli et al. [146] determined the three-step thermal unfolding of zinc-dependent alcohol dehydrogenase from hyper thermophilic archeon microorganism with 2D IR. Zhang et al. [142] and Wu et al. [230] used concatenated 2D IR for the determination of the reversibility of thermally induced folding, unfolding and globule to coil transition of bovine pancreatic ribonuclease A. Ashton and Blanch [267] studied the pH-dependent conformational transition of bovine α-lactalbumin with 2D Raman. Brewster et al. [322,337] reported the 2D Raman study of glycosilation status of protein by varying the concentration of native ribonuclease A and ribonuclease B, as well as chemically induced protein unfolding with different guanidine hydrochloride denaturant dose. Shao et al. [339] studied the conformational change of glucose oxidase upon adsorption onto graphine oxide with different protein concentration with 2D IR. Nowak et al. [348] reported the 2D SEIRAS study of membrane redox protein cytochrome c oxidase with varying electrical potential. Zhang and Wu [362] analyzed a number of proteins, including lysozyme, human serum albumin, ubiquitin, and ribonuclease A, by using 2D IR with structural and hydration changes under pressure.

Structure dynamics of proteins was explored by 2D correlation spectroscopy. Shashilov and Lednev [375] discussed the analysis of protein structure and dynamics by using 2D Raman spectroscopy, which is sensitive to conformations. Lednev et al. [77] reported the 2D deep UV resonance Raman study of the H/D exchange of *in vivo* protein structural evolution of amyloid fibril at the early stage of fibrillation. Lednev and Sikirzhytski [376] gave more discussion on the use of deep UV 2D Raman to probe protein fibrillation mechanisms. De la Arada et al. [62] used 2D IR to study the aggregation process of amyloid fibril formation for bovine and human serum albumin with varying incubation time. Piccirilli et al. [363] used 2D IR to examine the pressure effect on aggregation of bovine pancreatic insulin amyloid.

Li and Li [144] used 2D correlation fluorescence to probe the temperature-induced denaturation process of collagen dissolved in glycerol or 2-propanol. Chen et al. [147] used 2D IR to study the thermal denaturation of uncrosslinked and crosslinked collagen. Guo et al. [148] studied the temperature-induced denaturation of aqueous collagen solution by 2D IR. Chys et al. [243] used 2D IR to study the thermal responses of alkali-pretreated gelatin fractions to investigate the sequences of conformational changes. Wu et al. [288] used 2D fluorescence to study the concentration dependence of aggregation of type I collagen in acidic solution. Tan et al. [330] reported the 2D IR study of conformational changes and specific interaction of blends of collagen and hyaluronic acid with varying compositions. Tian et al. [332] studied the conformational change and specific interaction of blends of collagen and chondroitin sulfate with 2D IR.

Many other types of proteins were studied. Sakurada et al. [105] studied the time-dependent secondary structure changes of Ca^{2+}-binding protein calmodulin with its antagonist by 2D IR. Saguer et al. [107,161] investigated the heat-induced aggregation and gelation of whole porcine blood plasma and serum proteins with 2D IR. Fabian et al. [139] used 2D IR to determine the sequential order of the thermal unfolding of Cro repressor of the λ phage and its variants. Popescu et al. [140] used 2D IR to examine the mechanism of temperature-induced secondary protein structure changes of soluble elastin. Gao et al. [143] used 2D IR to study the thermally induced conformational change of an apoptosis inhibitor protein surviving. Sovová et al. [145] studied the thermal dynamics of natural killer cell receptor proteins with 2D IR and 2D Raman.

Tian et al. [150] investigated the thermally induced conformational transition of soy protein with 2D IR. Scirè et al. [151] used 2D IR to probe the temperature effect on rat odorant-binding protein. Ashton et al. [270] used 2D Raman and 2D ROA to study the pH effect on protein phosphorylation process. Ashton et al. [377] also used 2D Raman for the analysis of flow-induced conformational changes of proteins by using a Taylor-Couette flow cell. Weingarth et al. [378] applied 2D covariance processing for time, resolution and sensitivity gain to the NMR study microcrystalline proteins. Li et al. [379] studied microcrystalline proteins by 2D covariance NMR. Ren et al. [380] studied the conformational changes under heat treatment of ovotransferrin with 2D IR. Pastrana-Rios et al. [149] developed a 2D IR method for determining the aggregation, stability and viability of proteins, peptides and peptoids.

Various peptides were investigated. Le Bihan et al. [19] used LC-MS based 2D mass spectrometry to study peptide fragments obtained from cytoplasmic proteins of a cell extract. Caerdà-Costa et al. [113] investigated the temperature-induced conformational reorganization and aggregation of activation domain of human procarboxypeptide as a function of incubation time at 90 °C by using 2D IR. De la Arada et al. [138] studied the temperature-induced conformational transition of peptide with 2D IR. Sikirzhytski et al. [106] used 2D deep UV resonance Raman to determine the sequence of fibrillation process of genetically engineered model polypeptide. Ma et al. [273] reported the 2D UV-resonance Raman study of pH dependent side chain electrostatic interactions of poly-L-lysine. Zhang et al. [361] investigated the pressure-induced conformational change of poly-L-lysine with different initial conformation with 2D IR.

Sosa et al. [152] reported the 2D IR study of thermally induced structural changes of complex between a calcium binding protein centrin and model peptide melittin. Pienpinijtham et al. [276] and Podstawska-Proniewicz et al. [326] carried out the 2D SERS study of neurotensin, a peptide known to stimulate tumor growth, with various modifications. Podstawka et al. [345] also reported the 2D SERS study of phenylalanine-substituted bombesin fragment peptides adsorbed on various electrode surfaces under different electrode potential. Lafon et al. [381] reported 2D covariance NMR study of chiral molecules dissolved in polypeptide liquid crystalline mesophase.

4.4. Other biomolecules

Other biomolecules, such as lipids, saccharides, and DNA, were also studied. Popescu and Vasile [196] used 2D IR to study the temperature induced melting and partial miscibility of poly(tetrahydrofuran) and cholesteryl palmitate. Szwed et al. [213] applied 2D correlation to the temperature-dependent ATR IR spectra to examine the effect of incorporating fluphenazine into a model bilayer membrane of dipalmitoylphosphatidylcholin. Wu et al. [214] used 2D IR to study the temperature induced phase transition between lamellar and micellar phase of amphiphilic lysophospholipid 1-stearoyllysophosphatidylcholin to probe the cooperativity of phase transition phenomenon. Morita and Kitagawa [225] reported the moving-window 2D correlation analysis of the temperature effect of poly(2-methacryloyloxyetyl phophorylcholine). Litwińczuk et al. [275] used 2D polarized ATR IR to examine the pH dependence of orientation of solid-supported bilayer of phospholipid 1,2-dipalmitoyl-*sn*-glycero-3-phophocholine (DPPC). Leitch et al. [354] used 2D IRRAS to study the voltage dependent changes of phospholipid–cholesterol bilayer with cholera toxin B on Au(III) electrode surface.

Khesbak et al. [24] reported the 2D IR analysis of isothermal transition and conformational states of DNA based on transient IR spectra collected after pulsed hydration. Zhang et al. [68] used 2D NIR to detect glucose under the influence of various interring effect. Rao et al. [360] applied 2D SERS to single-molecule force spectroscopy by using a dual optical trapping of DNA near Ag nanoparticles. Rudd et al. [382,383] discussed the utility of 2D IR-CD hetero-spectral correlation for the study of glycosaminoglycans family of anionic polysaccharides, like heparin, titrated with copper (II) cation inhibitor.

4.5. Bio-based materials and whole biological samples

Samples generated from biological systems are usually complex mixtures and heterogeneous composites, instead of isolated pure compounds. Because of the unique features of sorting out overlapped and convoluted information, 2D correlation spectroscopy can be effectively applied to such bio-based samples. Even live microbial cells can be directly analyzed. For example, Kirwan et al. [110] used 2D correlation ^{31}P NMR to examine the growth process of a plant pathogen *Phytophthora palmivora* with and without phophonate. Nishi et al. [111] used 2D NIR-IR hetero-spectral correlation for directly monitoring the ethanol content during the fermentation process. Ricci et al. [112] reported the time course study of yeast *Saccharomyces cerevisiae* fermentation with different ethanol concentration by statistical 2D ^{13}C NMR. Liu et al. [384] used thermal fingerprinting 2D IR for powder of cyanobacterium *Spilulina* with and without gamma irradiation.

Natural fibers were studied by 2D correlation spectroscopy. Liu et al. [20] examined the water desorption process from water-soaked cotton fibers by using 2D IR. Liu et al. [103] and Liu [104] characterized with 2D IR cotton fibers with different maturity stages, determined by the days after flowering, which will have different crystalline and amorphous cellulose contents. Sun et al. [385] discussed the detection method for natural bamboo fibers based on chemical treatment of fiber samples followed by 2D IR analysis.

Wood products undergoing a degradation processes were studied. Popescu et al. [115–117] studied lime wood *Tilia cordata* Mill. exposed for different time period to soft-rot fungi, such as *Trichoderma viride* Pers. or *Chaetomium globosum* to induce decay. The degradation of wood can be controlled by chemical coating treatment. Popescu and Simionescu [96] studied the environmental weathering process of lime wood coated with acrylic treatment by using 2D IR. Popoescu et al. [118] studied the degradation of lime wood by other mechanisms, such as hydrolysis, oxidation, and decarboxylation reactions with varying amount of treatment time.

Many other biological systems were also studied. Quaroni et al. [83] reported the 2D synchrotron FT IR study of living retinal rod cells based on time-resolved spectra collected after photo-stimulation. Wang et al. [109] used 2D IR to determine the biopolymer degradation sequence during the composting process of rapeseed meal and what bran. Harvey et al. [260] used 2D IR to study plant-derived bio char samples produced by a heat treatment with rising temperature under oxygen-limited condition. via et al. [263] used ATR IR-NIR hetero-spectral correlation to characterize the biomass changes of sweet gum, Loblolly pine and switch grass during the torrefaction or roasting process.

De Almeida et al. [319] used 2D ATR IR to study zein-based biofilms with different concentration of a xanthan gum additive. Xu et al. [334] used 2D visible/NIR to examine the mixture of goose down and duck down with different composition. Liu et al. [386] reported the application of a correlation method to a UV–visible reflectance monitoring study based on the remote sensing for wetland vegetation growth. Wu et al. [387] applied 2D IR to discriminate bee pollens from different plants. Bingol and Brüschweiler [388] studied *E. coli* cell lysate by 2D covariance NMR.

4.6. Food products

Application of 2D correlation spectroscopy in food science has been very active, and a number of publications on this topic appeared during this survey period. For example, Rodriguez et al. [84] characterized beer samples under forced aging with 2D correlation NMR. Chen et al. [38] used 2D IR for the quantitative discrimination of seemingly similar samples of sweet and dry wine based on the room temperature volatilization behavior. Cozzolino et al. [257] used 2D MS electric nose for the headspace analysis of wine. Ferrari et al. [324] analyzed red wine samples, which had been color-enhanced with anthocyanins from grapevine or black rice, by using NIR-NMR hetero-spectral correlation. Fudge et al. [338] used 2D IR for the identification of smoke-affected wine. Zhang et al. [389] compared red wine samples and their dried residues with different sugar contents (i.e., dryness) and manufactures by the three-step IR macro-fingerprint method by using temperature-based 2D IR.

Cozzolino et al. [129] used 2D NIR reflectance to analyze red grape homogenate exposed to different microwave heating time. Giangiacomo et al. [33] studied the osmotic dehydration process of apple with hypertonic sugar solution with 2D NIR analysis. Sinelli et al. [25,34] used 2D diffuse reflectance NIR for monitoring the osmo-air dehydration process of blueberries. Yu et al. [331] reported the 2D IR study of edible oil blends. Chen et al. [390] used 2D NIR for the discrimination of edible vegetable oils. Chen et al. [252] also discussed the use of 2D fluorescence as an identification method for edible vegetable oils. By using 2D correlation chromatography, Andary et al. [134] analyzed the valorization of olive stones by dilute acid hydrolysis followed by varying the duration of over-liming process to increase sugar content.

Katayama et al. [32] studied the rehydration process of 100% amylopectin starch obtained from glutinous rice flour, which is capable of gelatinization either by heating or rehydration without heating, by using IR-NIR 2D hetero-spectral correlation. Piccinini et al. [61] used 2D NIR FT Raman to investigate the starch retrogression process by aging of Semolina bread crumb. Luo et al. [66] used 2D NIR for the on-line detection of time-dependent variations of sugar content of jujube. Shinzawa et al. [308] used 2D NIR to study Thai fish sauce samples with varying nitrogen contents. Lei et al. [391] used 2D IR to compare milk powder products with different levels of added lactose. Lü et al. [392] used 2D NIR diffuse reflectance for the rapid identification and classification of fishmeal and soybean meal protein feed. Sun et al. [393] used 2D fluorescence to analyze the oxidation reaction of ground meat.

4.7. Environmental samples

2D correlation spectroscopy has also been utilized to analyze complex mixture samples encountered in the field of environmental science. Yu et al. [108] studied the extracellular polymeric substances in biofilms developed during composting by using 2D IR, 2D NMR and IR-NMR hetero-spectral correlation. Mecozzi et al. [114] analyzed the aggregate formation process of marine mucilage with 2D IR and UV–visible-IR hetero-correlation. Pietroletti et al. [135] used 2D IR to study the pollutant removal by marine alga *Caulerpa racemosa* exposed to various hydrocarbons. Hur et al. [123] studied leaf litter humic substance and Suwannee River fulric acid under different UV irradiation time with 2D fluorescence. Hur and Lee [302,303] used 2D fluorescence to study the metal binding capability of dissolved organic matter in environment and heterogeneous distribution of copper-binding characteristics of ultrafiltered size fractions of soil humic acid.

Abdulla et al. [304] reported the 2D IR, 2D ^{13}C NMR correlation, and IR-NMR hetero-correlation studies of dissolved organic matter along an estuarine transect with varying salinity to identify the nature and origin of components. Abdulla et al. [305] further reported the use of Fourier transform ion cyclotron resonance based 2D MS and MS-NMR hetero-correlation to analyze the ultrafiltered dissolved organic matter from the lower Chesepeake Bay with varying salinity. Li et al. [369] used 2D IR to analyze the diagenesis of organic matter in Lake Superior sediment at different depth of core sampling. Forouzanghar et al. [394] carried out the NMR-IR and NMR-NIR hetero-correlation studies of soil organic matter for band assignment.

4.8. Medical, physiological, and pharmaceutical applications

Various forms of 2D correlation spectroscopy techniques were used in the field of medical, physiological, and pharmaceutical applications. Andraka et al. [88] used 2D IR to detect the metabolic changes of normal and cancerous keratinocyte cells with time after irradiation with different dosage. Gasper et al. [119] reported the 2D IR study of human prostate cancer cells in the presence of two different cardenolides with different incubation time after the exposure. Bálint et al. [271] used 2D SERS to determine a proper marker band for pH dependence of Raman spectrum of 4-mercaptobenzoic acid used as local pH monitoring within cancer cells.

Kirwan et al. [98] reported the metabonomics time study of human blood plasma obtained from subjects recovering from exhaustive exercise with ingestion of controlled diet by using 2D correlation NMR. Robinette et al. [99] analyzed the time variation of rat urine during the L-arginine induced pancreatitis development by statistical 2D correlation NMR. Sonker et al. [100] studied the transient metabolic flux of phage infection with statistical 2D NMR. Xu et al. [101] reported the statistical hetero-sample correlation between urine and serum ^{1}H NMR spectra from metabolomic data sets. Blaise et al. [395] used statistical 2D NMR to identify connections within the perturbed metabolic network. Aher et al. [396] reported the use of statistical 2D NMR-MS hetero-spectral correlation applied to the metabonomics study of biofluids and tissues. Posma et al. [397] used a variant form of statistical 2D NMR for biomarker differentiation from a large number of urine samples. Zhang et al. [336] used 2D ATR-IR to examine the blood glucose concentration.

Various pharmaceutical samples were examined by using 2D correlation spectroscopy. Kachrimanis and Griesser [26] used 2D IR to analyze the dehydration process of a pharmaceutical ingredient carbamazepine dihydridate. Zimmermann and Baranović et al. [264] used 2D IR for the study of polymorphs of analgesic and antipyretic compound paracetamol. Jiang et al. [300] reported the 2D UV study of the molar ratio dependence of different forms of Al(III) complex with curcumin obtained from turmeric for the possible prevention of Alzheimer's disease. Chruszcz-Lipska et al. [272] reported the 2D Raman study of pH-dependence of oxirane ring opening reaction of antibiotic fosfomycyn. Masuda et al. [398] used 2D covariance NMR to improve the S/N to detect weak cross peaks arising from site specific interaction between curcumin and amyloid β-protein fibrils. Rudd et al. [328,399] reported the 2D NMR study of heparin with compositional changes caused by contaminants or natural structural variability.

Hattori and Otsuka [43] used 2D NIR to examine the water penetration into and interaction with disaccharide excipient of pharmaceutical tablets. Shinzawa et al. [132] applied 2D correlation to the time-dependent NIR spectra during the spontaneous evaporation of moisture from cellulose excipient for pharmaceutical tablets to probe the effect of preparatory grinding process which lowers the crystallinity and consequently the contents of absorbed, bound and free water. Pressure-induced variation of cellulose affecting the packing and crystallinity was also examined [340,365]. Shinzawa et al. [157] also reported 2D X-ray diffraction (XRD), and hetero-correlation between XRD and dissolution profile of active ingredient or XRD and water absorption profile of pharmaceutical tablets containing cellulosic excipient and pentoxifylline under different compressive deformation, affecting both crystallinity and compaction. Shinzawa et al. [400] further reported the use of 2D NIR in the analysis of imaging data of cellulose tablets made under different grinding time, which induces crystallinity changes and other transitions.

4.9. Traditional Chinese medicines

Holistic discrimination of complex traditional Chinese herbal and related medicines by 2D correlation spectroscopy was pioneered by Sun [265]. So-called macro-fingerprinting 2D IR spectra with distinct visual characteristics associated with individual samples are generated from the correlation analysis of IR spectra obtained under the programed heating of samples from the room temperature to near decomposition. This technique is extensively utilized especially in China for rapid qualitative discrimination of complex mixture samples due to its sensitivity to subtle variations in the chemical compositions and morphological features arising from different origins of samples, including counterfeit products and even geographic variations.

Sun et al. [401] published a book written in Chinese dealing with IR analysis of traditional medicines. Three-step macro-fingerprinting method, involving FT IR, the second derivative analysis of IR spectra, and temperature-based 2D IR analysis, was described. Han et al. [402] successfully discriminated Kudzu root (*radix puerariae*) from different geographies by this technique. Huang et al. [403] compared Huanqi, i.e., *Astragalus membranaceus* (Fisch) Bge. Var. mongholicus (Bge.) Hsiao, and its counterfeit Ciguogancao (*Glycyrrhiza pallidiflora* Maxim.). Wang et al. [404] reported the analysis of different species of dendrobium. Yang et al. [405] reported the differentiation of cordyceps, which is a parasitic fungus on lava and caterpillar, of different origins and counterfeit products.

Chen et al. [406] reported the discrimination of ganoderma species by multi-step IR macro-fingerprint method. Lei et al. [407] compared alcohol extracts of dried stems of *Cistanche deserticola* by using different concentration of alcohol. Li et al. [408] compared five species of *Beimu* (*Bilbus Fritillariae*) and their alkaloid extracts. Liu et al. [409] used macro IR fingerprinting for deer antler based medicine. Sun et al. [410] reviewed with many examples the analysis of traditional Chinese medicine with thermal perturbation based 2D IR analysis as a fingerprinting technique. Tan et al. [411] reported the multistep IR macro-fingerprinting analysis of traditional herbal leaves of *Phyllagathis praetermissa* from different localities in Malaysia. Tu et al. [412] analyzed traditional medicine *Cao Wu* (Radix *Aconite kusnezoffi*) subjected to different processing methods, which resulted in different influence on product constituents.

Wu et al. [413] reported the discrimination of *Agrimonia Pilosa* Ledeb and its extracts. Xu et al. [414] evaluated various traditional medicines for aiding blood circulation. Xu et al. [415] compared different sources of *Herba cistanche*. Yao et al. [416] reported the differentiation of eight species of fruit of various *Lycium barbarum*. Yin et al. [417] analyzed Da Xue Teng or *Sargentodoxa cuneata* (*oliv*) Rehd. etwils in the original herbal form, extracts with water or with anthraquinone, and residues. Zhang [418] applied the three-step macro-fingerprint to differentiate one of the most important classes of traditional Chinese medicines ginseng (*Panax ginseng* C.A. Meyer) root samples with different growth environments and growth years. Zhang et al. [419] reported the analysis of the crude form and extract of radix *Scutellariae biclensis* Georgi.

Zhou et al. [420] examined the quality difference of licorice (*Glycyrrhiza uralensis* Fisch.) from different ecological habitats with varying climate, which could not be effectively detected by HPLC analysis of only select components, like glycyrrhizic acid and liquiritin. Adiana et al. [421] applied the macro-fingerprinting of tropical medicinal plant *Senna Alata* L., commonly known as candle bush, by holistic analysis of chemical constituents. Choong et al. [422] reported the differentiation of water extract of medicinal mushroom *Ganoderma lucidum*. Li et al. [423] described the thermal perturbation 2D IR of leech commonly used in traditional Chinese medicine before and after processing, and protein structure changes and oxidation of fatty acids and cholesterol components were detected. Tan et al. [424] discussed the macro-fingerprinting identification and quality control of herbal medicine, *Phyllagathis rotundifolia* and *Phyllagathis praetermissa*.

Wang et al. [425] reported the discrimination of various horns used in traditional medicine. Zhang et al. [426] carried out the identification of alcoholic extracts and residues of *Cinstanche deserticola*. Abdullah et al. [427] reported the authentication of three different medicinal herbs *Libisia pumila*. Cui et al. [428] analyzed the ultrasonic extract of actives from larch bark. Lu et al. [429,430] carried out the discrimination of traditional Chinese medicine Danshen, root and rhizome of *Salvia miltiorrhiza* Bunge, from different regions and of different growth year. Xu et al. [431] reported the rapid discrimination of three different Radix Puerariae and their extracts. Sun et al. [432] compared genuine *Herba geranium* and those from other geography.

Traditional Chinese medicines are also studied by 2D correlation spectroscopy techniques other than controlled thermal decomposition study. For example, Zhang et al. [142] used concatenated 2D IR analysis for the discrimination of *Astragus zhenheiqi* samples by comparing temperature-dependent spectral data to that of reference material. Zhou et al. [289] examined the concentration of analyte in *Ginko biloba* extracts by using 2D NIR correlation to select informative spectral intervals for chemometrics analysis.

4.10. Pure liquids and solution mixtures

Specific interactions, associations and aggregations in pure liquids and solution mixtures are important topics studied with 2D correlation spectroscopy. Sun et al. [153] used 2D NIR to examine the hydrogen bonding and transformation of aggregate species of pyrrole from polymer to dimer to monomer form. Tang et al. [154] studied the self-association of 2-pyrrolidone in the pure liquid. Haufa et al. [164] reported the 2D NIR study of aminoalcohols in the pure liquid state, as well as in CCl_4 and water. Liu et al. [165] reported the 2D NIR study of methanol and ethanol to probe the evolution of different hydrogen bonding association structures. Ryu et al. [172] studied temperature dependent IR spectra of ethylene glycol. Czarnecki [173] discussed the 2D NIR study of the temperature-induced peak position shift of hydrogen-bonded cyclohexanol.

Radice et al. [170] studied the hydrogen bonding in fluorinated amide by 2D IR. Sloop et al. [223] reported the 2D Raman study of the temperature-induced phase transition phenomenon and keto–enol and enol–enol tautomerization of fluorinated aryl β-diketones. Koeppe et al. [280] studied the hydrogen-bonded complexes formation of 2-chlore-4-nitrophenol with acetate ion by using 2D UV–visible and NMR hetero-spectral correlation. Unger et al. [194] and Shinzawa et al. [157] reported the 2D IR study of the recrystallization and self-assembly process of oleic acid. Czarnecki [433] reviewed various 2D correlation spectroscopy studies of hydrogen-bonded systems.

Solution systems consisting of several components with their molecular interaction behaviors were investigated. Li et al. [37] studied with 2D IR solutions of oleic acid or linoleic acid in ethanol. Szyc et al. [168] used 2D IR to probe the complexation chemistry of 2-pyridone, which can also isomerizes to 2-hydroxypyridine, in CD_2Cl_2. Liu et al. [166] used 2D IR to study the interaction between 4-aminopyridine and methacrylic acid. Ryu et al. [171,172] analyzed acetone in a mixture of $CHCl_3$ and CCl_4 by 2D IR. Czarnecki [174] studied the hydrogen bonding of diamine and water mixture with 2D NIR. Tong et al. [278] studied the mixture of 1-propanol and water with 2D IR. Unger et al. [281] used 2D IR for solution mixtures of *N*,*N*-dimethyl formamide or *N*,*N*-dimethyl acetamide in methanol.

Chen et al. [282] studied the system of iodine–benzene mixture in CCl_4 with 2D UV–visible and 2D IR spectroscopy. Li et al. [285,313] studied acetone or DMF and butanone mixture in CCl_4 by 2D IR. Szostak et al. [286,287] used 2D Raman to study the self-aggregation of trichloroacetaldehyde in CCl4 and deutrated cyclohexane. Morita et al. [307] discussed the study of evaporation of ethanol from a mixture with oleic acid. Shinzawa and Ritthiruangdej [308] studied the ethanol and oleic acid mixture by 2D IR. Li et al. [312] investigated the mixture of butanone and dimethyl formamide in CCl_4. Mello et al. [434] reported the 2D Raman study of the composition dependence of ethanol and methanol mixture, and microscopically non-ideal solution behavior, suggesting the possible formation of clusters, was observed.

A number of mixture systems involving ionic liquids were studied. Czarnecki et al. [163] reported the 2D NIR study of hydrogen bonding interaction for ionic liquid in cyclohexanol and water mixtures. Liu et al. [166] studied the temperature dependent interaction between 4-aminopyridine and methacrylic acid. Sun and Wu [167] studied the thermally induced evolution of a mixture of water and an ionic liquid 1-butyl-3-methylimidazolium tetrafluoroborate. Wu et al. [290] used 2D NIR to probe the effect of ethanol addition with different concentration to aqueous solution of ionic liquid. Park et al. [291] used 2D IR to study the concentration-dependent hydrogen bonding interactions of zwitterion-type ionic liquids in water.

Wang et al. [292] studied an ionic liquid, 1-butylpyridinium tetrafluoroborate, in water or DMSO. Zhang et al. [293] use 2D IR to probe the interaction between ionic liquid and water with varying concentration affecting the hydrogen bonding. Aleska et al. [294] reported the 2D Raman study of aqueous solutions of ionic liquid, 1-decyl-3-methyl-imidazolium bromide, with increasing water content to detect different states of water. He et al. [295] used 2D IR to study the molecular interaction in a mixture of methanol and ionic liquid, 1-ethyl-3-methylimidazolium lactate.

4.11. Colloids, interfaces, and electrode surfaces

The state and interaction of molecules at various interfaces are often analyzed by using 2D correlation spectroscopy. Haider et al. [17] applied 2D correlation to the time-resolved adsorption–desorption IR spectra by selectively poisoning colloidal Au catalysis with thiols. Chowdhury [18] studied the adsorption of 2-aminobenzithiazole onto nano-colloidal silver surface. Takumi et al. [29] used 2D external reflection–absorption IR to analyze the time-dependent adsorption dynamics of hexadecylpyridinium and sodium dodecyl sulfate to air and water interface. Yang et al. [30] reported the 2D IR study of the dynamic adsorption of catechol on goethite, which was found to be influenced by pH but not by ionic strength. Yan et al. [31] used 2D IR to probe the effect of dissolved organic matter on the desorption process of enrofloxacin onto montmorillonite under different pH.

Mäkie et al. [136] used 2D DRIFTS for the adsorption study of trimethyl phosphate onto nanomarticles of hematite, maghemite, or goethite. Park et al. [155] used 2D DRIFTS to examine the temperature effect on self-assembled thin films of sensitizing dye for solar cells on nanocrystalline TiO_2 surfaces. Murawska et al. [240] used 2D IR to study the structural changes during the heating of two-component liposome. Jung et al. [259] reported the 2D DRIFTS study of the surface-induced thermal degradation mechanism of self-assembled thin film of ruthenium complex dye containing polypyridyl ligand anchored on TiO_2 surface, which are used for dye-sensitized solar cells. Lindegren et al. [266] used 2D IR to study the pH dependence on the adsorption of citrate and tricarballylate onto goethite suspended in water.

Olsson et al. [269] reported the 2D IR study of the adsorption, desorption, and surface-promoted hydrolysis of glucose-1-phospahte based on pH-dependent surface complexes formation on goethite. Chandra et al. [309] used 2D SERS to investigate the concentration dependence of 3-thiophene carboxylic acid adsorption onto silver nano colloids. Simanova et al. [310] studied the reaction of oxalate or $Fe(C_2O_4)_3^{3-}$ adsorbed at water–geothite interface. Song and Boily [329] reported the 2D IR study of the concentration dependence of surface hydroxyl groups of akaganéite (β-FeOOH) particles. Yu et al. [335] used 2D IR to probe the binding of organic ligands with Al(III) in soil dissolved organic matter with different Al(III) concentration.

2D correlation spectroscopy is often used in the analysis of reactions at the electrode interface. Yan et al. [86] used 2D SEIRAS to investigate the electrochemical reaction of water at CO predosed Pt electrode interface under strong hydrogen evolution. Aldon and Perea [297] reported the 2D Mössbauer study of the electrochemical reaction of Li extraction from positive electrode. Boily [341] used 2D IR to study the oxyanions adsorbed on solid surfaces with electric field. Podstawka and Niaura [342] used 2D SERS for the analysis of neurotransimitter bombesin chemisorbed on electrochemically roughened electrode surfaces. Podstawka et al. [345] reported the 2D SERS study of peptides adsorbed onto various electrode surfaces. Ambrosio and Laredo et al. [346] studied the gold-supported biomimetic membrane phospholipid bilayer containing ion channel peptide with electrode potential.

Naumann et al. [347] reported the 2D SEIRAS study of the electrochemistry of protein tethered bilayer lipid membrane as a function of potential. Nowak et al. [348] investigated the membrane redox protein cytochrome c oxidase under varying electrical potential. Ambrosio and Gewirth [349] used 2D SERS to probe the reactions of alkaline aqueous solution at Ag electrode by cyclic voltametry. Colina et al. [350] investigated with 2D Raman the electrochemical oxidation of transparent single-walled carbon nanotubes during anodic voltametric scan. Butcher et al. [352] used 2D Raman to investigate the electrical potential dependent assembly of 2,2′-bipyridine on Au(100) and Au(111). Park et al. [296,298,344,353] reported a number of electrochemistry studies at the electrode–electrolyte interface of $LiCoO_2$/Li cell. Litch et al. [354] used 2D IRRAS for voltage-dependent changes of phospholipid and cholesterol bilayer with cholera toxin B on Au(III) electrode surface. Su et al. [355] studied with 2D IRRAS the electrochemistry of lipid bilayer assembled at Au(III) electrode surface.

4.12. Inorganic–organic hybrids and ionic species

A number of hydrothermally synthesized coordinated metal compounds with organic ligands were studied by 2D IR using thermal and magnetic perturbations. Chai et al. [176] analyzed the hydrothermally synthesized compound from bismuth and a flexible ligand *N*,*N*′-diacetic acid imidazolium chloride by 2D IR. Rare earth 3-bi-pyridine polymer was studied by Chen et al. [177], divalent transition metal carboxyarylphosphonates by Lei et al. [178], crystals of carboxylate metal coordination compounds hydrothermally synthesized with 3-methylbenzoic acid by Chen et al. [179], and porous organic–inorganic hybrid compound of polyoxovanadium borate by Li et al. [180,181].

Hydrothermally synthesized polyoxometalates with different carboxylic ligands and photocatalytic activities was investigated by Chen et al. [182], organically template aluminoborte with quasi-aromaticity by Hu et al. [183], lanthanide 2-hydroxynicotinic acid coordination polymer by Mei et al. [184], and polyoxovanadium borate organic–inorganic hybrid was analyzed by Sun et al. [185]. Keggin-type heteropolytungustates was studied by Chai et al. [186] and nitrogen-heterocyclic β-octamolybdate supported metal–organic compounds by Chen et al. [187]. Cadmium thiolato-carboxylate coordination complexes was investigated by Ge et al. [188], manganese complex with 4,4′-bipyridine and methyl benzoate ligands by Wu et al. [189], and rare earth compounds with 3-methylbenzoic acid by Zhao et al. [190].

Metal endohedral fullerenes were studied with 2D XANES and 2D IR by Marcelli et al. [237]. Ionic transport in crystalline ionic gel electrolytes was studied with 2D IR by Park et al. [301]. The energy transfer among lanthanide ions during the luminescence process was investigated with 2D UV–visible and fluorescence hetero-spectral correlation by Huang et al. [435]. Zinc organic phosphate was analyzed with 2D IR by Sun et al. [436].

4.13. Industrial chemicals, reaction systems, and miscellaneous compounds

2D correlation spectroscopy was used in the analysis of a number of industrial chemicals. For example, Feng et al. [343] discussed the use of 2D NIR for the prediction of viscosity index of engine oil. Kim et al. [251] and Kim and Chung [437] used 2D Raman for the analysis of lube base oil and adulterated olive oil. Pereira and Pasquini [320] analyzed gasoline by 2D IR. Gu et al. [284] used 2D NIR for the detection of organophosphorous insecticide phoxin in water. Kwok and Taylor [368] used 2D Raman imaging for the detection of counterfeit pharmaceutical packaging.

Various chemical reaction systems were examined by using 2D correlation spectroscopy. Competing amidation of oxirane ring opening and amide formation reactions in epoxidized methyl oleate and aniline was analyzed with 2D NIR by Del Rio et al. [79]. Isomerization of *o*-xylene catalyzed by zeolite was studied with 2D IR by Fernandez et al. [80]. Cu(I)-catalyzed azide–alkyne "click" cycloaddition was examined with 2D IR by Sun and Wu [81]. Chemical reaction dynamics of sterically hindered alkanolamine and CO_2 was investigated with 2D IR by Cheon et al. [89]. The conversion of carbanion to bicarbonaion in the aqueous reaction of CO_2 and NH_3 was analyzed with 2D IR by Choi et al. [90]. The reaction of phenol with phenylisocyanate to produce diphenylurethane isomers was investigated with 2D NIR by Spegazzini et al. [94]. Bergman cyclization reaction of enediyne was studied with 2D IR by Gredičak et al. [256]. Titration of protonated Schiff base of n-butylretinal titrated with trifluoroacetic acid was examined with 2D IR by Biliškov et al. [279].

A variety of chemical compounds are also studied. Dielectric silicon oxcarbide thin films made by plasma enhanced chemical vapor was studied with 2D IR by Hwang et al. [21]. Oxidation reaction of tyrosine was examined with 2D fluorescence by Sun et al. [85]. Polyhedral oligomeric silsequioxanes undergoing hydrolytic condensation reaction was analyzed with 2D IR by Qu et al. [93]. Degradation reaction of organophosphane compounds on hematite or goethite nanoparticles by sun light was studied with 2D DRIFTS by Mäkie et al. [128]. Gelation of *N*-octyl-D-gluconamide upon cooling was analyzed with 2D NIR by Sun et al. [159]. Hydrogen-bonded aggregates of matrix-isolated propanol clusters were probed using 2D IR by Balevicius et al. [169].

The 2D IR detection of phase transition of polymorphic or mesomorphic compounds was proposed by Zimmermann and Baranović [206]. Fermi dyads of CO_2 with different local density were investigated with 2D Raman by Idrissi et al. [248]. 2D SERS study of the mechanism of pH-dependent signal enhancement effect for p-aminobenzenethiol on Ag nanoparticles was reported by Ji et al. [274]. Optimization of the detection of SO_2, NO, and NO_2 gases with 2D IR was reported by Wang et al. [306]. Diurea crosslinked bridged silsequioxanes derived from organosilane precursor with variable molecular composition of central spacer length were analyzed with 2D IR by Fernandes et al. [323]. Crystalline ^{13}C and ^{15}N-labeled amino acid was studied with covariance 2D NMR by Takeda et al. [438].

5. Analytical probes

One of the unique features of 2D correlation spectroscopy is its flexibility and versatility of allowing different types of analytical probes, such as IR, Raman, NIR, NMR and many others, to be freely selected for the examination of specific sample systems. The additional capability of this technique to combine datasets obtained with multiple probes by the hetero-spectral correlation analysis is also a very attractive feature. Fig. 4 shows the distribution of probes used among 461 published articles appeared during this survey period.

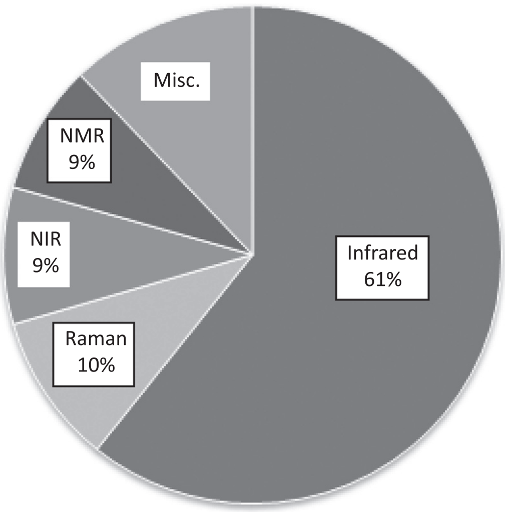

Fig. 4. Analytical probes used 2D correlation spectroscopy.

5.1. Infrared

IR is by far the most commonly used spectroscopic probe in 2D correlation analysis, representing about 60% of the probes found in 2D correlation spectroscopy literature reviewed here [11,14–17,20–24,26–32,35–42,44–50,52,53,58–60,62,65,67,69–76,80,81,83,86,88–90,92,93,95,96,103–105,107–109,113–122,124–128,130,135,136,138–143,145–153,155,156,158,160–162,166–172,175–196,199–202,204–206,208–222,224,226,228–240,243–245,247,25,33,34,43,51,54–57,61,63,64,66,68,77–79,82,84,85,87,91,94,97–102,106,110–112,123,129,131–134,137,144,154,157,159,163–165,173,174,197,198,203,207,223,225,227,241,242,246,248–256,258–264,266,269,275,277–279,281–283,285,291–293,295,299,301,304,306,307,310,312–314,316–319,323,327,329–333,335–339,341,346–348,353,354,356,357,361–363,369,372,374,380,382,384,385,387,389,391,394,401–403,405,406,408,410–432,436]. The use of IR spectroscopy had always been very strong in the past, but the overwhelming dominance of the use of IR probe indicates even greater popularity of 2D IR correlation spectroscopy as a well-established analytical technique in the field.

A notable trend during this review period for 2D correlation IR spectroscopy studies has been the increased reference to attenuated total reflection (ATR), reflecting the popularity of this measurement technique in many applications [15,17,20,30–32,37,39,42,44–47,67,72,81,86,92,103,120,206,213,253,263,269,275,278,281,291,293,295,310,319,329,336,339,157]. Other IR techniques employed in conjunction with 2D correlation analysis include diffuse reflectance infrared Fourier transform spectroscopy (DRIFTS) [65,128,136,155,259], infrared reflection absorption spectroscopy (IRRAS) [202,205,346,353,354], surface enhanced IR absorption spectroscopy (SEIRAS) [86,347,348], photoacoustic spectroscopy (PAS) [14], IR dichroism [356], as well as the use of synchrotron radiation source [83]. Several examples of hetero-spectral correlation studies were reported, combining IR spectroscopy with other probes, such as Raman [145], NIR [75,111,263], NMR [69,108,394], and XPS [204].

5.2. Raman

Raman probe [18,35,61,64,77,106,137,145,203,223,241,242,248,251,267,270,271,273,274,276,286,287,289,294,309,320,322,326,337,342,345,346,349,350,352,353,359,360,367,368,375,377,272,444] is also used extensively in 2D correlation spectroscopy. A number of techniques associated with Raman spectroscopy, such as surface enhanced Raman spectroscopy (SERS) [18,64,137,271,274,276,309,326,342,345,349,360], Raman optical activities (ROA) [270,439], deep UV resonance Raman [77,106,273,375], Raman microscopy [337], and spectral imaging [367], were found in various 2D Raman studies. The use of hetero-spectral correlation of Raman spectroscopy with IR [145] or XAS [353] measurement was also reported.

5.3. Near infrared

The application of 2D correlation in near infrared spectroscopy [3,25,32,34,43,49,61,66,68,75,79,94,111,122,132,153,154,159,163–165,167,173,174,232,263,277,284,289,290,308,315,324,327,340,343,365,390,392,394,400,404] is popular, especially for the investigation of hydrogen bonding and the characterization of samples in many practical applications. Hetero-spectral correlation of NIR spectroscopy with other analytical probes, such as IR [75,111,263], NMR [324], and visible spectroscopy [327], are reported. Although overshadowed by the huge growth of 2D IR applications, the actual numbers of publications for both NIR and Raman spectroscopy studies are steadily increasing.

5.4. UV–visible, THz and fluorescence

The range of optical spectroscopy applications analyzed by 2D correlation method extends to the ultraviolet and visible frequencies [78,102,114,177,280,282,300,311,334,382,393,435]. 2D UV–visible spectroscopy studies also included circular dichoisms (CD) [382] and reflectance measurements [95]. Hetero-spectral correlation studies of UV–visible spectroscopy combined with NMR [280], IR [311,382], NIR [334], and fluorescence spectroscopy [435] were reported. Spectroscopic studies utilizing pbobes like far IR or terahertz (THz) spectroscopy are also gaining popularity, and some promising applications of THz spectroscopy coupled with 2D correlation were reported [55–57,198]. Further growth in this emerging area is expected.

A sizable number of activities for 2D correlation analysis were also reported in the field of fluorescence spectroscopy [85,123,144,252,288,302,303,337,366,393,435]. Since the research activities in 2D fluorescence had been slowly declining in the past, this resurgence of the recent publication record is an encouraging sign for the renewed interest in using 2D correlation analysis for fluorescence data. Hetero-spectral correlation of fluorescence with UV–visible spectroscopy [435] was also reported.

5.5. NMR

Conventional 2D NMR spectroscopy, carried out by the application of a train of multiple radio frequency pulses followed by the double Fourier transformation of a set of detected free induction decay traces, is widely practiced. Survey of this type of 2D NMR is beyond the scope of the current review. An alternative approach to 2D NMR spectroscopy based on the generalized 2D correlation analysis is reviewed in this section. This form of 2D NMR was first reported by Eads and Noda [440], and similar ideas called statistical NMR techniques which use of covariance or correlation coefficientis [441,442] were forwarded later. Kirwan et al. [98] provided an excellent perspective on the development of various statistical 2D NMR techniques. NMR is probably one of the most rapidly growing areas of the application of 2D correlation spectroscopy.

A sizable number of applications of 2D correlation analysis in the field of NMR, mostly the statistical covariance or correlation coefficient analysis, were reported [69,84,90,98–101,108,110,112,250,273,304,305,324,328,346,378,379,388,394–399,438,443–454]. The statistical 2D NMR techniques are essentially the covariance or correlation coefficient analysis. Synchronous 2D correlation analysis can be readily applied to the NMR study of a single sample under multiple perturbations or pulse probes, multiple sample systems, or even in conjunction with different analytical probes, just as in the case of other hetero-sample or hetero-spectral 2D correlation analysis.

Ebbels et al. [443] discussed various forms of the statistical 2D NMR in the review of NMR bioinformatics. Various hetero-spectral correlation with other probes, such as IR [69,108,394], NIR [324,394], UV–visible [273], and mass spectrometry [305,396], were also explored. While some workers have recently started incorporating the broader concept of generalized 2D correlation into their analysis of NMR data, many others still utilize only the synchronous covariance or correlation coefficient portion of the statistical 2D NMR. It may provide a fertile future growth opportunity for NMR spectroscopists to explore this area of possibilities.

5.6. X-ray and scattering techniques

2D correlation analysis was used in some investigations using X-ray probes. They include small angle X-ray scattering (SAXS) [51,54], wide angle X-ray diffraction (WAXD) [51,54,364], X-ray adsorption near edge structure (XANES) [237], X-ray photoelectron spectroscopy (XPS) [204,298,334], and X-ray absorption spectroscopy (XAS) [298,353]. Hetero-correlation between SAXS and WAXD [51], XPS and IR [204], as well as XAS and Raman [353] were reported. 2D correlation in time-resolved scattering of light [63] and enhanced Rayleigh scattering [268] were also reported.

5.7. Other analytical probes

There were several examples of 2D correlation analysis applied to mass spectrometry [19,257,305,396,455] and its hetero-correlation with NMR [305,396]. Other spectroscopic or spectrometric probes used in the field include localized surface plasmon resonance [22], ultrafast spectroscopy [91], retardance [197], dynamic mechanical analysis [207,318], dielectric relaxation [359], and Mössbauer and gamma ray spectroscopy [297,456]. Data from size exclusion chromatography [133] and HPLC [134], as well as microscopic images [368], were also analyzed by using 2D correlation method. More unusual potential applications of 2D correlation analysis include dynamic temperature modulation [87], thermogravimetry [131], molecular dynamics simulation [249], cyclic voltametery [351], as well as dissolution profiles of pharmaceutical tablets [364].

6. Concluding remarks

In this survey, some of the noteworthy experimental practices, which are advancing forward the frontiers of the field of two-dimensional 2D correlation spectroscopy, are reviewed with the focus on various perturbation methods currently used to induce spectral changes, pertinent examples of applications in various fields, and types of analytical probes employed. Types of perturbation methods found in the published literature are very diverse, encompassing both dynamic and static effects. Fields of applications covered by the literature are also amazingly broad, ranging from fundamental research to practical applications in a number of physical, chemical and biological systems. Aside from IR spectroscopy, which is the most commonly used tool, many other analytical probes are used in 2D correlation analysis.

Dynamic perturbations surveyed here relate to not only time-dependent physical processes, such as acoustic or pulsed mechanical perturbations, sorption, penetration, diffusion and evaporation, crystallization and other transient physical phenomena, but also chemical reactions, like polymerization and crosslinking, and biological processes, as well as duration of exposure to various stimuli. Static perturbations, much more commonly employed today in 2D correlation spectroscopy than dynamic counterpart, is dominated by the effect of temperature, which include various phenomena, such as conformational changes of proteins, association, self-assembly and gelation, hydrogen bonding interactions, melting, crystallization, and glass transition, and other transition phenomena, various structural changes, and temperature-induced chemical reactions. The influence of concentration, such as pH effect, compositions of solution mixtures, ionic liquids, ionic species, dissolved gasses, blends and composites, and the use of designed concentration series, are reported. Other static perturbations include various electro-magnetic effects, mechanical deformation, pressure and compression, and even spatial distributions.

Polymers are extensively studied, including bio-based and biodegradable polymers, thermo-responsive polymers, water-soluble polymers, liquid crystalline polymers, thermosetting polymers, block copolymers and blends, a number of conventional polymers, as well as polymer matrices incorporating small molecules within. Other materials studied by 2D correlation spectroscopy include nano particles and nano composites, proteins, and peptides, and other biomolecules, bio-based materials and biological samples like living cells, food products, and environmental samples. 2D correlation spectroscopy is used in medical, physiological, and pharmaceutical applications, traditional Chinese medicines, pure liquids and solution mixtures, colloids, interfaces, and electrode surfaces, inorganic–organic hybrids and ionic species, industrial chemicals, and various reaction systems.

Analytical probes employed are currently dominated by infrared, but other probes are also used, such as Raman, near infrared, UV–visible, THz and fluorescence, NMR, X-ray spectroscopy and scattering techniques, and other analytical methods, like mass spectrometry and chromatography. The ever expanding trend in depth, breadth and versatility of 2D correlation spectroscopy techniques and their broad applications all point to the robust and healthy state of the field.

References

[1] I. Noda, A.E. Dowrey, C. Marcott, Appl. Spectrosc. 47 (1993) 1317.
[2] I. Noda, in: Y. Ozaki, I. Noda (Eds.), Two-Dimensional Correlation Spectroscopy, AIP Press, Melville, 2000, pp. 3–17.
[3] I. Noda, Vib. Spectrosc. 36 (2004) 143.
[4] I. Noda, J. Mol. Struct. 799 (2006) 2.
[5] I. Noda, J. Mol. Struct. 883–884 (2008) 2.
[6] I. Noda, J. Mol. Struct. 974 (2010) 3.
[7] I. Noda, J. Mol. Struct. 1069 (2014) 3.
[8] I. Noda, J. Am. Chem. Soc. 111 (1989) 8116.
[9] I. Noda, Appl. Spectrosc. 44 (1990) 550.
[10] I. Noda, Appl. Spectrosc. 47 (1993) 1329.
[11] I. Noda, Appl. Spectrosc. 54 (2000) 994.
[12] I. Noda, A.E. Dowrey, C. Marcott, G.M. Story, Y. Ozaki, Appl. Spectrosc. 54 (2000) 236A.
[13] I. Noda, Y. Ozaki, Two-dimensional Correlation Spectroscopy—Applications in Vibrational and Optical Spectroscopy, Wiley, Chichester, 2004.
[14] B.B. Li, P.D. Zhang, Sci. China Chem. 53 (2010) 1190.
[15] Y. Nishikawa, T. Nakano, I. Noda, Appl. Spectrosc. 63 (2009) 1204.
[16] M. Rivallan, E. Seguin, S. Thomas, M. Lepage, N. Takagi, H. Hirata, F. Thibault-Starzyk, Angew. Chem. Int. Ed. 99 (2010) 785.
[17] P. Haider, A. Urakawa, E. Schmidt, A. Baiker, J. Mol. Catal. 305 (2009) 161.
[18] J. Chowdhury, Vib. Spectrosc. 52 (2009) 85.
[19] T. Le Bihan, R. Grima, S. Martin, T. Forster, Y. Le Bihan, Rapid Commun. Mass Spectrom. 24 (2010) 1093.
[20] Y. Liu, G. Gamble, D. Thibodeaux, Appl. Spectrosc. 64 (2010) 1355.
[21] C.-S. Hwang, H.-B. Kim, J. Korean Phys. Soc. 55 (2009) 622.
[22] B. Tang, S. Xu, J. Tao, Y. Wu, W. Xu, Y. Ozaki, J. Phys. Chem. C 114 (2010) 20990.
[23] M. Kawabe, K. Futamura, S. Morita, Y. Ozaki, Nippon Setchaku Gakkaishi 47 (2011) 421.
[24] H. Khesbak, O. Savchuk, S. Tsushima, K. Fahmy, J. Am. Chem. Soc. 133 (2011) 5834.
[25] N. Sinelli, E. Casiraghi, S. Barzaghi, A. Brambilla, G. Giovanelli, Food Res. Int. 44 (2011) 1427.
[26] K. Kachrimanis, U.J. Griesser, Pharm. Res. 29 (2012) 1143.
[27] P. Musto, G. Mensitieri, M. Lavorgna, G. Scarinzi, G. Scherillo, J. Phys. Chem. B 116 (2012) 1209.
[28] H. Lai, P. Wu, Polym. Chem. 4 (2013) 3323.
[29] H. Takumi, M. Noda, H. Matsubara, T. Takuie, M. Aratono, Chem. Lett. 41 (2012) 1218.
[30] Y. Yang, W. Yan, C. Jing, Langmuir 28 (2012) 14588.
[31] W. Yan, J. Zhang, C. Jing, J. Colloid Interface Sci. 390 (2013) 196.
[32] N. Katayama, M. Kondo, M. Miyazawa, J. Mol. Struct. 974 (2010) 179.
[33] R. Giangiacomo, P. Pani, S. Barzaghi, J. Near Infrared Spectrosc. 17 (2009) 329.
[34] N. Sinelli, G. Giovanelli, A. Brambilla, S. Barzaghi, E. Casiraghi, in: Proc. 5th CIGR Section VI Int. Symp. Food Proc. Monitor. Technol. Bioproc. Food Quality Manag., Potsdam, Germany, 2009, p. 19.
[35] I. Noda, J. Mol. Struct. 974 (2010) 108.
[36] I. Noda, J. Mol. Struct. 974 (2010) 116.
[37] F. Pi, H. Shinzawa, M.A. Czarnecki, M. Iwahashi, M. Suzuki, Y. Ozaki, J. Mol. Struct. 974 (2010) 40.
[38] J. Chen, Q. Zhou, I. Noda, S. Sun, Appl. Spectrosc. 63 (2009) 920.
[39] W. Wang, Y. Jin, Z. Su, J. Phys. Chem. B 113 (2009) 15742.
[40] L. Li, Y. Yu, H. Su, G. Zhan, S. Li, P. Wu, Appl. Spectrosc. 64 (2010) 458.
[41] M. Wang, P. Wu, Polymer 52 (2011) 769.
[42] M. Wang, P. Wu, S.S. Sengupta, B.I. Chadhary, J.M. Cogen, B. Li, Ind. Eng. Chem. Res. 50 (2011) 6447.
[43] Y. Hattori, M. Otsuka, Vib. Spectrosc. 57 (2011) 275.
[44] Y. Jin, W. Wang, Z. Su, J. Memb. Sci. 379 (2011) 121.
[45] Y. Jin, W. Wang, Z. Su, Macromolecules 44 (2011) 2132.
[46] Y. Fu, L.-T. Lim, Polym. Test 31 (2012) 56.
[47] H. Lai, Z. Wang, P. Wu, B.I. Chaudhary, S.V. Sengupta, J.M. Cogen, B. Li, Ind. Eng. Chem. Res. 51 (2012) 9365.
[48] J. Shi, P. Wu, L. Li, T. Liu, L. Zhao, Polymer 50 (2009) 5598.
[49] K. Zheng, R. Liu, Y. Huang, Polym. J. 42 (2010) 81.
[50] K. Liu, Y. Yuan, J. Zhang, Vib. Spectrosc. 57 (2011) 81.
[51] D.S. Smirnova, J.A. Kornfield, D.J. Lohshe, Macromolecules 44 (2011) 6836.
[52] Y. Ando, H. Sato, H. Shinzawa, M. Okamoto, I. Noda, Y. Ozaki, Vib. Spectrosc. 60 (2012) 158.
[53] Z. Chen, J.-N. Hay, M.J. Jenkins, Eur. Polym. J. 48 (2012) 1586.
[54] L. Guo, N. Spegazzini, H. Sato, T. Hashimoto, H. Masunaga, S. Sasaki, M. Takata, Y. Ozaki, Macromolecules 45 (2012) 313.
[55] H. Hoshina, Bunko Kenkyu 61 (2012) 44.
[56] H. Hoshina, S. Ishii, Y. Morisawa, H. Sato, I. Noda, Y. Ozaki, C. Otani, Appl. Phys. Lett. 100 (2012) 011907.
[57] H. Hoshina, S. Ishii, S. Yamamoto, Y. Morisawa, H. Sato, T. Uchiyama, Y. Ozaki, C. Otani, IEEE Trans. Terahertz Sci. Technol. 3 (2013) 248.
[58] J. Zhou, Z. Xin, Polym. Compos. 33 (2012) 371.
[59] J.-Z. Xu, Y.-Y. Liang, G.-J. Zhong, H.-L. Li, C. Chen, L.-B. Li, Z.-M. Li, J. Phys. Chem. Lett. 3 (2012) 530.
[60] X. Wang, K. Xiang, Y. Nie, G. Huang, J. Wu, Z. Su, Macromol. Res. 21 (2013) 493.
[61] M. Piccinini, S. Fois, N. Secchi, M. Sanna, T. Roggio, P. Catzedu, Food Anal. Methods 5 (2012) 1145.
[62] I. de la Arada, C. Seiler, W. Mäntele, Eur. Biophys. J. 41 (2012) 931.
[63] X. Tang, L. Li, L. Zhao, H. Zhang, P. Wu, Chin. J. Polym. Sci. 29 (2010) 63.
[64] W.-H. Park, Z.H. Kim, Nano Lett. 10 (2010) 4040.
[65] S. Kim, S.B. Kim, H.C. Choi, Bull. Korean Chem. Soc. 23 (2012) 194.
[66] H. Luo, Q. Lu, H. Ding, H. Gao, L. Guo, Spectrosc. Spectr. Anal. (Guangpuxue Yu Guangpu Fenxi) 32 (2012) 1225.
[67] Y. Park, C. Hashimoto, T. Hashimoto, Y. Hirokawa, Y.M. Jung, Y. Ozaki, Macromolecules 46 (2013) 3587.
[68] W. Zhang, R. Liu, W. Zhang, H. Jia, K. Xu, Biomed. Opt. Exp. 4 (2013) 789.
[69] S.R. Ryu, W.M. Bae, W.J. Hong, K.J. Ihn, Y.M. Jung, Vib. Spectrosc. 60 (2012) 168.
[70] Z. Su, Z. Jiang, G. Huang, L. Li, X. Wang, J. Macromol. Sci. 52 (2013) 22.
[71] K.-W. Huang, S.-W. Kuo, Macromol. Chem. Phys. 211 (2010) 2301.
[72] N. Spegazzini, I. Ruisánchez, M.S. Larrechi, A. Serra, A. Mantecón, Appl. Spectrosc. 64 (2010) 104.
[73] N. Spegazzini, I. Ruisánchez, A. Serra, A. Mantecón, M.S. Larrechi, Appl. Spectrosc. 64 (2010) 177.
[74] Y. Yu, X. Zhong, H. Su, A. Serra, Polymer 51 (2010) 1563.
[75] H. Yamasaki, S. Morita, J. Appl. Polym. Sci. 119 (2011) 871.
[76] B. Chae, S.H. Lee, S.B. Kim, Y.M. Jung, S.W. Lee, Vib. Spectrosc. 60 (2012) 137.
[77] I.K. Lednev, V. Shashilov, M. Xu, Current Sci. 97 (2009) 180.
[78] B. Tang, S. Xu, J. An, B. Zhao, W. Xu, J.R. Lombardi, Phys. Chem. Chem. Phys. 11 (2009) 10286.
[79] V. Del Rio, N. Spegazzini, M.P. Callao, M.S. Larrechi, J. Near Infrared Spectrosc. 18 (2010) 281.
[80] C. Fernandez, I. Stan, J.-P. Gilson, K. Thomas, A. Vicente, A. Bonilla, J. Pérez-Ramírez, Chem. Eur. J. 16 (2010) 6224.
[81] B. Sun, P. Wu, J. Phys. Chem. A 114 (2010) 8331.
[82] A. Mezzetti, L. Blanchet, A. de Juan, W. Leibl, C. Ruckebusch, Anal. Bioanal. Chem. 399 (2011) 1999.
[83] L. Quaroni, T. Zlateva, E. Normand, Anal. Chem. 83 (2011) 7371.
[84] J.A. Rodrigues, A.S. Barros, B. Carvalho, T. Brandão, A.M. Gil, Anal. Chim. Acta 702 (2011) 178.
[85] Q.Y. Sun, W. Wang, L. Wu, X. Jia, Spectrosc. Spectr. Anal. (Guangpuxue Yu Guangpu Fenxi) 31 (2011) 1838.
[86] Y.-G. Yan, B. Peng, Y.-Y. Yang, W.-B. Cai, A. Bund, U. Stimming, J. Phys. Chem. C 115 (2011) 5584.
[87] K. Zrelli, T. Barilero, E. Cavatore, H. Berthoumieux, T. Le Saux, V. Croquette, A. Lemarchand, C. Gosse, I. Jullien, Anal. Chem. 83 (2011) 2476.
[88] N. Andraka, J. Gonzalez-Valasco, J. Celeiro, J.R. Arrondo, P. Bilbao, Vib. Spectrosc. 60 (2012) 189.
[89] Y. Cheon, Y.M. Jung, J. Lee, H. Kim, J. Im, M. Cheong, H.S. Kim, H.S. Park, ChemPhysChem 13 (2012) 3365.
[90] B.G. Choi, H.S. Park, G.H. Kim, Y.M. Jung, K.B. Yi, J.-N. Kim, W.H. Hong, J. Ind. Eng. Chem. 18 (2012) 98.
[91] S.C. Doan, G. Kuzmanich, M.N. Gard, M.A. Garcia-Garibay, B.J. Schwartz, J. Phys. Chem. Lett. 3 (2012) 81.
[92] P. Musto, M. Abbate, M. Pannico, G. Scarinzi, G. Ragosta, Polymer 53 (2012) 5016.
[93] Y. Qu, G. Huang, X. Wang, J. Li, J. Appl. Polym. Sci. 125 (2012) 3658.
[94] N. Spegazzini, H.W. Siesler, Y. Ozaki, Anal. Chem. 84 (2012) 8330.
[95] K. Xiang, X. Wang, G. Huang, J. Zheng, J. Huang, G. Li, Polym. Degrad. Stabil. 97 (2012) 1704.

[96] C.-M. Popescu, B.C. Simionescu, Appl. Spectrosc. 67 (2013) 606.

[97] P. Guyett, J. Glushka, X. Gu, M. Bar-Peled, Carbohyd. Res. 344 (2009) 1072.

[98] G.M. Kirwan, V.G. Coffey, J.O. Niere, J.A. Hawley, M.J. Adams, Anal. Chim. Acta 652 (2009) 173.

[99] S.L. Robinette, K.A. Veselkov, E. Bohus, M. Coen, H.C. Keun, T.M.D. Ebbels, O. Beckonert, E.C. Holmes, J.C. Lindon, J.K. Nicholson, Anal. Chem. 81 (2009) 6581.

[100] K. Sonker, R.N. Purusottam, N. Sinha, Anal. Chem. 84 (2012) 4063.

[101] J. Xu, S. Cai, X. Li, J. Dong, J. Ding, Z. Chen, Chemom. Intel. Lab. Syst. 112 (2012) 33.

[102] X. Yao, Y. Zhu, W. Feng, Y. Tian, W. Cao, Spectrosc. Spectr. Anal. (Guangpuxue Yu Guangpu Fenxi) 29 (2009) 2129.

[103] Y. Liu, D. Thibodeaux, G. Gamble, Appl. Spectrosc. 66 (2012) 198.

[104] Y. Liu, Materials 6 (2013) 299.

[105] D. Sakurada, W. Nunomura, Y. Takakuwa, Biochem. Biophys. Res. Commun. 423 (2012) 360.

[106] V. Sikirzhytski, N.I. Toplina, G.A. Takor, S. Higashiya, J.T. Welch, V.N. Uversky, I.K. Lednev, Biomacromolecules 13 (2012) 1503.

[107] E. Saguer, P.A. Alvarez, J. Sedman, A.A. Ismail, Food Hydrocolloids 33 (2013) 402.

[108] G.-H. Yu, Z. Tang, Y.-C. Xu, Q.-R. Shen, Environ. Sci. Technol. 45 (2011) 9224.

[109] L.-P. Wang, Q.-R. Shen, G.-H. Yu, W. Ran, Y.-C. Xu, Bioresource Technol. 105 (2012) 88.

[110] G.M. Kirwan, D.I. Fernandez, J.O. Niere, M.J. Adams, Anal. Biochem. 429 (2012) 1.

[111] T. Nishi, T. Genkawa, M. Watari, Y. Ozaki, Anal. Sci. 28 (2012) 1165.

[112] M. Ricci, M. Aggravi, C. Bonechi, S. Martini, A.M. Aloisi, C. Rossi, J. Biosci. 37 (2012) 749.

[113] N. Caerdà-Costa, I. De la Arada, F.X. Avilés, J.L.R. Arrondo, S. Villegas, Biochemistry 48 (2009) 10582.

[114] M. Mecozzi, M. Pietroletti, V. Gallo, M.E. Conti, Marine Chem. 116 (2009) 18.

[115] C.-M. Popescu, M.-C. Popescu, C. Vasile, Carohyd. Polym. 79 (2010) 362.

[116] C.-M. Popescu, M.-C. Popescu, C. Vasile, Microthermal J. 95 (2010) 377.

[117] C.-M. Popescu, M.-C. Popescu, C. Vasile, Int. J. Biol. Macromol. 48 (2011) 667.

[118] M.-C. Popescu, J. Froidevaux, P. Navi, C.-M. Popescu, J. Mol. Struct. 1033 (2013) 176.

[119] R. Gasper, T. Mijatovic, R. Kiss, E. Goormagtigh, Appl. Spectrosc. 65 (2011) 584.

[120] C. Palszkiewicz, A. Wesłucha-Birzyńska, E. Stodolak-Zych, M. Hasik, Vib. Spectrosc. 60 (2012) 185.

[121] Y.H. Kim, B. Chae, T.J. Lee, S.B. Kim, Y.M. Jung, S.W. Lee, J. Mol. Struct. 974 (2010) 30.

[122] S.H. Lee, B. Chae, H.-C. Kim, S.B. Kim, Y.M. Jung, S.W. Lee, J. Mol. Struct. 974 (2010) 35.

[123] J. Hur, K.-Y. Jung, Y.M. Jung, Water Res. 45 (2011) 2965.

[124] C.O. Lee, B. Chae, S.B. Kim, Y.M. Jung, S.W. Lee, Vib. Spectrosc. 60 (2012) 142.

[125] X. Zhong, Y. Liu, X. Tang, Q. Wu, L. Li, Y. Yu, Colloid Polym. Sci. 290 (2012) 1683.

[126] Y. Wang, Y. He, X. Wang, Polym. Bull. 68 (2012) 1731.

[127] Y. Wang, G. Ye, X. Wang, J. Mater. Chem. 22 (2012) 7614.

[128] P. Mäkie, P. Persson, L. Österlund, J. Phys. Chem. C 116 (2012) 14917.

[129] D. Cozzolino, W.U. Cynkar, R.G. Dambergs, Sens. Instrum. Food Qual. 5 (2011) 97.

[130] A.I. Gomaa, J. Sedman, A.A. Ismail, Vib. Spectrosc. 65 (2013) 101.

[131] H.L. Sui, X.Y. Liu, F.C. Zhong, X.Y. Li, X. Ju, Polym. Degrad. Stab. 98 (2013) 255.

[132] H. Shinzawa, K. Awa, I. Noda, Y. Ozaki, J. Mol. Struct. 974 (2010) 151.

[133] T.J. Kamerzell, M. Li, S. Arora, J.A. Ji, J. Wang, J. Pharmaceut. Sci. 100 (2011) 1341.

[134] J. Andary, J. Maalouly, R. Quaini, H. Chebib, D.N. Ruttledge, N. Quiani, Chemom. Intel. Lab. Syst. 113 (2012) 58.

[135] M. Pietroletti, A. Capobianchi, E. Ragosta, M. Mecozzi, Spectrochim. Acta A 77 (2010) 673.

[136] P. Mäkie, P. Persson, L. Österlund, J. Colloid Interface Sci. 392 (2013) 349.

[137] G. Das, F. Mecarini, F. Gentile, F. De Angelis, H.G.M. Kumar, P. Candeloro, C. Liberale, G. Cuda, E. Di Fabrizio, Biosensors Bioelectron. 24 (2009) 1693.

[138] I. de la Arada, J.-P. Julien, B.G. de la Torre, N. Huarte, D. Andreu, E.F. Pai, J.L. Arrondo, J.L. Nieva, J. Phys. Chem. B 113 (2009) 13626.

[139] H. Fabian, Z. Wu, Y. Wang, D. Naumann, J. Mol. Struct. 974 (2010) 203.

[140] M.-C. Popescu, C. Vasile, O. Craciunescu, Biopolymers 93 (2010) 1072.

[141] Q. Wang, W. Xu, P.W. Wu, H. Zhang, C. Cai, B. Zhao, J. Phys. Chem. B 114 (2010) 12754.

[142] L. Zhang, I. Noda, Y. Wu, Appl. Spectrosc. 64 (2010) 343.

[143] Y. Gao, M. Zhang, H. Zhang, X. Yu, W. Kong, X. Zha, Y. Wu, J. Phys. Chem. B 115 (2011) 7038.

[144] J. Li, C. Li, Int. J. Biol. Macromol. 48 (2011) 364.

[145] Ž. Sovová, V. Kopecký Jr., T. Pazderka, K. Hofbauerová, D. Rozbeský, K. Bezouška, R. Ettrich, J. Mol. Model. 17 (2011) 1353.

[146] A. Ausilli, A. Vitale, T. Labella, F. Rosso, A. Barbarisi, J.C. Gómez-Fernández, S. D'Auria, Arch. Biochem. Biophys. 525 (2012) 40.

[147] Y. Chen, H. Tian, J. Li, G. Li, Spectrosc. Spectr. Anal. (Guangpuxue Yu Guangpu Fenxi) 32 (2012) 1500.

[148] J. Guo, W. Zhang, X. Liao, B. Shi, J. Am. Leat. Chem. Assoc. 107 (2012) 205.

[149] B. Pastrana-Rios, I. Lloro-Manzano, United States Patent US 8,268,628 B1 (September 18, 2012).

[150] K. Tian, Z. Shao, X. Chen, J. Appl. Polym. Sci. 124 (2012) 2838.

[151] A. Scirè, A. Marabotti, M. Staiano, L. Briand, A. Varriale, E. Bertoli, F. Tanfani, S. D'Auria, J. Proteome Res. 8 (2009) 4005.

[152] L.del V. Sosa, E. Alifaro, J. Santiago, D. Naváez, M.C. Rosado, A. Rodríguez, A.M. Gómez, E.R. Schreiter, B. Pastrana-Rios, Proteins: Struct. Func. Bioinform. 72 (2011) 3132.

[153] S. Sun, H. Tang, P. Wu, Phys. Chem. Chem. Phys. 11 (2009) 7611.

[154] H. Tang, S. Sun, P. Wu, Appl. Spectrosc. 63 (2009) 1174.

[155] Y. Park, Y.M. Jung, S. Sarker, J.-J. Lee, Y. Lee, K. Lee, J.J. Oh, S.-W. Joo, Solar Energy Mater. Solar Cells 94 (2010) 857.

[156] J. Shi, P. Wu, F. Yan, Langmuir 26 (2010) 11427.

[157] H. Shinzawa, T. Genkawa, W. Kanematsu, J. Mol. Struct. 1028 (2012) 164.

[158] L. Jia, C. Guo, L. Yang, J. Xiang, Y. Tang, C. Liu, H. Liu, J. Colloid Interface Sci. 345 (2010) 332.

[159] S. Sun, P. Wu, Soft Matter 7 (2011) 6451.

[160] Z. Wang, P. Wu, J. Phys. Chem. B 115 (2011) 10604.

[161] E. Saguer, P. Alvarez, A.A. Ismail, Food Hydrocolloids 27 (2012) 208.

[162] W. Li, B. Sun, P. Wu, Carbohyd. Polym. 78 (2009) 454.

[163] M.A. Czarnecki, A.J. Muszyński, T. Troczyńska, J. Mol. Struct. 974 (2010) 60.

[164] K.Z. Haufa, M.A. Czarnecki, Appl. Spectrosc. 64 (2010) 351.

[165] H. Liu, J.P. Xu, L.B. Qu, R.R. Xiang, Sci. China Chem. 53 (2010).

[166] X. Liu, T. Zhou, X. Wang, J. Zhang, Anal. Bioanal. Chem. 397 (2010) 339.

[167] B. Sun, P. Wu, J. Phys. Chem. B 114 (2010) 9209.

[168] L. Szyc, J. Guo, M. Yang, J. Dreyer, P.M. Tolstoy, E.T.J. Nibbering, B. Czarnik-Matusewicz, T. Elsaesser, H.-H. Limbach, J. Phys. Chem. A 114 (2010) 7749.

[169] V. Balevicius, V. Sablinskas, I. Doroshenko, V. Pogorelov, Ukr. J. Phys. 56 (2011) 855.

[170] S. Radice, A. Milani, C. Castiglioni, Macromol. Symp. 305 (2011) 81.

[171] S.R. Ryu, I. Noda, Y.M. Jung, Bull. Korean Chem. Soc. 32 (2011) 2332.

[172] S.R. Ryu, I. Noda, C.-H. Lee, P.H. Lee, H. Hwang, Y.M. Jung, Appl. Spectrosc. 65 (2011) 359.

[173] M.A. Czarnecki, Vib. Spectrosc. 58 (2012) 193.

[174] M.A. Czarnecki, Vib. Spectrosc. 62 (2012) 207.

[175] C. Li, J. Liu, J. Li, F. Shen, Q. Huang, H. Xu, Polymer 53 (2012) 5423.

[176] X.-C. Chai, H.-H. Zhang, S. Zhang, R. Lei, Y.-P. Chen, Y.-Q. Sun, R.-Q. Sun, Q.-Y. Yang, Chinese J. Struct. Chem. (Jiegou Huaxue) 28 (2009) 1348.

[177] Y. Chen, L. Zhao, H. Zhang, Q. Yan, R. Sun, H. Fu, Spectrosc. Spectr. Anal. (Guangpuxue Yu Guangpu Fenxi) 30 (2010) 174.

[178] R. Lei, X. Chai, H. Mei, H. Zhang, Y. Chen, Y. Sun, J. Solid State Chem. 183 (2010) 1510.

[179] X.-Y. Chen, C.-M. Li, H.-B. Hu, Y.-P. Chen, C.-X. Li, Q.-Y. Yang, Y.-Q. Sun, H.-H. Zhang, R.-G. Luo, Chinese J. Struct. Chem (Jiegou Huaxue) 30 (2011) 839.

[180] G.-M. Li, H.-X. Mei, X.-Y. Chen, Y.-P. Chen, Y.-Q. Sun, H.-H. Zhang, X.-P. Chen, Chinese J. Struct. Chem. (Jiegou Huaxue) 30 (2011) 785.

[181] G. Li, H. Mei, S. Deng, Y. Sun, H. Hu, Y. Chen, H. Zhang, Spectrosc. Spectr. Anal. (Guangpuxue Yu Guangpu Fenxi) 31 (2011) 3026.

[182] X. Chen, Y. Chen, Z. Xia, H. Hu, Y. Sun, W. Huang, Dalton Trans. 41 (2012) 10035.

[183] H. Hu, X. Chen, S. Deng, F. Cai, Y. Sun, Y. Chen, J. Mol. Struct. 1010 (2012) 67.

[184] H. Mei, G. Li, S. Deng, Y. Sun, Y. Chen, H. Zhang, Spectrosc. Spectr. Anal. (Guangpuxue Yu Guangpu Fenxi) 32 (2012) 166.

[185] Y.-Q. Sun, G.-M. Li, Y.-P. Chen, Dalton Trans. 41 (2012) 5774.

[186] F. Chai, Y.-P. Chen, Z.-C. You, Z.-M. Xia, S.-Z. Ge, Y.-Q. Sun, H.-H. Huang, J. Solid State Chem. 202 (2013) 161.

[187] X.-Y. Chen, Y.-P. Chen, F. Chai, Y.-Q. Sun, B.-H. Huang, J. Mol. Struct. 1035 (2013) 462.

[188] S.-G. Ge, Q. Liu, S. Deng, Y.-Q. Sun, Y.-P. Chen, J. Inorg. Organomet. Polym. 23 (2013) 571.

[189] X.-J. Wu, Y.-P. Chen, Z.-M. Xia, S.-Z. Ge, F. Chai, L.-Y. Zhao, J. Mol. Struct. 1035 (2013) 318.

[190] L. Zhao, Y. Chen, X. Chai, G. Cui, L. Ren, Y. Yang, H. Zhang, X. Deng, J. Mol. Struct. 1032 (2013) 213.

[191] M. Unger, S. Morita, H. Sato, Y. Ozaki, H. Siesler, Appl. Spectrosc. 63 (2009) 1027.

[192] M. Unger, S. Morita, H. Sato, Y. Ozaki, H. Siesler, Appl. Spectrosc. 63 (2009) 1034.

[193] M. Unger, H. Sato, Y. Ozaki, H.W. Siesler, Macromol. Symp. 305 (2011) 90.

[194] M. Unger, D. Chaturvedi, S. Mishra, P. Tandon, H.W. Siesler, Spectrosc. Lett. 46 (2013) 21.

[195] H. Zhou, J. Feng, P. Wu, Appl. Spectrosc. 63 (2009) 1303.

[196] M.-C. Popescu, C. Vasile, Soft Mater. 8 (2010) 386.

[197] S. Watanabe, I. Noda, Y. Ozaki, J. Mol. Struct. 974 (2010) 165.

[198] H. Hoshina, Y. Morisawa, H. Sato, H. Minamide, I. Noda, Y. Ozaki, C. Otani, Phys. Chem. Chem. Phys. 13 (2011) 9173.

[199] Y. Li, T. Zhou, Z. Chen, J. Hui, L. Li, A. Zhang, Polymer 52 (2011) 2059.

[200] Z. Chen, T. Zhou, J. Hui, L. Li, Y. Li, A. Zhang, T. Yuan, Vib. Spectrosc. 62 (2012) 299.

[201] Y. Guo, Y. Jin, Z. Su, Soft Mater. 8 (2012) 2907.

[202] M.K. Kim, S.R. Ryu, I. Noda, Y.M. Jung, Vib. Spectrosc. 60 (2012) 163.

[203] H. Shinzawa, Y. Ozaki, H. Chung, Vib. Spectrosc. 60 (2012) 154.

[204] H.C. Choi, S.R. Ryu, H. Ji, S.B. Kim, I. Noda, Y.M. Jung, J. Phys. Chem. B 114 (2010) 10979.

[205] M.K. Kim, S.R. Ryu, I. Noda, y.M. Jung, Bull. Korean Chem. Soc. 32 (2011) 4005.

[206] B. Zimmermann, D. Vrsaljko, Polym. Testing 29 (2010) 849.

[207] X. Wang, G. Huang, J. Wu, Y. Nie, X. He, J. Phys. Chem. B 115 (2011) 1775.

[208] B. Zimmermann, G. Baranović, Appl. Spectrosc. 63 (2009) 1152.

[209] V. Kurz, M. Grunze, P. Koelsch, ChemPhysChem 11 (2010) 1425.

[210] H. Lai, P. Wu, Polymer 51 (2010) 1404.
[211] S. Sun, J. Hu, H. Tang, P. Wu, J. Phys. Chem. B 114 (2010) 9761.
[212] S. Sun, P. Wu, Macromolecules 43 (2010) 9501.
[213] J. Szwed, K. Cieślik-Boczula, B. Czarnik-Matusewicz, A. Jaszczyszyn, K. Gąsiorowski, P. Świątek, W. Maliknka, J. Mol. Struct. 974 (2010) 192.
[214] F.-G. Wu, N.-N. Wang, J.-S. Yu, J.-J. Luo, Z.-W. Yu, J. Phys. Chem. B 114 (2010) 2158.
[215] L. Zhang, I. Noda, Y. Wu, J. Mol. Struct. 974 (2010) 80.
[216] L. Zhang, Z. Xu, H. Li, I. Noda, J. Mol. Struct. 974 (2010) 46.
[217] T. Zhou, Z. Wu, Y. Li, J. Luo, Z. Chen, J. Xia, H. Liang, A. Zhang, Polymer 51 (2010) 4249.
[218] Y.-H. Cheng, W.-P. Chen, Z. Shen, X.-H. Fan, M.-F. Zhu, Q.-F. Zhou, Macromolecules 44 (2011) 1429.
[219] J. Luo, T. Zhou, X. Fu, H. Liang, A. Zhang, Eur. Polym. J. 47 (2011) 230.
[220] S. Sun, J. Hu, H. Tang, P. Wu, Phys. Chem. Chem. Phys. 13 (2011) 5061.
[221] B. Sun, H. Lai, P. Wu, J. Phys. Chem. B 115 (2011) 1335.
[222] S. Sun, P. Wu, J. Phys. Chem. B 115 (2011) 11609.
[223] J.C. Sloop, P.D. Boyle, A.W. Fountain, W.F. Pearman, J.A. Swann, Eur. J. Org. Chem. 5 (2011) 936.
[224] H. Wang, S. Sun, P. Wu, J. Phys. Chem. 115 (2011) 8832.
[225] S. Morita, K. Kitagawa, Vib. Spectrosc. 60 (2012) 217.
[226] M.-C. Popescu, B.C. Simionescu, Spectrochim. Acta A 92 (2012) 398.
[227] S. Sun, W. Zhang, W. Zhang, P. Wu, X. Zhou, Soft Matter 8 (2012) 3980.
[228] Z. Wang, H. Lai, P. Wu, Soft Matter 8 (2012) 11644.
[229] Z. Wang, P. Wu, RSC Adv. 2 (2012) 7099.
[230] Y. Wu, L. Zhang, I. Noda, Vib. Spectrosc. 60 (2012) 220.
[231] L. Zhang, I. Noda, Y. Wu, Vib. Spectrosc. 60 (2012) 200.
[232] Y. Jin, P. Wu, Cellulose 20 (2013) 67.
[233] S. Sun, H. Wang, P. Wu, Soft Matter 9 (2013) 2878.
[234] S. Sun, P. Wu, Macromolecules 46 (2013) 236.
[235] S. Sun, P. Wu, W. Zhang, W. Zhang, X. Zhu, Soft Matter 9 (2013) 1807.
[236] H. Lai, G. Chen, P. Wu, Z. Li, Soft Mater. 8 (2012) 2662.
[237] A. Marcelli, W. Xu, L. Liu, C. Wang, W. Chu, Z. Wu, J. Nanophotonics 3 (2009) 031975.
[238] W. Li, P. Wu, Appl. Spectrosc. 63 (2009) 926.
[239] S. Morita, K. Kitagawa, J. Mol. Struct. 974 (2010) 56.
[240] A. Murawska, K. Cieślik-Boczula, B. Czarnik-Matusewicz, J. Mol. Struct. 974 (2010) 183.
[241] H. Tang, S. Sun, J. Wu, P. Wu, X. Wan, Polymer 51 (2010) 5482.
[242] H. Zhou, Z. Lai, P. Wu, Appl. Spectrosc. 64 (2010) 912.
[243] P. Chys, C. Gielens, F. Meersman, Biochim. Biophys. Acta 1814 (2011) 318.
[244] S. Morita, H. Yamasaki, H. Shinzawa, Y. Ozaki, Setchaku no Gijutsu 32 (2012) 49.
[245] E.F.-J. Rettler, M.V. Unger, R. Hoogenboom, H.W. Siesler, U.S. Schubert, Appl. Spectrosc. 66 (2012) 1145.
[246] S. Sun, H. Tang, P. Wu, J. Phys. Chem. B 114 (2010) 3439.
[247] M. Wang, S. Sun, P. Wu, Appl. Spectrosc. 64 (2010) 1396.
[248] A. Idrissi, C. Ruckebusch, B. Debus, L. Boussekey, P. Damay, J. Mol. Liq. 164 (2011) 11.
[249] I. Vyalov, M. Kiselev, T. Tassaing, J.C. Soetens, M. Federov, P. Damay, A. Idrissi, J. Mol. Liq. 159 (2011) 31.
[250] H. Shinzawa, M. Nishida, W. Kanematsu, T. Tanaka, K. Suzuki, I. Noda, Analyst 137 (2012) 1913.
[251] M. Kim, S. Lee, K. Chang, H. Chung, Y.M. Jung, Anal. Chim. Acta 748 (2012) 58.
[252] B. Chen, P. Tian, D. Lu, L. Yu, Chinese Patent Application CN 103115910A, May 22, 2013.
[253] H. Yamasaki, S. Morita, Appl. Spectrosc. 66 (2012) 926.
[254] S.I. Vdovenko, I.I. Gerus, H.A. Fedorenko, V.P. Kukhar, Spectrochim. Acta A 103 (2013) 368.
[255] H. Du, T. Zhou, J. Zhang, X. Liu, Anal. Bioanal. Chem. 397 (2010) 3127.
[256] M. Gredičak, I. Matanović, B. Zimmermann, I. Jerić, J. Org. Chem. 75 (2010) 6219.
[257] D. Cozzolino, W. Cynkar, R. Dambergs, P. Smith, Sensors Actuators B 145 (2010) 628.
[258] H. Peng, Y. Hu, T. Liu, W.C. Tjiu, C. He, Thermochim. Acta 502 (2010) 1.
[259] Y.M. Jung, Y. Park, S. Sarker, J.-J. Lee, U. Dembereldorj, S.-W. Joo, Solar Energy Mater. Solar Cells 95 (2011) 326.
[260] O.R. Harvey, B.E. Herbert, J.-L. Kuo, P. Louchouran, Environ. Sci. Technol. 46 (2012) 10641.
[261] J.D. Badia, L. Santonja-Blasco, A. Martínez-Felipe, A. Ribes-Greus, Bioresource Technol. 114 (2012) 468.
[262] J.D. Badia, L. Santonja-Blasco, A. Martínez-Felipe, A. Ribes-Greus, Bioresource Technol. 114 (2012) 622.
[263] B.K. Via, S. Adhikari, S. Taylor, Bioresource Technol. 133 (2013) 1.
[264] B. Zimmermann, G. Baranović, J. Pharmaceut. Biomed. Anal. 54 (2011) 295.
[265] S.-Q. Sun, Q. Zhou, Z. Qin, Atlas of Two-dimensional Correlation Infrared Spectroscopy for Traditional Chinese Medicine Identification, Chemical Industry Press, Beijing, 2003.
[266] M. Lindegren, J.S. Loring, P. Person, Langmuir 25 (2009) 10639.
[267] L. Ashton, E.W. Blanch, J. Mol. Struct. 974 (2010) 132.
[268] Y. Li, H. Li, X. Chen, F. zhu, J. Yang, Y. Zhu, J. Ploym. Sci. B: Polym. Phys. 48 (2010) 1847.
[269] R. Olsson, R. Giesler, J.S. Loring, P. Person, Langmuir 26 (2010) 18760.
[270] L. Ashton, C. Johannessen, R. Goodacre, Anal. Chem. 83 (2011) 7978.
[271] Š. Bálint, S. Rao, M. Marro, P. Miškovský, D. Petrov, J. Raman Spectrosc. 42 (2011) 1215.
[272] K. Chruszcz-Lipska, K.K. Zborowski, E. Podstawka-Proniewicz, S. Liu, Y. Xu, L.M. Proniewicz, J. Mol. Struct. 986 (2011) 49.
[273] L. Ma, Z. Ahmed, S.A. Asher, J. Phys. Chem. B 115 (2011) 4251.
[274] W. Ji, N. Spegazzini, Y. Kitahama, Y. Chen, B. Zhao, Y. Ozaki, J. Phys. Chem. Lett. 3 (2012) 3204.
[275] A. Litwińczuk, J. Petrus, B. Czarnik-Matusewicz, Vib. Spectrosc. 60 (2012) 173.
[276] P. Pienpinijtham, E. Proniewicz, Y. Kim, Y. Ozaki, J.R. Lombardi, L.M. Proniewicz, J. Phys. Chem. C 116 (2012) 16561.
[277] Y. Geng, B. Xiang, J. Mol. Struct. 974 (2010) 173.
[278] H.-J. Tong, J.-Y. Yu, Y.-H. Zhang, J.P. Reid, J. Phys. Chem. A 114 (2010) 6795.
[279] N. Biliškov, J. Novak, M. Petković, G. Zgrablić, G. baranović, N. Došlić, Croat. Chem. Acta 84 (2011) 221.
[280] B. Koeppe, P.M. Tolstoy, J. Guo, E.T.J. Nibbering, T. Elsaesser, J. Phys. Chem. Lett. 2 (2011) 1106.
[281] M. Unger, B. Harnacke, I. Noda, H.W. Siesler, Appl. Spectrosc. 65 (2011) 892.
[282] J. Chen, Q. Bi, S. Liu, X. Li, Y. Liu, Y. Zhai, Y. Zhao, L. Yang, Y. Xu, I. Noda, J. Wu, J. Phys. Chem. A 116 (2012) 10904.
[283] J. Díaz-Visurraga, C. Daza, C. Pozo, A. Becerra, C. von Plessing, A. Garcia, Int. J. Nanomed. 7 (2012) 3597.
[284] C. Gu, B. Xiang, J. Xu, Spectrochim. Acta A 97 (2012) 594.
[285] X. Li, Q. Bi, S. Liu, J. Chen, S. Yue, Y. Wei, K. Huang, Y. Zhao, H. Liu, Y. Zhai, Y. Xu, I. Noda, J. Wu, J. Mol. Struct. 1034 (2013) 101.
[286] R. Szostak, Chem. Phys. Lett. 514 (2011) 49.
[287] R. Szontak, J. Raman Spectrosc. 42 (2011) 1185.
[288] K. Wu, W. Liu, G. Li, Spectrochim. Acta A 102 (2013) 186.
[289] X. Zhou, B. Xiang, M. Zhang, Anal. Lett. 46 (2013) 340.
[290] B. Wu, Y. Zhang, H. Wang, J. Phys. Chem. B 113 (2009) 12332.
[291] H.S. Park, Y.M. Jung, S.P. Yang, W. Shin, J.K. Kang, H.S. Kim, H.J. Lee, W.H. Hong, ChemPhysChem 11 (2010) 1711.
[292] N.-N. Wang, Q.-G. Zhang, F.-G. Wu, Q.-Z. Li, Z.-W. Yu, J. Phys. Chem. B 114 (2010) 8689.
[293] Q.-G. Zhang, N.-N. Wang, Z.-W. Yu, J. Phys. Chem. B 114 (2010) 4747.
[294] V. Aleksa, J. Kausteklis, V. Klimavicius, Z. Gdaniec, V. Balevicius, J. Mol. Struct. 993 (2011) 91.
[295] H. He, H. Chen, Y. Zheng, X. Zhang, X. Yao, Z. Yu, S. Zhang, Aust. J. Chem. 66 (2013) 50.
[296] Y. Park, N.H. Kim, J.Y. Kim, I.-Yong. Eom, Y.U. Jeong, M.S. Kim, S.M. Lee, H.C. Choi, Y.M. Jung, Vib. Spectrosc. 53 (2010) 60.
[297] L. Aldon, A. Perea, J. Power Sources 196 (2011) 1342.
[298] Y. Park, N.H. Kim, J.M. Kim, Y.C. Kim, Y.K. Jeong, S.M. Lee, H.C. Choi, Y.M. Jung, Appl. Spectrosc. 65 (2011) 320.
[299] Y.-C. Yen, C.-C. Cheng, S.-W. Kuo, F.-C. Chang, Macromolecules 43 (2010) 2634.
[300] T. Jiang, L. Wang, S. Zhang, P.-C. Sun, C.-F. Ding, Y.-Q. Chu, P. Zhou, J. Mol. Struct. 1004 (2011) 163.
[301] H.S. Park, S.R. Kwon, Y.M. Jung, H.S. Kim, H.J. Lee, W.H. Hong, Chem. Commun. 42 (2009) 6388.
[302] J. Hur, B.-M. Lee, Chemosphere 83 (2011) 1603.
[303] J. Hur, B.-M. Lee, Sci. World J. 11 (2011) 1865.
[304] H.A.N. Abdulla, E.C. Minor, P.G. Hatcher, Environ. Sci. Technol. 44 (2010) 8044.
[305] H.A.N. Abdulla, R.L. Sleighter, P. Hatcher, Anal. Chem. 85 (2013) 3895.
[306] Y. Wang, J. Yang, N. Li, W. Zheng, Spectrosc. Spectr. Anal. (Guangpuxue Yu Guangpu Fenxi) 29 (2009) 1835.
[307] S. Morita, H. Shinzawa, Y. Ozaki, Bunko Kenkyu 60 (2011) 245.
[308] H. Shinzawa, P. Ritthiruangdej, Y. Ozaki 65 (2011) 549.
[309] S. Chandra, J. Chowdhury, M. Ghosh, G.B. Talapatra, J. Phys. Chem. C 115 (2011) 14309.
[310] A.A. Simanova, J.S. Loring, P. Persson, J. Phys. Chem. C 115 (2011) 21191.
[311] C. Zhang, K. Huang, H. Li, J. Chen, S. Liu, Y. Zhao, D. Wang, Y. Xu, J. Wu, I. Noda, Y. Ozaki, J. Phys. Chem. A 113 (2009) 12142.
[312] X. Li, Q. Pan, J. Chen, S. Liu, A. He, C. Liu, Y. Wei, K. Huang, L. Yang, J. Feng, Y. Zhao, Y. Xu, Y. Ozaki, I. Noda, J. Wu, Appl. Spectrosc. 65 (2011) 901.
[313] X. Li, S. Liu, J. Chen, S. Yue, C. Liu, Y. Wei, K. Huang, Y. Zhao, Y. Xu, I. Noda, J. Wu, Vib. Spectrosc. 60 (2012) 212.
[314] K.-W. Huang, L.-W. Tsai, S.-W. Kuo, Polymer 50 (2009) 4876.
[315] Ž. Jelčić, N. Vranješ, V. Rek, Macromol. Symp. 290 (2010) 1.
[316] S.-W. Kuo, W.-C. Liu, J. Appl. Polym. Sci. 119 (2011) 300.
[317] S. Nurkhamidha, E.M. Woo, I.-H. Huang, C.C. Su, Colloid. Polym. Sci. 289 (2011) 1563.
[318] X. Wu, H. Wang, Z. Zhu, C.S. Liu, J. Phys. Chem. B 117 (2013).
[319] C.B. De Almeida, K.T. Catelam, M.L. Cornélio, J.L. Filho, Food Technol. Biotechnol. 48 (2010) 19.
[320] C.F. Pereira, C. Pasquini, Appl. Spectrosc. 64 (2010) 507.
[321] S. Radice, M. Tommasini, C. Castiglioni, J. Mol. Struct. 974 (2010) 73.
[322] V.L. Brewster, L. Ashton, R. Goodacre, Anal. Chem. 83 (2011) 6074.
[323] M. Fernandes, S.S. Nobre, Q. Xu, C. Carcel, J.N. Cachia, X. Cattoen, J.M. Sousa, R.A.S. Ferreira, L.D. Carlos, C.V. Santilli, M.C.M. Wong, V. de Zea Bermudez, J. Phys. Chem. B 115 (2011) 10877.
[324] E. Ferrari, G. Foca, M. Vignali, L. Tassi, A. Ulrici, Anal. Chim. Acta 701 (2011) 139.
[325] H.S. Park, H.S. Kim, Y.M. Jung, J. Phys. Chem. B 115 (2011) 1743.
[326] E. Podstawska-Proniewicz, A. Kudelski, Y. Kim, L.M. Proniewicz, J. Phys. Chem. B 115 (2011) 6709.
[327] M.-C. Popescu, C. Vasile, Spectrochim. Acta A 79 (2011) 45.

[328] T.R. Rudd, D. Gaudesi, M.A. Lima, M.A. Skidmore, B. Mulloy, G. Torri, H.B. Nader, M. Guerrini, E.A. Yates, Analyst 136 (2011) 1390.
[329] X. Song, J.-F. Boily, J. Phys. Chem. C 115 (2011) 17036.
[330] Q. Tan, Z. Tian, G. Li, Spectrosc. Spectr. Anal. (Guangpuxue Yu Guangpu Fenxi) 31 (2011) 970.
[331] X. Yu, F.R. van de Voort, J. Sedman, J. Gao, Anal. Bioanal. Chem. 401 (2011) 315.
[332] H. Tian, Y. Chen, C. Ding, G. Li, Carbohyd. Polym. 89 (2012) 542.
[333] Q.-Y. Wu, X.-N. Chen, L.-S. Wan, Z.-K. Xu, J. Phys. Chem. B 116 (2012) 8321.
[334] H. Xu, B. Song, W. Wan, Y. Zhou, Y. Ying, Spectrosc. Spectr. Anal. (Guangpuxue Yu Guangpu Fenxi) 32 (2012) 974.
[335] G.-H. Yu, M.-J. Wu, G.-R. Wei, Y.-H. Luo, W. Ran, B.-R. Wang, J. Zhang, Q.-R. Shen, Environ. Sci. Technol. 46 (2012) 6102.
[336] W. Zhang, Y. Cao, R. Liu, K. Xu, Spectrosc. Spectr. Anal. (Guangpuxue Yu Guangpu Fenxi) 32 (2012) 1507.
[337] V.L. Brewster, L. Ashton, R. Goodacre, Anal. Chem. 85 (2013) 3570.
[338] A.L. Fudge, K.L. Wilkinson, R. Ristik, D. Cozzolino, Food Chem. 139 (2013) 115.
[339] Q. Shao, Y. Qian, P. Wu, H. Zhang, C. Cai, Colloid Surf. B: Biointerface 109 (2013) 115.
[340] H. Shinzawa, K. Awa, I. Noda, Y. Ozaki, Appl. Spectrosc. 67 (2013) 163.
[341] J.-F. Boily, Phys. Chem. Chem. Phys. 11 (2009) 8133.
[342] E. Podstawka, G. Niaura, J. Phys. Chem. B 113 (2009) 10974.
[343] X. Feng, M. Lei, L. Guan, Cinese Patent (Faming Zhuanli Shenqing Gongkai Shuoming Shu) CN 101726451 A, 2010.
[344] Y. Park, N.H. Kim, S.B. Cho, J.M. Kim, G.C. Kim, M.S. Kim, S.M. Lee, I.-Y. Eom, H.C. Choi, Y.M. Jung, J. Mol. Struct. 974 (2010) 139.
[345] E. Podstawka, G. Niaura, L.M. Proniewicz, J. Phys. Chem. B 114 (2010) 1010.
[346] T. Laredo, J.R. Dutcher, J. Lipkowski, Langmuir 27 (2011) 10072.
[347] R.L.C. Naumann, C. Nowak, W. Knoll, Soft Matter 7 (2011) 9535.
[348] C. Nowak, T. Laredo, J. Gebert, J. Lipkowski, R.B. Gennis, S. Ferguson-Miller, W. Knoll, R.L.C. Naumann, Metallomics 3 (2011) 619.
[349] R.C. Ambrosio, A.A. Gewirth, Anal. Chem. 82 (2010) 1305.
[350] A. Colina, V. Ruiz, A. Heras, E. Ochoteco, E. Kauppinen, J. López-Palacios, Electrochim. Acta 56 (2011) 1294.
[351] L.R. Whitman, K.P. Bork, Y. Tang, J. Electroanal. Chem. 661 (2011) 100.
[352] D.P. Butcher, S.P. Boulos, C.J. Murphy, R.C. Ambrosio, A.A. Gewirth, J. Phys. Chem. C 116 (2012) 5128.
[353] Y. Park, N.H. Kim, H.C. Choi, S.M. Lee, H. Hwang, Y.U. Jeong, Y.M. Jung, Vib. Spectrosc. 60 (2012) 226.
[354] J.J. Leitch, C.L. Brosseau, S.G. Roscoe, K. Bessonov, J.R. Dutcher, J. Lipkowski, Langmuir 29 (2013) 965.
[355] Z.-F. Su, Y.-X. Jiang, M. Velázquez-Manzanares, J.J. Leitch, A. Kycia, J. Electroanal. Chem. 688 (2013) 78.
[356] M. Unger, H.W. Siesler, Appl. Spectrosc. 63 (2009) 1351.
[357] C.M. Burba, L. Woods, S. Miller, J. Pallie, Electrochim. Acta 57 (2011) 165.
[358] Z. Liu, L. Hu, J. Liu, C. Qiu, H. Zhou, D.P. Hashim, G. Shi, C. Peng, S. Najmaei, L. Sun, J. Lou, P.M. Ajayan, Nano Lett. 11 (2011) 5117.
[359] X. Wang, G. Huang, J.R. Wu, Y. Nie, X. He, K.W. Xiang, Appl. Phys. Lett. 99 (2011) 121902.
[360] S. Rao, S. Raj, B. Cossins, M. Marro, V. Gualler, D. Petrov, Biophys. J. 104 (2013) 156.
[361] M. Zhang, L. Zhang, Y. Wu, Vib. Spectrosc. 57 (2011) 319.
[362] M. Zhang, Y. Wu, Anal. Sci. 27 (2011) 1139.
[363] F. Piccirilli, S. Magialardo, P. Postorino, L. Baldassarre, S. Lupi, A. Perucci, Soft Matter 8 (2012) 11867.
[364] H. Shinzawa, K. Awa, Y. Ozaki, Anal. Methods 4 (2012) 1530.
[365] H. Shinzawa, K. Awa, I. Noda, Y. Ozaki, Vib. Spectrosc. 65 (2013) 28.
[366] M. Zhang, Y.-Q. Dang, T.-Y. Liu, H.-W. Li, Y. Wu, Q. Li, K. Wang, B. Zou, J. Phys. Chem. C 117 (2013) 639.
[367] H.H. Richardson, D. Wang, J. Mol. Struct. 974 (2010) 52.
[368] K. Kwok, L.S. Taylor, Vib. Spectrosc. 61 (2012) 176.
[369] H. Li, E.C. Minor, P.K. Zigah, Org. Geochem. 58 (2013) 125.
[370] Y. Doi, Microbial Polyesters, VCH, New York, 1990.
[371] I. Noda, S.B. Lindsey, D. Carraway, in: G.-Q. Chen (Ed.), Plastics from Bacteria: Natural Functions and Applications, Microbiology Monographs, vol. 14, Springer, Berlin, 2010, pp. 237–255.
[372] S. Sun, H. Tang, P. Wu, X. Wan, Phys. Chem. Chem. Phys. 11 (2009) 9861.
[373] J.D. Badia, A. Martinez-Felipe, L. Santonja-Blasco, A. Ribes-Greus, J. Anal. Appl. Pyrol. 99 (2013) 191.
[374] S.-W. Kuo, Y.-C. Wu, C.-F. Wang, K.U. Jeong, J. Phys. Chem. C 113 (2009) 20666.
[375] V.A. Shashilov, I.K. Lednev, J. Raman Spectrosc. 40 (2009) 1749.
[376] I.K. Lednev, V. Sikirzhytski, Am. Pharmaceut. Rev. 15 (2012) 1.
[377] L. Ashton, J. Dusting, E. Imomoh, S. Balabani, E.W. Blanch, Biophys. J. 98 (2010) 707.
[378] M. Weingarth, P. Tekely, R. Brüschweiler, G. Bodenhausen, Chem. Commun. 46 (2010) 952.
[379] Y. Li, Q. Wang, Z. Zhang, J. Yang, B. Hu, Q. Chen, I. Noda, F. Deng, J. Magn. Reson. 217 (2012) 106.
[380] G. Ren, A. Guo, F. Geng, M. Ma, Q. Huang, X. Wu, Spectrosc. Spectr. Anal. (Guangpuxue Yu Guangpu Fenxi) 32 (2012) 11780.
[381] O. Lafon, B. Hu, J.-P. Amoureux, P. Lesot, Chem. Eur. J. 17 (2011) 6716.
[382] T.R. Rudd, E.A. Yates, M. Hricovíni, Curr. Med. Chem. 16 (2009) 4750.
[383] T.R. Rudd, M.A. Skidmore, M. Guerrini, M. Hricovini, A.K. Powell, G. Silligardi, E.A. Yates, Curr. Opin. Struct. Biol. 20 (2010) 567.
[384] H.J. Liu, C.H. Xu, Q. Zhou, F. Wang, W.M. Li, Y.M. Ha, S.Q. Sun, Radiat. Phys. Chem. 85 (2013) 210.
[385] B. Sun, J. Liu, Y. Wang, A. Huang, Chinese Patent (Faming Zhuanli Shenqing) (2012). 102661929A.
[386] X. Liu, W. Zhao, X. Guo, Y. Wang, Y. Sun, Q. Miao, Spectrosc. Spectr. Anal. (Guangpuxue Yu Guangpu Fenxi) 32 (2012) 465.
[387] J. Wu, Q. Zhou, L. Wu, J. An, S. Sun, F. Hu, Spectrosc. Spectr. Anal. (Guangpuxue Yu Guangpu Fenxi) 30 (2010) 353.
[388] K. Bingol, R. Brüschweiler, Anal. Chem. 83 (2011) 7412.
[389] Y. Zhang, J. Chen, Y. Lei, Q. Zhou, S. Sun, I. Noda, J. Mol. Struct. 974 (2010) 144.
[390] B. Chen, P. Tian, D.-L. Lu, Z.-Q. Zhou, M.-L. Shao, Anal. Method 4 (2012) 4310.
[391] Y. Lei, Q. Zhou, Y. Zhang, J. Chen, S. Sun, I. Noda, J. Mol. Struct. 974 (2010) 88.
[392] C. Lü, L. Chen, Z. Yang, L. Han, Trans. Chinese Soc. Agric. Machinery (Nongye Jixie Xuebao) 43 (2012) 141.
[393] Y.-H. Sun, X.-L. Jia, J.-X. Meng, M.-L. Peng, Spectrosc. Spectr. Anal. (Guanpuxue yu Guanpufenxi) 33 (2013) 1014.
[394] M. Forouzanghar, D. Cozzolino, R.J. Smernik, J.A. Baldock, S.T. Forrester, D.J. Chittleborough, R.S. Kookana, Vib. Spectrosc. 66 (2013) 76.
[395] B.J. Blaise, V. Navratil, L. Emsley, P. Toulhoat, J. Proteome Res. 10 (2011) 4342.
[396] A.D. Maher, L.A. Cysique, B.J. Brew, C.D. Rae, J. Proteome Res. 10 (2011) 1737.
[397] J.M. Posma, I. Garcia-Perez, M. De Iorio, J.C. Lindon, P. Elliott, E. Holmes, T.M.D. Ebbels, J. Nicholson, Anal. Chem. 84 (2012) 10694.
[398] Y. Masuda, M. Fukuchi, T. Yatagawa, M. Tada, K. Takeda, K. Irie, K. Akagi, Y. Monobe, T. Imazawa, K. Takegoshi, Bioorg. Med. Chem. 19 (2011) 5967.
[399] T.R. Rudd, E. Macchi, C. Gardini, L. Muzi, M. Guerrini, E.A. Yates, G. Torri, Anal. Chem. 84 (2012) 6841.
[400] H. Shinzawa, K. Awa, I. Noda, Y. Ozaki, J. Mol. Struct. 974 (2010) 25.
[401] S. Sun, Q. Zhou, J. Chen, Analysis of Traditional Chinese Medicine by Infrared Spectroscopy, Chemical Industry Press, Beijing, 2010.
[402] M. Han, Q. Zhou, Q. Li, S. Sun, Spectrosc. Spectr. Anal. (Guangpuxue Yu Guangpu Fenxi) 29 (2009) 1851.
[403] D. Huang, S. Sun, Y. Xu, X. Chen, Spectrosc. Spectr. Anal. (Guangpuxue Yu Guangpu Fenxi) 29 (2009) 2396.
[404] C. Wang, B. Xiang, W. Zhang, J. Chemom. 23 (2009) 463.
[405] P. Yang, P. Song, S.-Q. Sun, Q. Zhou, S. Feng, J.-X. Tao, Spectrochim. Acta A 74 (2009) 983.
[406] X. Chen, D. Huang, S. Sun, J. Cao, S. Wang, Spectrosc. Spectr. Anal. (Guangpuxue Yu Guangpu Fenxi) 30 (2010) 78.
[407] Y. Lei, Q. Zhou, Tu-ya, J. Chen, S. Sun, I. Noda, J. Mol. Struct. 974 (2010) 156.
[408] D. Li, Z. Jin, Q. Zhou, J. Chen, Y. Lei, S. Sun, J. Mol. Struct. 974 (2010) 68.
[409] Y. Liu, G.-J. Zhang, S.-Q. Sun, I. Noda, J. Pharmaceut. Biomed. Anal. 52 (2010) 631.
[410] S. Sun, J. Chen, Q. Zhou, G. Lu, K. Chan, Planta Med. 76 (2010) 1987.
[411] H.-P. Tan, S.-K. Ling, C.-H. Chuah, Vib. Spectrosc. 52 (2010) 48.
[412] Y. Tu, P. Yang, S. Sun, Q. Zhou, X. Bao, I. Noda, J. Mol. Struct. 974 (2010) 103.
[413] X. Wu, Z. Jin, S. Sun, R. Jin, C. Wang, Spectrosc. Spectr. Anal. (Guangpuxue Yu Guangpu Fenxi) 30 (2010) 3222.
[414] M. Xu, H. Li, Q. Zhou, Q. Yin, S. Sun, X. Wu, Spectrosc. Spectr. Anal. (Guangpuxue Yu Guangpu Fenxi) 30 (2010) 640.
[415] R. Xu, S. Sun, Y. Liu, J. Chen, T. Liu, S. Chen, Spectrosc. Spectr. Anal. (Guangpuxue Yu Guangpu Fenxi) 30 (2010) 897.
[416] X. Yao, Y. Peng, Q. Zhou, P. Xiao, S. Sun, J. Mol. Struct. 974 (2010) 161.
[417] Q. Yin, H. Li, Q. Zhou, M. Xu, S. Yan, S. Sun, X. Wu, Spectrosc. Spectr. Anal. (Guangpuxue Yu Guangpu Fenxi) 30 (2010) 54.
[418] Y. Zhang, J. Chen, Y. Lei, Q. Zhou, S. Sun, I. Noda, J. Mol. Struct. 974 (2010) 94.
[419] C. Zhang, G. Zhang, S. Sun, Y. Tu, Spectrosc. Spectr. Anal. (Guangpuxue Yu Guangpu Fenxi) 30 (2010) 1774.
[420] Y. Zhou, H. Yu, Y. Zhang, S. Sun, S. Chen, R. Zhao, Q. Zhou, I. Noda, J. Mol. Struct. 974 (2010) 127.
[421] M.A. Adiana, M.P. Mazura, J. Mol. Struct. 991 (2011) 84.
[422] Y.K. Choon, S.-Q. Sun, Q. Zhou, Z. Ismail, B.A.A. Rashid, J.-X. Tao, Vib. Spectrosc. 57 (2011) 87.
[423] B. Li, Y. Wu, J. Ouyang, S. Sun, S. Chen, Spectrosc. Spectr. Anal. (Guangpuxue Yu Guangpu Fenxi) 31 (2011) 979.
[424] H.P. Tan, S.K. Ling, C.H. Chuah, J. Mol. Struct. 1006 (2011) 297.
[425] Y. Wang, C.-H. Xu, P. Wang, S.-Q. Sun, J.-B. Chen, J. Li, T. Chen, J.-B. Wang, Spectrochim. Acta A 83 (2011) 265.
[426] S. Zhang, C. Xu, J. Chen, Q. Zhou, S. Sun, Spectrosc. Spectr. Anal. (Guangpuxue Yu Guangpu Fenxi) 31 (2011) 2923.
[427] F. Abdullah, S.K. Ling, S. Man, A.L. Tan, H.P. Tan, Z. Abdullah, Vib. Spectrosc. 62 (2012) 200.
[428] X. Cui, X. Zhang, H. tang, L. Zhang, C. Xu, S. Sun, Spectrosc. Spectr. Anal. (Guangpuxue Yu Guangpu Fenxi) 32 (2012) 1810.
[429] X. Liu, C. Xu, S. Sun, J. Huang, K. Zhang, G. Li, Y. Zhu, Q. Zhou, Z. Zhang, J. Wang, Spectroschim. Acta A 97 (2012) 290.
[430] X.-H. Liu, H.-J. Xu, S.-Q. Sun, J. Huang, G.Y. Li, Y. Zhu, H.-Y. Gao, Z.-C. Zhang, J.-H. Wang, Anal. Method 4 (2012) 3344.
[431] B. Xu, G. Zhang, S. Sun, C. Xu, J. Chen, Y. Tu, Q. Zhou, M. Cui, J. Wang, C. Wen, J. Mol. Struct. 1018 (2012) 88.
[432] R.-S. Sun, Z.-X. Jin, Z.-P. Zhang, C.-H. Xu, S.-Q. Sun, Spectrosc. Spectr. Anal. (Guanpuxue yu Guanpufenxi) 33 (2013) 81.
[433] M.A. Czarnecki, Appl. Spectrosc. Rev. 46 (2011) 67.
[434] C. Mello, T. Mello, E. Sevéri, L. Coelho, D. Ribeiro, A. Marangoni, R. Poppi, I. Noda, J. Chem. Phys. 131 (2009) 084501.

[435] K. Huang, J. Chen, S. Liu, X. Gao, Q. Pan, C. Zhang, Y. Liu, J. Xia, J. Qi, Y. Xu, J. Wu, Spectrosc. Spectr. Anal. (Guangpuxue Yu Guangpu Fenxi) 30 (2010) 1181.
[436] R. Sun, J. Hu, H. Zhang, Y. Cao, Z. Ye, Y. Wang, Y. Chen, Spectrosc. Spectr. Anal. (Guangpuxue Yu Guangpu Fenxi) 30 (2010) 2215.
[437] M. Kim, H. Chung, Analyst 138 (2013) 1515.
[438] K. Takeda, Y. Kusakabe, Y. Noda, M. Fukuchi, K. Takegoshi, Phys. Chem. Chem. Phys. 14 (2012) 9715.
[439] T. Pazderka, V. Kopecký Jr., Vib. Spectrosc. 60 (2012) 193.
[440] C.D. Eads, I. Noda, J. Am. Chem. Soc. 124 (2002) 1111.
[441] Y. Chen, F. Zhang, D. Snyder, Z. Gan, L. Brüschweiler, R. Brüschweiler, J. Biomol. NMR 38 (2007) 73.
[442] E. Holmes, R.L. Loo, O. Cloarec, M. Coen, H. Tang, E. Maibaum, S. Bruce, Q. Chan, P. Elliott, J. Stamler, L.D. Wilson, J.C. Lindon, J.K. Nicholson, Anal. Chem. 79 (2007) 3740.
[443] T.M.D. Ebbels, R. Cavill, Prog. Nucl. Magn. Reson. Spectrosc. 55 (2009) 361.
[444] C.J. Sands, M. Coen, A.D. Maher, T.M.D. Ebbels, E. Holmes, J.C. Lindon, J.K. Nicholson, Anal. Chem. 81 (2009) 6458.
[445] D.A. Snyder, R. Brüschweiler, J. Phys. Chem. A 113 (2009) 12898.
[446] B.J. Blaise, V. Navratil, C. Domange, L. Shintu, M.-E. Dumas, B. Elena-Hermann, L. Emsley, P. Toulhoat, J. Proteome Res. 9 (2010) 4531.
[447] F. Zhang, L. Bruschweiler-Li, R. Brüschweiler, J. Am. Chem. Soc. 132 (2010) 16922.
[448] R.L.E.G. Aspers, P.E.T.J. Geutjes, M. Honing, Magn. Reson. Chem. 49 (2011) 425.
[449] G.E. Martin, B.D. Hilton, M.R. Willcott III, K.A. Blinov, Magn. Reson. Chem. 49 (2011) 641.
[450] G.N.M. Reddy, S. Caldarelli, Chem. Commun. 47 (2011) 4297.
[451] C.J. Sands, M. Coen, T.M.D. Ebbels, E. Holmes, J.C. Lindon, J.K. Niocholson, Anal. Chem. 83 (2011) 2075.
[452] A.D. Mahler, J.M. Fonville, M. Coen, J.C. Lindon, C.D. Rae, J.K. Nicholson, Anal. Chem. 84 (2012) 1083.
[453] Y. Chen, Z. Zhang, G. Shen, S. Cai, C. Cai, Z. Chen, Chem. Phys. Lett. 563 (2013) 102.
[454] Y. Li, B. Hu, Q. Chen, Q. Wang, Z. Zhang, J. Yang, I. Noda, J. Trébosc, O. Lafon, J.-P. Amoureux, F. Deng, Analyst 138 (2013) 2411.
[455] P. Wang, Mod. Phys. Lett. B 26 (2012) 1250065.
[456] R. Trainham, J. Tinsley, Rev. Sci. Instrum. 84 (2013) 013502.